New Approaches towards the Asymmetric Allylation of the Formyl and Imino Groups

via Strained Silane Lewis Acids

Alexander Buitrago Santanilla

Submitted in partial fulfillment of the

Requirements for the degree

of Doctor of Philosophy

In the Graduate School of Arts and Sciences

COLUMBIA UNIVERSITY

2013

ABSTRACT

New Approaches towards the Asymmetric Allylation of the Formyl and Imino Groups via

Strained Silane Lewis Acids

Alexander Buitrago Santanilla

This dissertation presents new approaches towards the asymmetric allylation of the imino and formyl functionalities by using strained silanes as Lewis acids. Here in the Laboratory of Professor James L. Leighton, chiral homoallylic alcohols and amines are considered privileged products given their important role as building blocks in natural product synthesis. The new approaches reported herein are focused on expanding the scope of imine allylation reactions and gaining full synthetic utility of the corresponding homoallylic amine products by means of economic and user-friendly protocols. In addition, the discovery of a novel catalytic and mild approach to the asymmetric allylation of aldehydes will be the focus of discussion at the end of this works. Chapter 1 will give a brief introduction about general concepts in asymmetric allylation of aldehydes and imines as well as in applications of strained silane Lewis acids in these reactions. Chapter 2 will discuss the development of a novel asymmetric allylation method for *N*-heteroaryl hydrazones and the *N*-heteroaryl cleavage from the product to unmask the corresponding free amines. Chapter 3 will carry on these studies into different imine activating groups in search for a more general and user-friendly approach towards both allylation and cleavage protocols. Finally, Chapter 3 will discuss the development of a new methodology in which chiral bismuth (III) complexes can catalyze the asymmetric allylation of aldehydes with achiral strained allylsilanes.

Table of Contents

3. Chapter 3 - Asymmetric Allylation of Aminomethylnaphthol-derived Imines

4. Chapter 4 - Bi(OTf)$_3$ – PyBox Catalyzed Asymmetric Allylation of Aldehydes via Strained Silanes

List of Figures

Chapter 4

List of Schemes

Chapter 1

Chapter 3

Chapter 4

List of Tables

Acknowledgements

As I finally reach this section of my dissertation, a million or perhaps more people come to my mind, just making me realize how much I have to thank for. Whether it was love, company, support, help, friendship, a laugh, a tear, a hug, a kiss, or simply a hand shake, many people have inspired me to go on with my dreams and goals, regardless of how unreachable they seem to be.

I would like to start by thanking my fellow graduate students. We all came here for the same purpose, and we all have given up a lot for science. Without all of you, walking in the hallways, riding the elevator, getting a tea and a cookie, going to happy hour, or just going to lab would not be the same. I do know that sometimes chemists do not get along, but that is just simply understandable since we all have the same girlfriend: chemistry! I also want to thank our Faculty, especially those who talk to the students and share their knowledge and experience as mentors. I must confess I can be intimidated by some of you, but that is just because I really look up to you. Also, many thanks to Dr.'s Decatur, Itagaki, and Avila: research would be impossible without your help.

I have some special thanks reserved for the women who have driven me crazy during these last years: Anđela Šarić, Dr. Sharon Lee, and the greatest of all Dr. Heike Schönherr. I would certainly not have learned several life lessons without all the drama. I love you all for the wonderful moments and anecdotes we shared. Angie, my sweet heart, thanks for saying hi that very first day of STAT. I knew we were going to be good friends (Remember who we totally checked out as he entered?). Shaley!!! OMG! You are the

person I have seen the most every day of my life so far besides my mom. Words cannot explain how grateful I am for having he chance to be your friend. I miss our cooking nights, our after lunch nap breaks, the blasting OVO and Pink Martini from Cirque du Soleil in Lab, your bird food and its consequences, and the times we shared outside of lab. Oh yeah! No JACS ASAPS at Central Park. I guess we never did that. Thank you very much for taking me under your wing when I was a first year student. I learned lots from you. Schneiky Schoenhey, love is a small word compared to everything that you are. Thanks for being in the fun times, the bad times, and the lab times! You and Tim Cernak are my angels in this city. Thanks for being in my life, and for bringing so much joy to it. I am very proud of you two and wish you the best in life.

To my New York City friends, graduate school would not have been any fabulous without you in my life. I am sorry for flaking most Saturday afternoons whenever a great brunch or afternoon at the park awaited. Alex Andrade, you have been my sunshine all these years, and I love you for your warmth and great friendship. Thanks for all the fun times and courage you gave me to make it to the end. Bri Bri, Esteban, Willermina, Selena, Alexis, Constantine, Ricky, Bobby Christina, Kawohi, Christian, Amalia, Ellie Kardouz: many thanks for making me live such great moments.

To my friends in Los Angeles and Colombia: Thank you all for the support and the motivation. Mi Julissa divina, mi angel. JuanPa, Walter, Sebastian, Daniel, Pao, Jesus, Ivan, Johnathan, Carlitos, Juanito, Henry, Luis, Orlando, Liliana. Mis primas, mis primos, mis tios y tias: A todos mil gracias! In France: Ashley Megrelis thanks for your inspiration!

A Dios, mi Madre, y Familia. . .

CHAPTER 1

Strained Silanes in the Allylation of the Carbonyl and Imino Groups

1.1. Introduction

It is an unquestionable reality that the literature is flooded with the concept of asymmetric allylation. A simple Scifinder® search for those two simple words yields 1,920 references, which comes as no surprise since the corresponding homoallylic alcohols or amines derived from asymmetric allylation are perhaps among the most valuable and versatile chiral building blocks in natural product synthesis[1]. Throughout the years, several stoichiometric and catalytic approaches to access these types of products have demonstrated high levels of creativity from the researchers involved in their development[2]. One of the most exploited approaches to these products is the asymmetric metal-allyl fragment addition to aldehydes and imines, which many researchers have studied in great detail in terms of substrate and reagent control.

The asymmetric addition of metal-allyl fragments to carbonyl and imino groups has been mechanistically categorized in three major types:[3] Type I, II, and III (Scheme 1-1). We will use aldehydes for simplicity to portray examples of those categories. Type I allylation invokes a closed chair-like six-membered transition state, in which the metal or metalloid serves a dual function: acting as a Lewis acid to activate the aldehyde and transferring the allyl fragment. This highly organized transition state renders the allyl transfer diastereospecific, in which the (*E*)-allyl fragment gives the *anti*-product, and the (*Z*)-allyl fragment gives the *syn*-product. Type II allylation invokes the use of nucleophilic metal-

allyl fragments, in which the metal is not Lewis acidic. Thus, an external Lewis acid is required to activate the aldehyde as well as a promoting nucleophile to attack the silicon. The major consequence of this requirement is that the reaction proceeds via an open transition state, in which the *syn*-product is the most favorable outcome as it bypasses more severe *gauche* interactions in the transition state. Finally, Type III allylation invokes the use of a Lewis acidic metal-allyl fragment in rapid isomerization to the *E* isomer regardless of the initial *E/Z* content. The reaction occurs via a closed transition state like in Type I, resulting in the *anti*-diastereomer as the major product.

Scheme 1-1: Types of Allylation Reactions
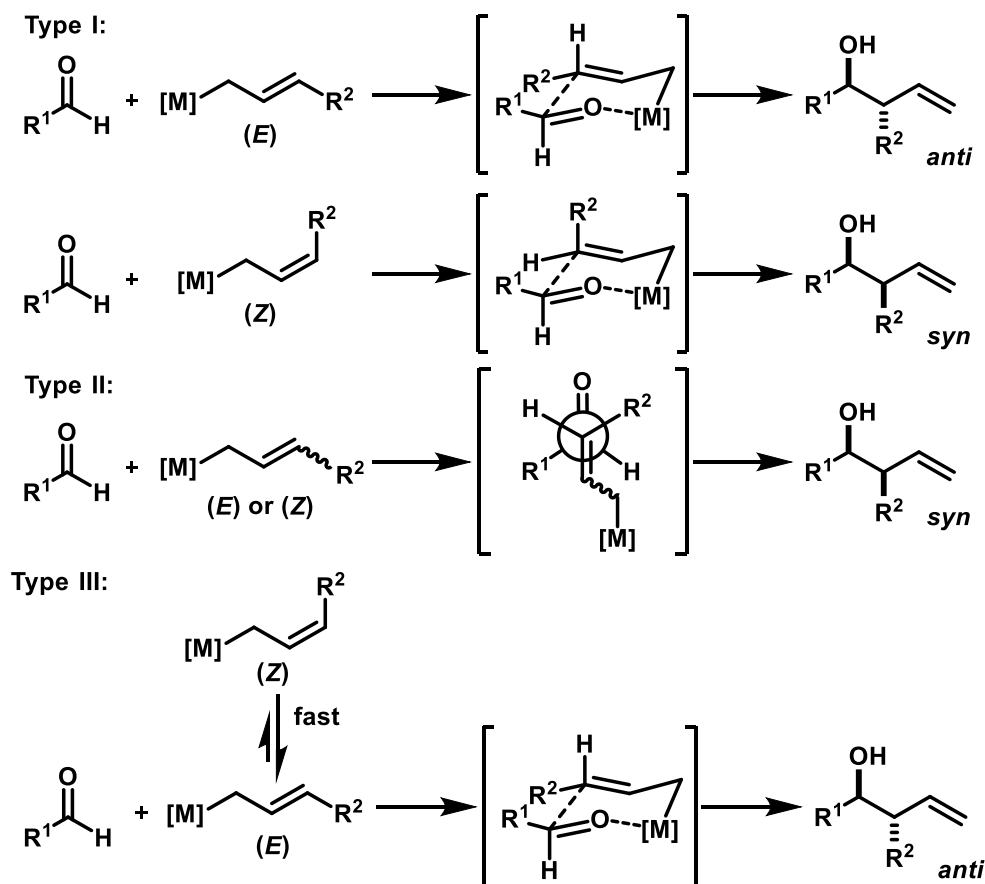
1.1.1. Asymmetric Allylation of Aldehydes

From the scheme above, it becomes clear that there are several advantages and limitations within each allylation type. For instance, in Type I, while one can access each product diastereomer, it is required to separately synthesize the (*E*) and (*Z*) reagents which can turn out to be cumbersome in certain cases. A relevant example to this type of allylation is the Brown crotylation[4] of aldehydes, in which high levels of enantio and diastereoselectivity are achieved at the expense of inconvenient reaction conditions such as rigorous timing and cryogenic monitoring for high selectivity and byproduct separation (Scheme 1-2).

Scheme 1-2: Brown Crotylation of Aldehydes
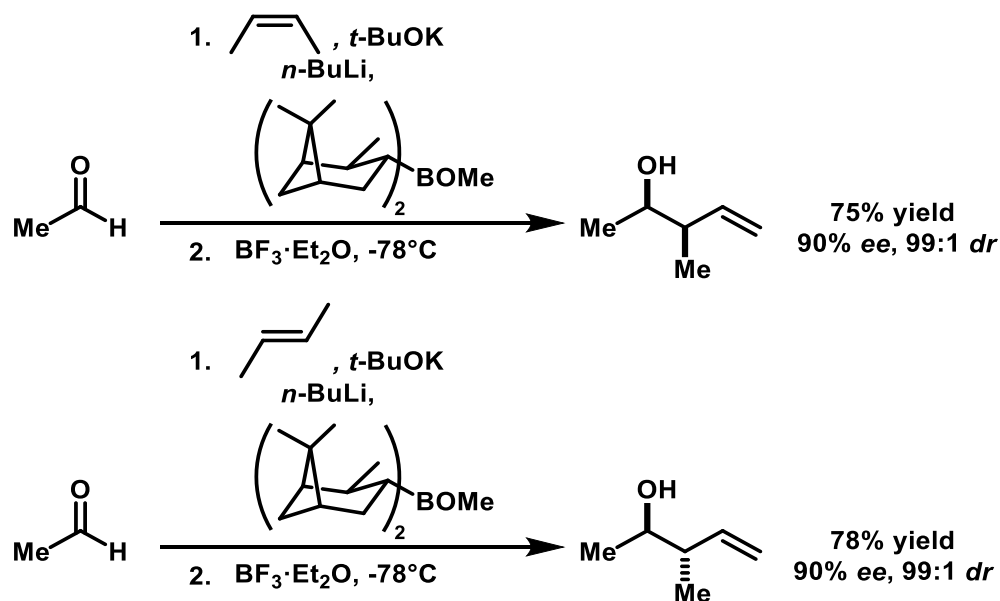
In Type II allylation, a clear disadvantage is that one can only or most exclusively access the *syn*-product. An example of Type II allylation is that of Kumada and coworkers[5] in which optically active trimethylsilanes are added to aldehydes in the presence of titanium tetrachloride as an external Lewis acid (Scheme 1-3).

Scheme 1-3: Addition of Chiral Crotyltrimethylsilanes to Aldehydes

syn-product is major

anti-product is major
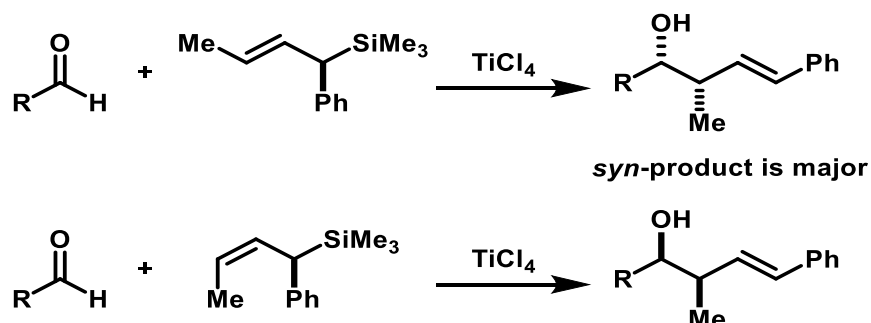
Similarly, in Type III allylations one can only or almost exclusively access the *anti*-product. A relevant example of Type III allylation is the addition of chiral crotyltitanium reagents to aldehydes developed by Hafner and coworkers[6] (Scheme 1-4). The crotyltitanium reagent is obtained from the corresponding chlorotitanium precursor and (*E*)-crotylmagnesium chloride or (*Z*)-crotylpotassium. However, fast isomerization to the (*E*)-crotyltitanium reagent accounts for the high stereospecificity for the *anti*-product given that the reaction goes through a closed transition state.

Scheme 1-4: Addition of Chiral Crotyltitanium Reagents to Aldehydes

anti-product is major
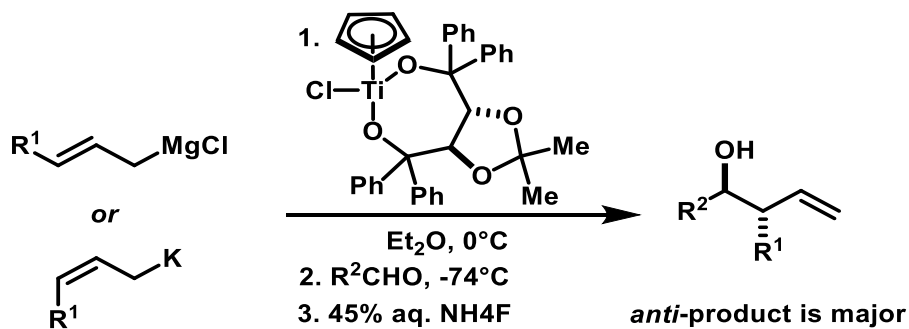
While all of the examples discussed so far correspond to stoichiometric methods, there are also reported catalytic variants for the asymmetric allylation of aldehydes[7]. One

very major discovery of this type and relevant to the contents of this thesis was that of Denmark and coworkers[8]. In this method, an achiral (*E*) or (*Z*) crotyltrichlorosilane activated by complexation with catalytic amounts of a chiral bisphosphoramide can asymmetrically crotylate aldehydes, albeit only aromatic, via the Type I mechanism in good yields and enantioselectivities and excellent diastereoselectivities (Scheme 1-5).

Scheme 1-5: Denmark Catalytic Crotylation of Aldehydes
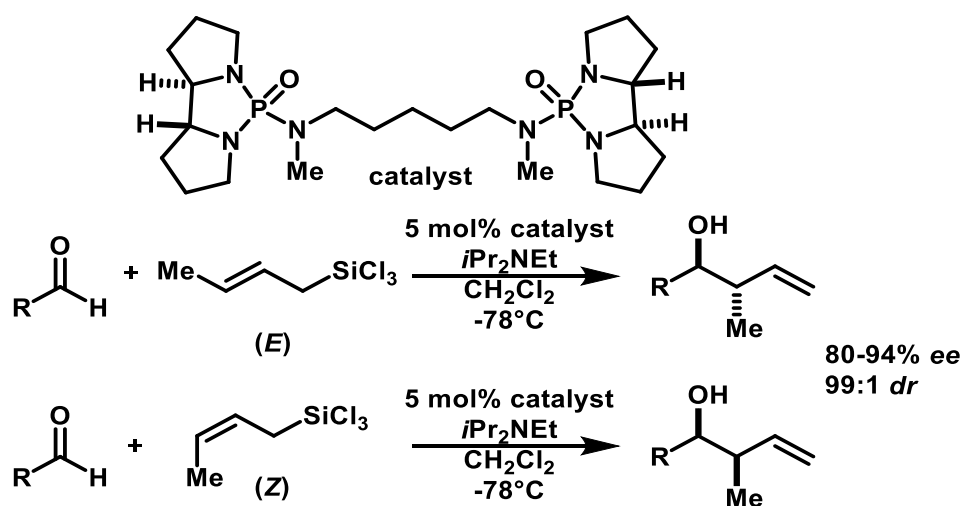
1.1.2. Asymmetric Allylation of Imines

Besides aldehyde allylation, which was exemplified in all cases above, imines may also undergo allylation reactions of the same types. However, approaches to imine allylation are more diverse and complex since there is plenty of exploratory room to control reactivity and selectivity from the substrate itself by means of chiral auxiliaries or activators on the imine nitrogen or by means of chiral reagents[9]. Also, new challenges arise since not all imines are configurationally stable and may undergo *E/Z* isomerization and/or tautomerization to the corresponding enamine in the case of enolizable imines (Figure 1-1).

Figure 1-1: Challenges in Asymmetric Imine Allylation
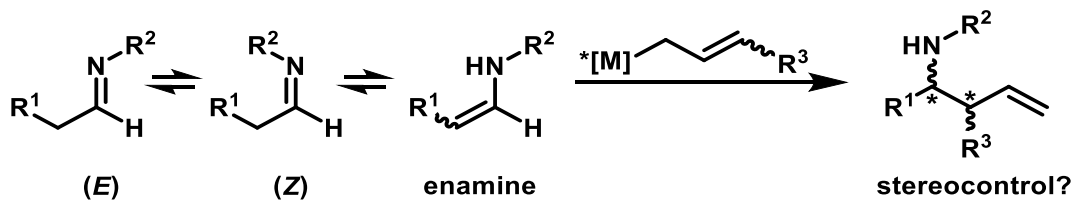
In fact, structural features of the imine itself redefine the outcome of products in Type I allylation. For instance, the lone pair *trans* to the R^1 group in an aldehyde does not exist in a typical (*E*)-imine as this position is substituted with another group R^2 (Figure 1-2). Thus, in order to involve the imine nitrogen lone pair in the closed transition state, the R^1 group will now occupy the pseuodoaxial position of the chair unless there are other conformers involved, such as a boat, or *in situ*-bound imine isomerization to the (*Z*) geometry.

Figure 1-2: Type I Allylation in Imines
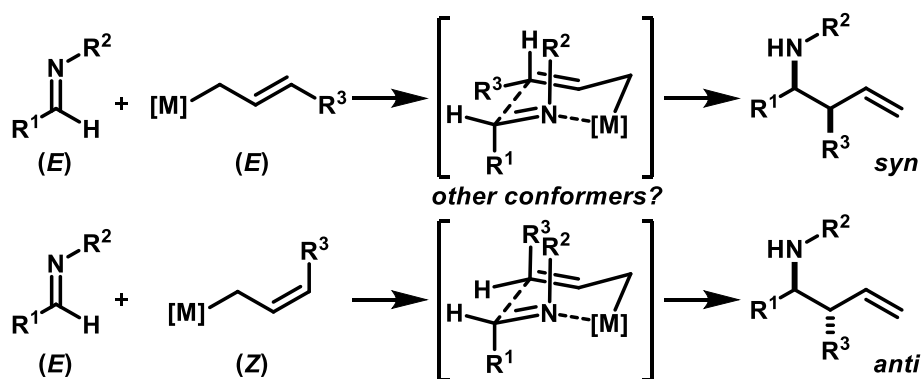
Asymmetric addition of an unsubstituted allyl group to an imine has been greatly exploited[10]. However, when it comes to addition of more complex allyl fragments to imines such as crotyl or cinnamyl groups, additional problematic issues come afloat. One major

issue is the synthesis of the required complex allyl fragments and their incorporation as part of the allyl transfer reagent. Similarly, the design, installation, and cleavage of an activating group on the imine nitrogen can be a complex if not cumbersome task, which can in the end render methods highly substrate dependent and/or disabling the relevant synthetic utility of the resulting allylation products (Figure 1-3).

Figure 1-3: Additional Challenges in Imine Asymmetric Allylation
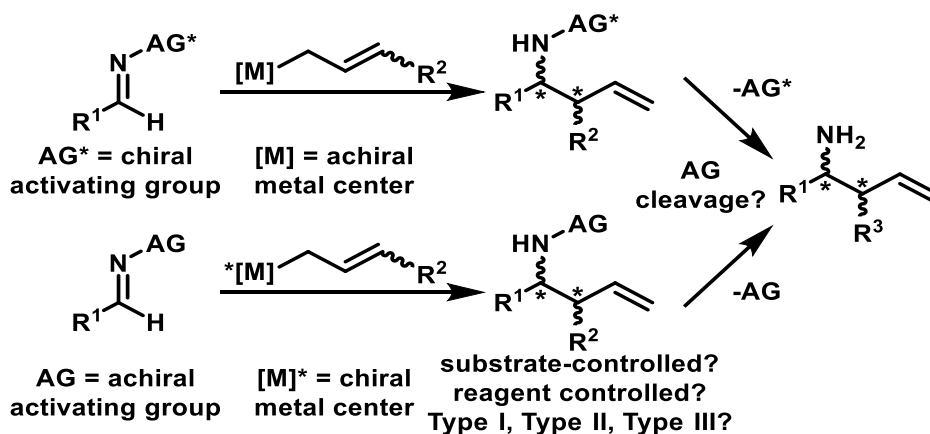
Indeed, there are only a few examples in the literature in which complex allyl fragments such as cinnamyl groups are added to imines with high enantio and diastereoselectivity[11]. The first example of truly asymmetric cinnamylation of imines was that of Sato and coworkers[12] in which a chiral *N*-(α-methylbenzyl)-derived imine **3** is subjected to an *in situ* generated cinnamyltitanium reagent to give the corresponding *syn*-cinnamylation product in good yield and excellent diastereoselectivity (Sheme 1-6).

Scheme 1-6: First Asymmetric Cinnamylation of Imines
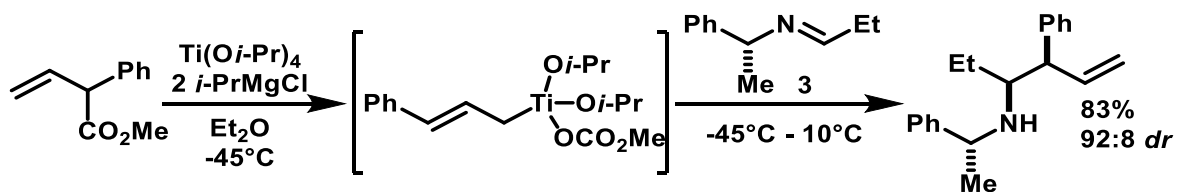
Another variant of this reaction is the addition cinnamylzinc bromide to chiral glyoxamide-derived imine **5** by Hanessian and coworkers[13] to obtain the corresponding cinnamylation product in good yield and excellent diastereoselectivity (Scheme 1-7).

Scheme 1-7: Asymmetric Glyoxamide-derived Imine Cinnamylation
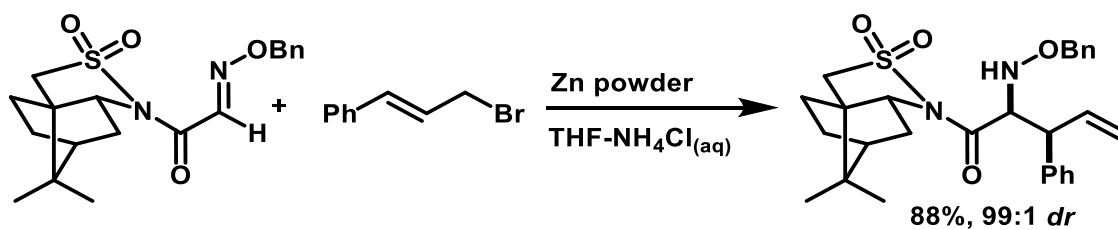
Almost a decade later from the method above, Lee and coworkers[14] reported the use of phenylglycinamide-derived imines in the asymmetric addition of cinnamylzinc bromide, obtaining moderate yields and only modest stereoselectivities (Scheme 1-8).

Scheme 1-8: Asymmetric Glycinamide-derived Imine Cinnamylation
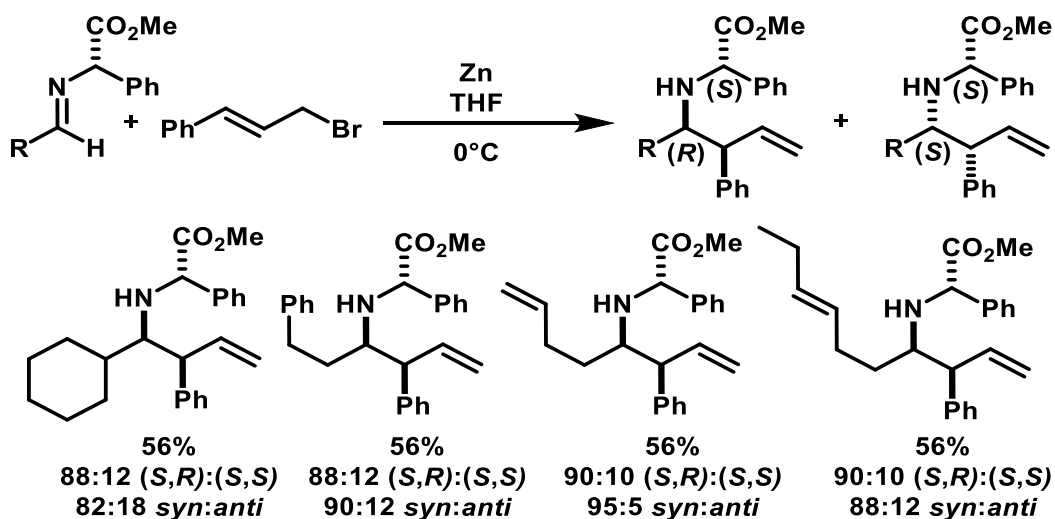
More recently, Reddy and coworkers[15] have reported the cinnamylation of chiral *N*-*tert*-butanesulfinylimines with cinnamylzinc reagents, being able to obtain the *syn* cinnamylation products in high yields and excellent diastereoselectivities (Scheme 1-9).

Scheme 1-9: Cinnamylation of Chiral *N*-*tert*-butanesulfinylimines
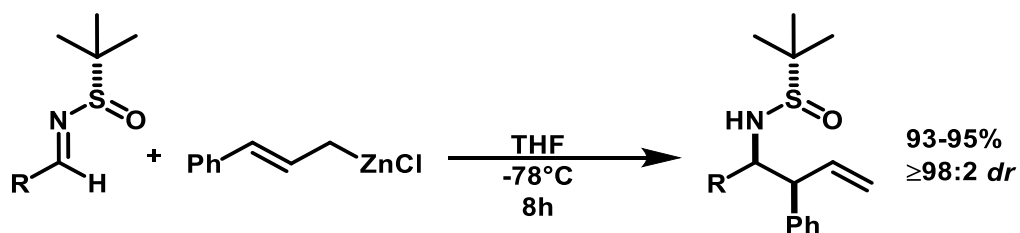
The methodologies presented above are highly substrate controlled as the activating group and chirality source have been designed to be part of the imine substrate. With the exception of the last example presented, those activating groups are not readily installed or removed. An example of reagent controlled cinnamylation of imines was earlier reported by

Nakamura and coworkers[16], in which a cinnamylzinc reagent complexed by chiral BOX ligands is able to cinnamylate cyclic imines in great yields, modest enantioselectivity, and excellent diastereoselectivity (Scheme 1-10).

Scheme 1-10: Asymmetric Cinnamylation of Cyclic Imines
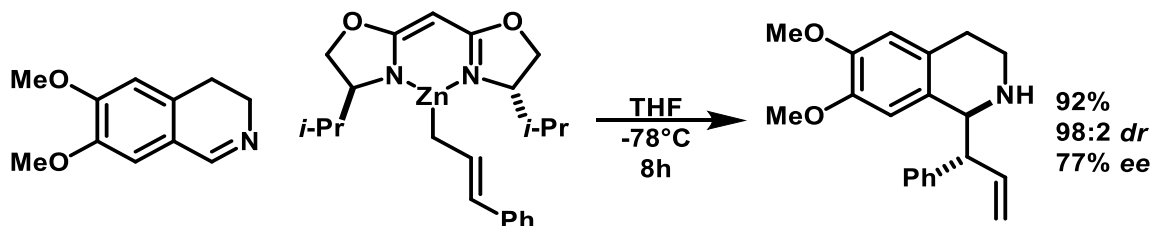
A noteworthy observation from the methods presented above is the almost exclusive access to one diastereomer, predominantly the *syn*-product. This can be attributed to the Type III nature of the cinnamyl-metal species, which seems to be rapidly isomerizing to the (*E*)-isomer regardless of the initial E/Z content, then reacting with the imine in a closed transition state to provide the observed *syn* product[17].

There have also been advances in the field of asymmetric catalysis for the allylation of imines[18]. Some of which have extended to the addition of more complex allyl fragments. One relevant and seminal example of such additions to imines is the asymmetric crotylation of *N*-acylhydrazones using crotyltrichlorosilanes with a chiral sulfoxide as the catalyst as reported by Kobayashi and coworkers[19] (Scheme 1-11). In this case, the chiral sulfoxide serves as a Lewis base to activate the crotyltrichlorosilane. The reaction proceeds via a Type I mechanism, with moderate to excellent yields and good to excellent enantio and diastereoselectivities albeit the inconvenient use of 300 mol% of the chiral sulfoxide and

cryogenic conditions. This method resembles much of the work of Denmark and coworkers presented earlier in the chapter on the catalytic crotylation of aldehydes using crotyltrichlorosilanes with chiral bisphosphoramides as catalysts.

Scheme 1-11: Chiral Sulfoxide Catalyzed Asymmetric Crotylation of Acylhydrazones
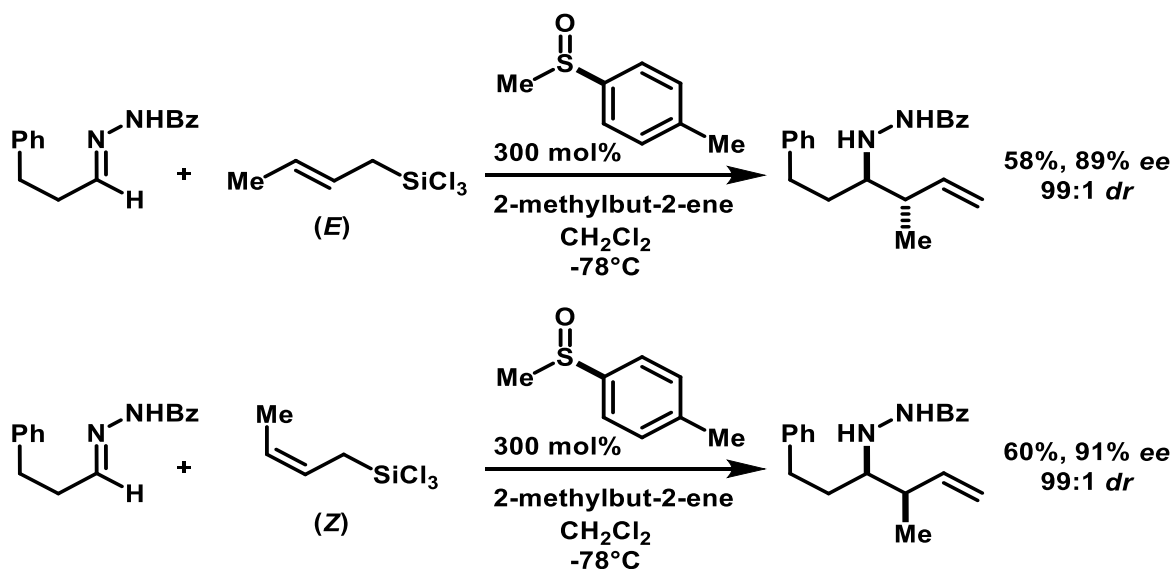
Another more recent and relevant method has been reported by Schaus and coworkers[20], in which *N*-benzoyl imines are asymmetrically crotylated using crotyl isopropyl boronates with chiral binaphthol as a catalyst (Scheme 1-12). This method has proven to be very broad in substrate scope for simple allylation reactions and very practical in experimental setup, but it suffers a major limitation in crotylation reactions as both the (*E*) and (*Z*) crotyltrichlorosilanes give exclusively the *anti*-product.

Scheme 1-12: Chiral Binaphthol Catalyzed Crotylation of *N*-benzoyl Imines
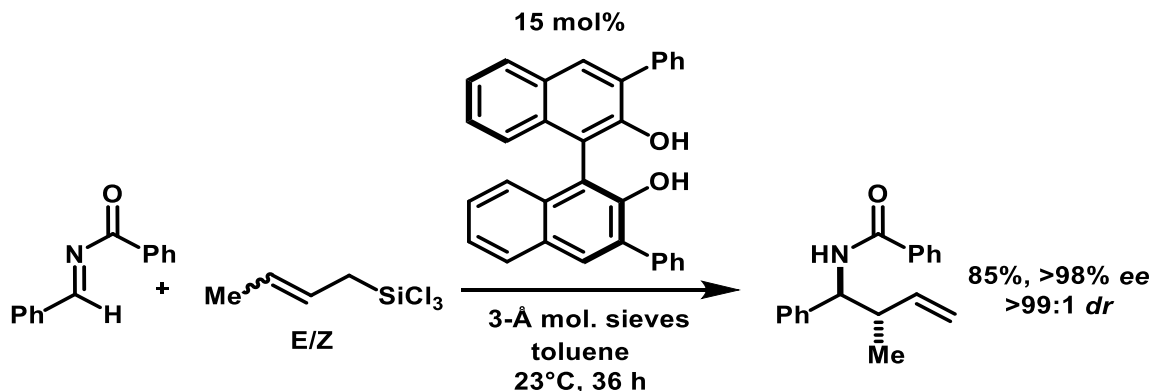
The representative examples for asymmetric aldehyde and imine allylation we provided above are among the best methods within that field[21]. One can then appreciate that there is much more work left to do in order to approach a more general and ideal asymmetric allylation protocol that allows for both simple and complex allyl transfer reactions to a broad scope of substrates, utilizing user-friendly conditions, and economic reagents. In the imine case, the activating group design is the most important consideration after the allyl transfer reaction itself as it determines the real synthetic utility of the homoallylic amine products.

With the picture of an ideal asymmetric allylation reaction in mind, the Leighton group here at Columbia University has been making progress in getting closer to that depiction. In particular, this has been by means of exploiting the idea of silicon strained-release Lewis acidity[22], which potential was overlooked in the previous years since its discovery. In synthetic organic chemistry, silicon is most widely seen in the realm of protecting groups, but the Leighton group has taken its potential far beyond that general

concept and used it in the development of several asymmetric allylation protocols, some of which will be discussed in the rest of this chapter.

1.2. Strained Allylsilicon Reagents

Allylsilicon reagents have been mostly known in the Hosomi-Sakurai-like reactions[23], in which a nucleophilic allylsilane adds to an exogenous Lewis acid-activated aldehyde (Scheme 1-13). These reactions commonly undergo Type II mechanisms, proceeding via an open transition state. The role of silicon in these reactions is to stabilize the buildup of positive charge at the β-carbon to it as the terminal olefin attacks the activated carbonyl. This stabilization is also known as the β-silicon effect[24]. A typical example of this kind of reaction was presented in section 1.1.1 where type II allylations were discussed.

Figure 1-4: The Hosomi-Sakurai Reaction
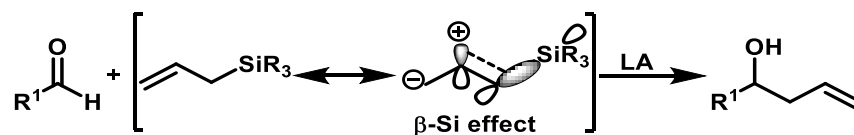
More than a decade after the discovery of the Hosomi-Sakurai reaction, Utimoto and coworkers[25] reported that allylsilacyclobutane **1.1** reacts with benzaldehyde to give the corresponding homoallylic product in 85% yield (Scheme 1-13). This was very groundbreaking at the time as trialkylsilanes typically require an exogenous Lewis acid-activated aldehyde for allyl transfer in a Type II fashion. In fact, allyldimethylphenylsilane **1.2** did not react with benzaldehyde even at higher temperature and extended reaction time.

Scheme 1-13: Allylsilacyclobutane Allylation of Benzaldehyde
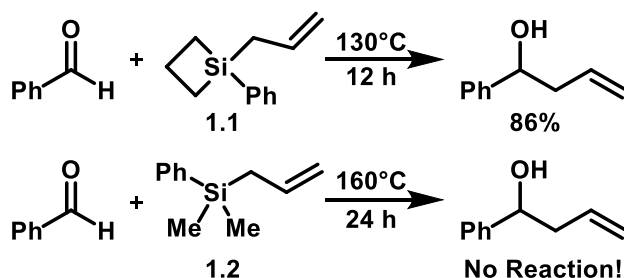
Interestingly, (*E*) and (*Z*) n-propyl analogues of silane **1.1** reacted with benzaldehyde to give highly diastereoselective *anti* and *syn* products, respectively (Scheme 1-14).

Scheme 1-14: Crotylsilacyclobutane Reactions with Benzaldehyde
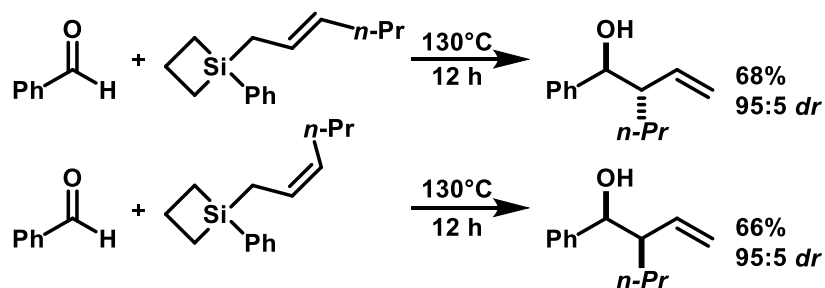
These results are typically diagnostic for a Type I allylation, implying that the silicon was also acting as a Lewis acid in order to engage the aldehyde in a closed transition state. These results were in agreement to the work of Myers[26] and Denmark[27] who reported uncatalyzed aldol additions to aldehydes from enoxysilacylobutanes. These observations were also unusual since silyl enol ethers were then known to require external Lewis acids to activate the aldehyde and promoting nucleophiles to attack the silicon in order to participate in Mukaiyama aldol reactions[28]. This newly discovered behavior of silicon acting as a Lewis acid when constrained in a small ring has since then been referred to strain release

Lewis acidity[29]. This behavior is a consequence from the compression of the C-Si-C bond angle in the silacyclobutane ring[30] which is about 78° compared to an ideal tetrahedral angle of 109°. One can imagine that such compression is due to longer Si-C bond lengths (1.894 Å) compared to typical C-C bond lengths in a cyclobutane (1.523 Å). As a result of this compression, this highly strained silacycle is very prone to accept nucleophiles or Lewis bases to adopt a trigonal bipyramidal hybridization to better accomodate the small angle[31]; thus, releasing the strain.

Not long after the observations by Utimoto, the Leighton group found that oxasilacyclopentane **1.3** also reacted with benzaldehyde under similar conditions[32] as the silacyclobutane **1.1** (Scheme 1-15). While the 95° O-Si-C angle[33] in **1.3** is larger than in **1.1**, it was still strained enough to act as a Lewis acid aided by the electron withdrawing power of the neighboring oxygen.

Scheme 1-15: Allyloxasilacyclopentane Reaction with Benzaldehyde
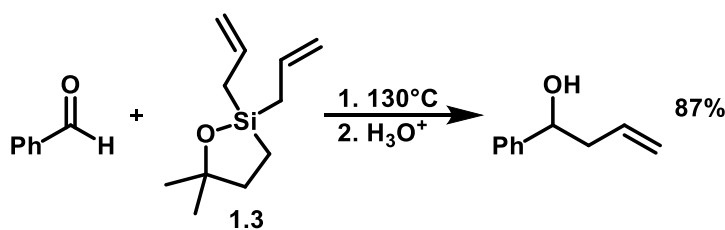
1.2.1. Chiral Strained Allylsilicon Reagents

This experimental result opened a new avenue for the discovery of potential chiral strained silane reagents such as the (*S,S*)-pseudoephedrine-derived silane[34] **1.4**. Although **1.4** exists as a 2:1 ratio of diastereomers, it reacts with several aldehydes (aromatic, alkenyl, aliphatic, branched, hindered, and α-oxyaliphatic) to give the corresponding homoallylic alcohols in good yields and modest to good enantioselectivities (Table 1-1). One if not the

best advantage of this reagent is that each enantiomer of the pseudoephedrine precursor is readily available and very inexpensive. Also, this silane can be easily synthesized and purified in large scales and stored for long periods of time in a freezer[35].

Table 1-1: Pseudoephedrine-Derived Silane Asymmetric Allylation of Aldehydes
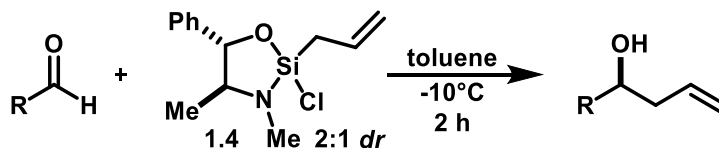
Entry	R	% Yield	% ee
1	Ph	80	81
2	PhCH=CH	59	78
3	PhCH$_2$CH$_2$	84	88
4	i-Bu	79	87
5	c-Hex	70	87
6	t-Bu	80	96
7	BnOCH$_2$	85	88
8	TBSOCH$_2$	71	89

A similar system was later designed with strained chiral diaminocyclohexane-derived silanes **1.5**. These reagents participated in highly enantio and diastereoselective Type I allylation[36] and crotylation[37] reactions with a wide range of aldehydes, proving to be even more selective than **1.4**. A representative example is given for hydrocinnamaldehyde (Scheme 1-16).

Scheme 1-16: Diamine-derived Silane Asymmetric Allylation of Aldehydes

R^1 = H,   R^2 = H; 90%, 98% ee
R^1 = Me, R^2 = H; 81%, 98% ee, >25:1 dr
R^1 = H, R^2 = Me; 83%, 97% ee, >25:1 dr
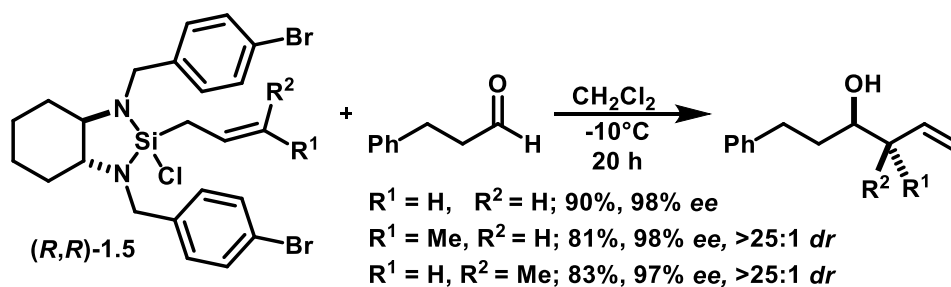
A powerful feature of the chiral diamine reagent is that it can override the inherent selectivity of chiral aldehydes in allylation reactions; thus, completely controlling the diastereochemical outcome in the product (Scheme 1-17).

Scheme 1-17: Asymmetric Allylation of Chiral Aldehydes
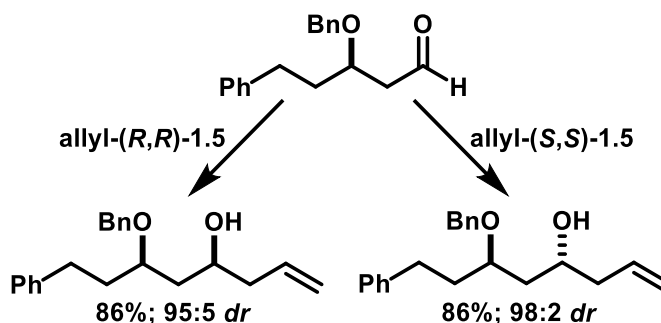
Several expansions in asymmetric allylation of the carbonyl group were later reported from the Leighton group[38], some of which will be discussed in Chapter 4, leading to the discovery of an asymmetric catalytic system for aldehydes using achiral strained silanes.

In analogy to aldehydes, pseudoephedrine silane **1.4** was found to allylate aldehyde[39] and ketone-derived[40] *N*-acylhydrazones in a highly enantioselective manner (Scheme 1-18).

Scheme 1-18: Enantioselective Allylation of *N*-acylhydrazones
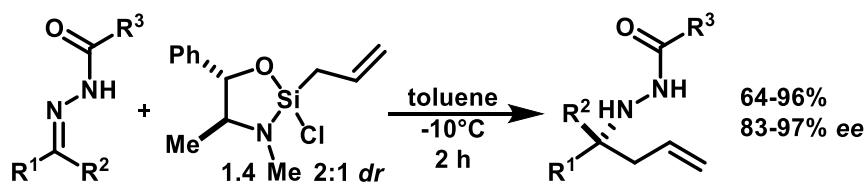
However, there is an important structural requirement for the imine that must be met in order to successfully participate in enantioselective allylation reactions with the Leighton

silanes. That major requirement is that the imine must bear a protic nucleophile, which has the crucial role of binding to the silane to displace the chloride. This occurs with concomitant generation of HCl, which protonates the pseudoephedrine backbone and provides a positive charge adjacent to the silicon; thus, further enhancing its Lewis acidity. In fact, when benzoyl hydrazone **1.6** is mixed with equimolar amounts of silane **1.6**, a single complex **1.7** can be isolated, and its crystal structure clearly depicts the product of this process[41] (Scheme 1-19). Additionally, it was observed that the imine had isomerized from (*E*) to (*Z*), which will play an important role later in our discussions about the diastereoselective outcome of crotylation and cinnamylation reactions. As further support to these findings, no reaction was observed when the chloride in the silane was replaced by methoxy or when the N-H proton in the hydrazone was replaced by methyl. The former observation due to the fact that methoxy is a lousy leaving group, so it does not get displaced, and even if it did, the resulting methanol would not protonate the nitrogen in the pseudoephedrine backbone. The latter observation is attributed to the lack of an available proton to acidify the silane backbone.

Scheme 1-19: Silane Hydrazone Complexation and X-Ray Characterization
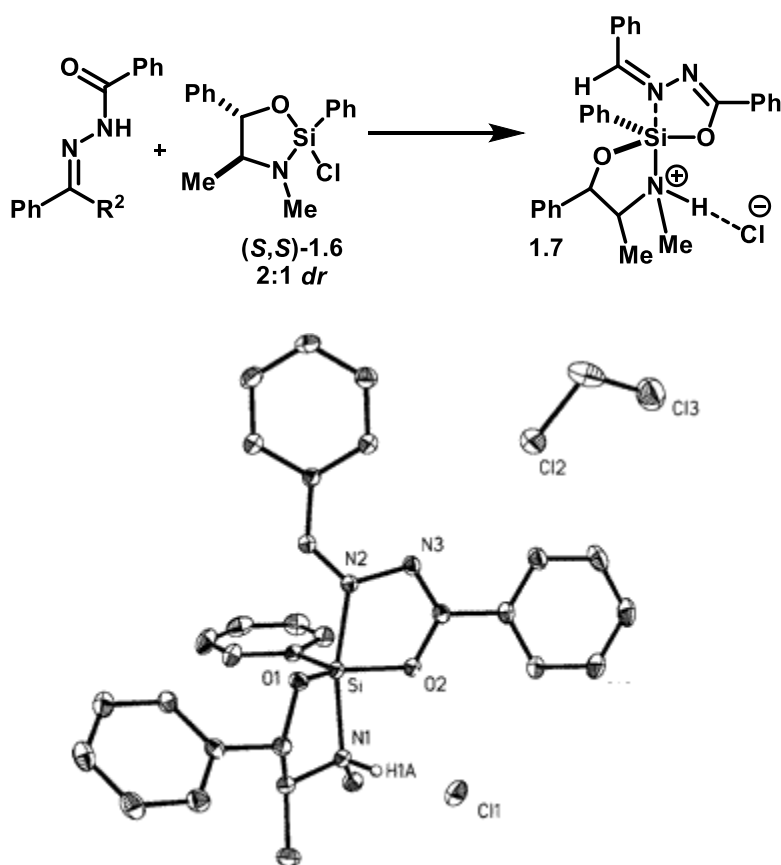
Unfortunately, the acyl hydrazones did not perform well in crotylation reactions[42] and the cleavage of the hydrazide products with samarium iodide to give the free amine was not ideal in terms of practicality and scalability. Since then, the Leighton group has begun a search for an ideal imine activating group that meets the requirements described above in an effort to broaden the scope of allylation reactions. This ideal activating group must not only facilitate the reaction, but also must be readily cleavable from the products in an efficient, orthogonal, and user-friendly manner so that the synthetic utility of the homoallylic amine products can be fully exploited. This will be the focus of the next two chapters.

1.3. References

1. See Following:

a) Denmark, S. E.; Almstead, N. G. In *Modern Carbonyl Chemistry*; Wiley-VCH Verlag GmbH, 2007; Chapter 10.

b) Chemler, S. R.; Roush, W. R. In *Modern Carbonyl Chemistry*; Wiley-VCH Verlag GmbH, 2007; Chapter 11.

c) Ding, H.; Friestad, G. K. *Synthesis* **2005**, 2815–2829.

d) Friestad, G. K.; Mathies, A. K. *Tetrahedron* **2007**, *63*, 2541–2569.

2. Santanilla A.B; Leighton, J.L. In *Science of Synthesis: Stereoselective synthesis. - 2. Stereoselective reactions of carbonyl and imino groups / vol. ed.: G. A. Molander* ; Georg Thieme, 2011; Chapter 2.8

3. Denmark, S. E.; Weber, E. J. *Helvetica Chimica Acta* **1983**, *66*, 1655–1660.

4. See Following:

a) Brown, H. C.; Jadhav, P. K. *Journal of the American Chemical Society* **1983**, *105*, 2092–2093.

b) Jadhav, P. K.; Bhat, K. S.; Perumal, P. T.; Brown, H. C. *Journal of Organic Chemistry* **1986**, *51*, 432–439.

c) Brown, H. C.; Bhat, K. S. *Journal of the American Chemical Society* **1986**, *108*, 5919–5923.

5. Hayashi, T.; Konishi, M.; Ito, H.; Kumada, M. *Journal of the American Chemical Society* **1982**, *104*, 4962–4963.

6. Hafner, A.; Duthaler, R. O.; Marti, R.; Rihs, G.; Rothe-Streit, P.; Schwarzenbach, F. *Journal of the American Chemical Society* **1992**, *114*, 2321–2336.

7. See references:

a) Yus, M.; González-Gómez, J. C.; Foubelo, F. *Chemical Reviews* **2011**, *111*, 7774–7854.

b) Denmark, S. E.; Fu, J. *Chemical Reviews* **2003**, *103*, 2763–2794.

c) Naodovic, M.; Yamamoto, H. *Chemical Reviews* **2008**, *108*, 3132–3148.

d) Mohr, J. T.; Stoltz, B. M. *Chemistry--An Asian Journal* **2007**, *2*, 1476–1491.

e) Yamamoto, H.; Wadamoto, M. *Chemistry--An Asian Journal* **2007**, *2*, 692–698.

f) A. Yanagisawa in *Comprehensive Asymmetric Catalysis, Vol. II* (Eds.: E. N. Jacobsen, A. Pfaltz, H. Yamamoto), Springer, Heidelberg, 1999, chap. 27.

8. Denmark, S. E.; Fu, J. *Journal of the American Chemical Society* **2001**, *123*, 9488–9489.

9. Yus, M.; González-Gómez, J. C.; Foubelo, F. *Chemical Reviews* **2013**. Article ASAP

10. See references:

a) Friestad, G. K.; Mathies, A. K. *Tetrahedron* **2007**, *63*, 2541–2569.

b) Ding, H.; Friestad, G. K. *Synthesis* **2005**, 2815–2829.

11. Yus, M.; González-Gómez, J. C.; Foubelo, F. *Chemical Reviews* **2013**. Article ASAP

12. Gao, Y.; Sato, F. *Journal of Organic Chemistry* **1995**, *60*, 8136–8137.

13. Hanessian, S.; Yang, R.-Y. *Tetrahedron Letters* **1996**, *37*, 5273–5276.

14. Lee, C.-L. K.; Ling, H. Y.; Loh, T.-P. *Journal of Organic Chemistry* **2004**, *69*, 7787–7789.

15. Reddy, L. R.; Hu, B.; Prashad, M.; Prasad, K. *Organic Letters* **2008**, *10*, 3109–3112.

16. Nakamura, M.; Hirai, A.; Nakamura, E. *Journal of the American Chemical Society* **1996**, *118*, 8489–8490.

17. Yamamoto, Y.; Maruyama, K.; Komatsu, T.; Ito, W. *Journal of the American Chemical Society* **1986**, *108*, 7778–7786.

18. See references:

a) Kobayashi, S.; Ishitani, H. *Chemical Reviews (Washington, D. C.)* **1999**, *99*, 1069–1094.

b) Friestad, G. K.; Mathies, A. K. *Tetrahedron* **2007**, *63*, 2541–2569.

c) Yus, M.; González-Gómez, J. C.; Foubelo, F. *Chemical Reviews* **2011**, *111*, 7774–7854.

19. (1) Kobayashi, S.; Ogawa, C.; Konishi, H.; Sugiura, M. *Journal of the American Chemical Society* **2003**, *125*, 6610–6611.

20. Lou, S.; Moquist, P. N.; Schaus, S. E. *Journal of the American Chemical Society* **2007**, *129*, 15398–15404.

21. Santanilla A.B; Leighton, J.L. In *Science of Synthesis: Stereoselective synthesis. - 2. Stereoselective reactions of carbonyl and imino groups / vol. ed.: G. A. Molander* ; Georg Thieme, 2011; Chapter 2.8

22. See references:

a) Westheimer, F. H. *Accounts of Chemical Research* **1968**, *1*, 70–78.

b) Perozzi, E. F.; Michalak, R. S.; Figuly, G. D.; Stevenson, W. H.; Dess, D.; Ross, M. R.; Martin, J. C. *The Journal of Organic Chemistry* **1981**, *46*, 1049–1053.

c) Denmark, S. E.; Jacobs, R. T.; Dai-Ho, G.; Wilson, S. *Organometallics* **1990**, *9*, 3015–3019.

d) Denmark, S. E.; Griedel, B. D.; Coe, D. M. *Journal of Organic Chemistry* **1993**, *58*, 988–990.

23. See references

a) White, J. M.; Clark, C. I. *Topics in Stereochemistry* **1999**, *22*, 137–200.

b) Denmark, S. E.; Fu, J. *Chemical Reviews* **2003**, *103*, 2763–2794.

24. Lambert, J. B.; Zhao, Y.; Emblidge, R. W.; Salvador, L. A.; Liu, X.; So, J.-H.; Chelius, E. C. *Accounts of Chemical Research* **1998**, *32*, 183–190.

25. Matsumoto, K.; Oshima, K.; Utimoto, K. *Journal of Organic Chemistry* **1994**, *59*, 7152–7155

26. Myers, A. G.; Kephart, S. E.; Chen, H. *Journal of the American Chemical Society* **1992**, *114*, 7922–7923.

27. See references:

a) Denmark, S. E.; Griedel, B. D.; Coe, D. M.; Schnute, M. E. *Journal of the American Chemical Society* **1994**, *116*, 7026–7043.

b) Denmark, S. E.; Griedel, B. D.; Coe, D. M. *Journal of Organic Chemistry* **1993**, *58*, 988–990.

28. See references:

a) Mukaiyama, T.; Narasaka, K.; Banno, K. *Chemistry Letters* **1973**, *2*, 1011–1014.

b) Mahrwald, R. *Chemical Reviews* **1999**, *99*, 1095–1120.

29. See references:

a) Westheimer, F. H. *Accounts of Chemical Research* **1968**, *1*, 70–78.

b) Perozzi, E. F.; Michalak, R. S.; Figuly, G. D.; Stevenson, W. H.; Dess, D.; Ross, M. R.; Martin, J. C. *The Journal of Organic Chemistry* **1981**, *46*, 1049–1053.

c) Denmark, S. E.; Jacobs, R. T.; Dai-Ho, G.; Wilson, S. *Organometallics* **1990**, *9*, 3015–3019.

d) Denmark, S. E.; Griedel, B. D.; Coe, D. M. *Journal of Organic Chemistry* **1993**, *58*, 988–990.

30. Omoto, K.; Sawada, Y.; Fujimoto, H. *Journal of the American Chemical Society* **1996**, *118*, 1750–1755.

31. Perozzi, E. F.; Michalak, R. S.; Figuly, G. D.; Stevenson, W. H.; Dess, D.; Ross, M. R.; Martin, J. C. *The Journal of Organic Chemistry* **1981**, *46*, 1049–1053.

32. Zacuto, M. J.; Leighton, J. L. *Journal of the American Chemical Society* **2000**, *122*, 8587–8588.

33. X-ray: Shaw, J. T.; Woerpel, K. A. *The Journal of Organic Chemistry* **1997**, *62*, 6706–6707.

34. Kinnaird, J. W. A.; Ng, P. Y.; Kubota, K.; Wang, X.; Leighton, J. L. *Journal of the American Chemical Society* **2002**, *124*, 7920–7921.

35. Santanilla, A. B.; Leighton, J.L. (4*S*,5*S*)-2-Allyl-2-chloro-3,4-dimethyl-5-Phenyl-1-oxa-3-aza-2-Silacyclopentane. *Encyclopedia of Reagents for Organic Synthesis* **2012**.

36. Kubota, K.; Leighton, J. L. *Angewandte Chemie (International ed. in English)* **2003**, *42*, 946–8.

37. Hackman, B. M.; Lombardi, P. J.; Leighton, J. L. *Organic letters* **2004**, *6*, 4375–7.

38. See Chapter 4

39. Berger, R.; Rabbat, P. M. A.; Leighton, J. L. *Journal of the American Chemical Society* **2003**, *125*, 9596–9597.

40. Berger, R.; Duff, K.; Leighton, J. L. *Journal of the American Chemical Society* **2004**, *126*, 5686–5687.

41. See crystal structure in the supporting information from previous reference.

42. Berger, R. The enantioselective allylation of aldehyde and ketone derived acylhydrazones using strained silacycles: A study of reactivity and mechanism, Columbia University: United States -- New York, 2004, pp. 22 – 24.

CHAPTER 2

The Asymmetric Allylation of *N*-Heteroaryl Hydrazones

2.1. Introduction

Chiral amines are innately important as they are commonly identified in biologically active natural products and pharmaceutical compounds[1]. Asymmetric nucleophilic addition to imines is perhaps the most widely used approach to make such compounds in high levels of enantioselectivity. One attractive transformation of this sort is the asymmetric allylation of imines since the corresponding products display several useful structural features such as an additional stereocenter adjacent to that of the carbinamine position and two synthetically valuable functionalities such as the terminal olefin and the amine nitrogen (Figure 2-1).

Figure 2-1:   Generic Asymmetric Allylation of Imines
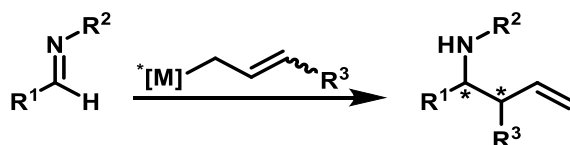
However, current methods available for the asymmetric synthesis of chiral homoallylic amines are generally limited in substrate scope (mostly effective for R^1 = aromatic). Moreover, the geometric availability/stability of the chiral metal ([M]*) allyl fragment coupling partners (*cis* vs. *trans* R^3) can be a difficult issue to deal with as the complexity of R^3 increases. In addition, chiral ligands on the metal can be expensive and/or cumbersome to access synthetically. Furthermore, some systems require the use of non-trivially made synthetic scaffolds as imine activating/directing groups (R^2), which can be

also problematic to remove orthogonally and efficiently in a user-friendly manner[2]. In the search for a novel and efficient method for asymmetric imine allylation, the Leighton group has reported the use of inexpensive chiral strained silane (*S,S*)-**2.1** as a Lewis acid for the allylation of aldehyde and ketone derived acyl hydrazones with moderate to excellent yields and good to excellent levels of enantioselectivity (Scheme 2-1)[3].

Scheme 2-1: Enantioselective Allylation of *N*-Acylhydrazones
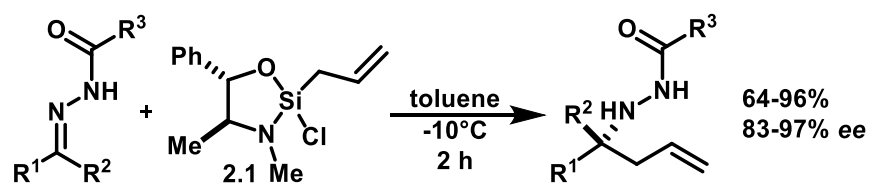
Despite the usefulness of this methodology, the substrate scope was limited to aromatic acyl hydrazones. In addition, these hydrazones did not perform well in crotylation and cinnamylation reactions. In order to address this problem, a new class of aminophenol and aminomethylphenol-derived imines was developed. These new imines were found to be suitable for the previously mentioned reactions using the corresponding Leighton reagents with moderate to good yields and excellent enantioselectivities (Scheme 2-2 and Scheme 2-3)[4].

Scheme 2-2: Asymmetric Allylation of Aminophenol-derived Imines
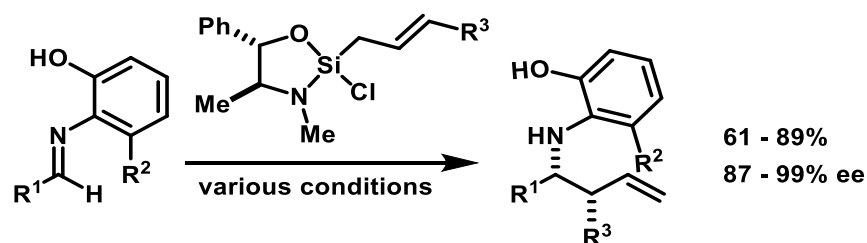
Scheme 2-3: Asymmetric Allylation of Aminomethylphenol-derived Imines
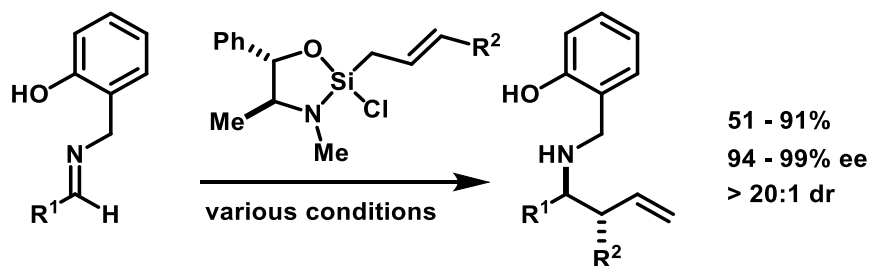
However, the problem of expanding the scope to aliphatic substrates remained in place as well as the removal of the *N*-bearing motif or activating group from the product. The cleavage protocols used for these groups in the previously mentioned methodologies were inconvenient, non-scalable, and in cases non-orthogonal since reagents such as samarium iodide and strong oxidants must be used. With these challenges in mind, the Leighton group continued its research journey by looking for an ideal activating group that provides both reactivity with the Leighton reagents and enough lability for efficient cleavage under mild and user-friendly conditions.

2.2. *N*-Hetrocyclic Hydrazones in perspective with the Leighton Silanes

The search for an ideal activating group led to the discovery of a new class of *N*-heteroaryl hydrazones[5]. These hydrazones were envisioned to react in a similar way as the acylhydrazones did with silane **2.2** to promote allyl transfer (Scheme 2-4)[6].

Scheme 2-4: *N*-Heteroaryl Hydrazones as Protic Nucleophiles to Leighton Allyl Silanes
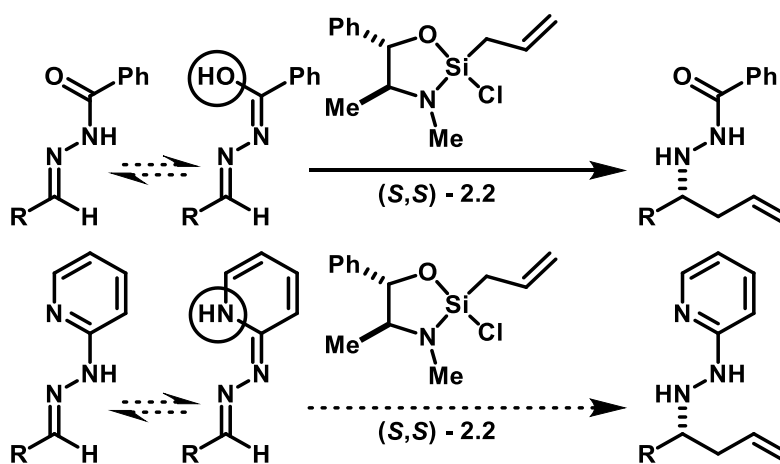
Note that the requirement of having a protic nucleophile tethered to the imine nitrogen, circled in Scheme 2-4 for emphasis, could be met by tautomerization of the corresponding hydrazone. Even though it is required that the heterocycle loses its aromaticity, this is not necessarily a problematic issue since the heterocycle already displays depressed aromatic character. This is a consequence from the electron withdrawing power of nitrogen which results in unequal sharing of the electron density in the ring and different N-C and C-C bond lengths.[7] In addition, it was envisioned that the N-N hydrazide bond in the resulting product could be cleaved by metal-catalyzed hydrogenation[8] in constrast to the acyl hydrazides which are cleaved with samarium (II) iodide.

The preparation of *N*-heteroaryl hydrazones is conveniently achieved by condensation of the desired aldehyde with an *N*-heteroaryl hydrazide. Some of the hydrazides are commercially available or inexpensively prepared from their corresponding dichloroheteroarene precursor[9] (Scheme 2-5).

Scheme 2-5: A Typical Preparation of *N*-Heteroaryl Hydrazones
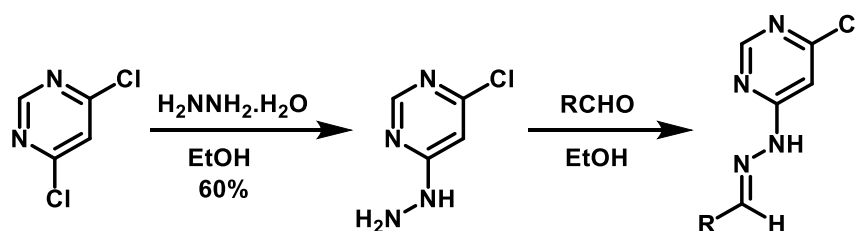
2.3. Asymmetric Allylation and Crotylation of *N*-Heterocyclic Hydrazones

After exhaustive screening of several heterocyclic motifs[10], it was found that benzoxazole-derived hydrazone **2.3** could be allylated with silane (*R,R*)-**2.2** in 64% yield and 91% ee, and cleaved under mild hydrogenolysis conditions with Pearlman's catalyst to give the corresponding free amine in 90% yield (Scheme 2-5).

Scheme 2-6: Allylation/Cleavage of Benzoxazole-derived Hydrazones*
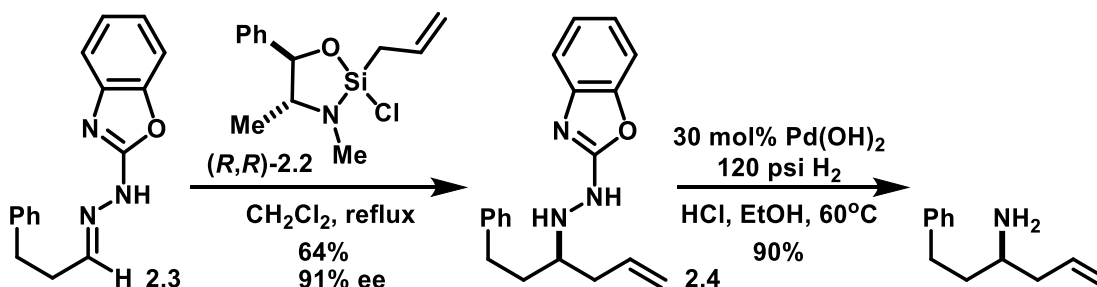
*Work by Dr. Miriam Inbar Feske

Similarly, 6-chloro-2-quinolyl-derived hydrazone **2.5** was subjected to silane (*R,R*)-**2.6** to give crotylation product **2.7** in 67% yield and 94% ee. This product was also cleaved via hydrogenolysis with Pearlman's catalyst (Scheme 2-6) to give its free amine in 98% yield. Several other aliphatic substrates besides **2.3** were also found to be effective in the crotylation reaction.[11]

Scheme 2-7: Crotylation/Cleavage of Benzoxazole-derived Hydrazones*

*With Dr. Miriam Inbar Feske
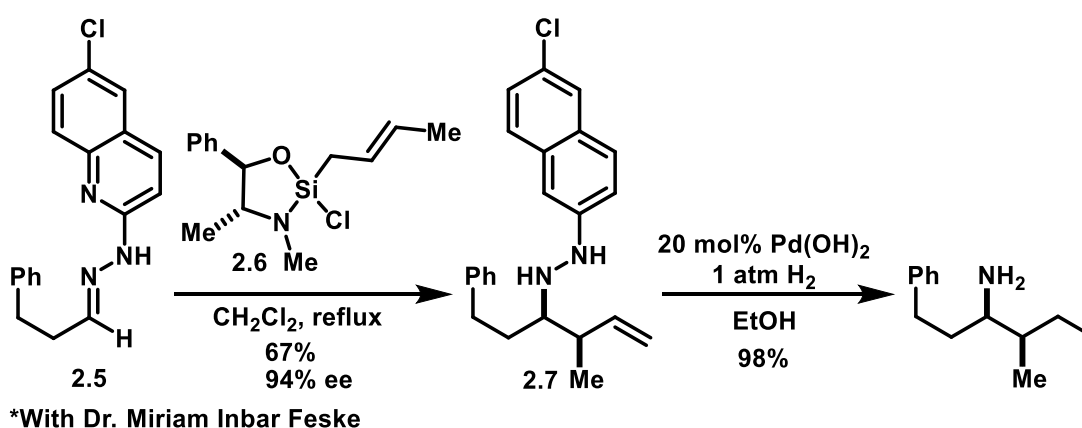
2.4. Asymmetric Cinnamylation of *N*-Heterocyclic Hydrazones

Unfortunately, none of the previously mentioned hydrazones performed well in the cinnamylation reaction with (*R,R*)-**2.8**. Thus, we attempted to screen several aryl motifs, silanes, and substrates (Figure 2-2) to fine-tune for an optimal single system for allylation, crotylation, and cinnamylaton of this class of imines (Table 2-1)

Figure 2-1: Proposed Variable Changes for Screening
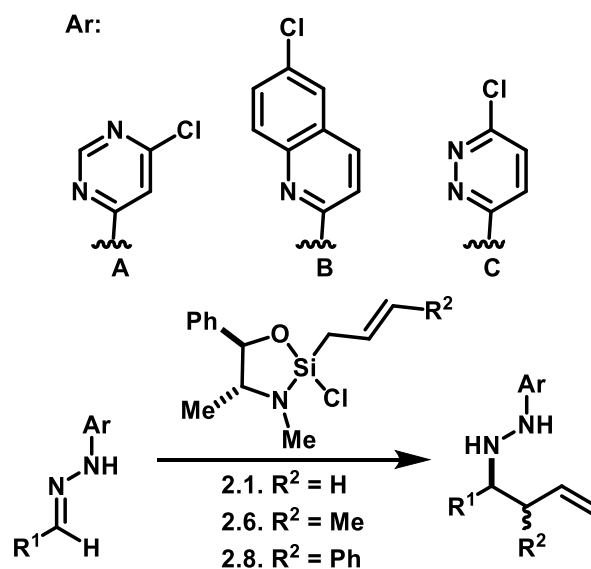
Table 2-1: Screen Results

Entry	Ar	R^1	Silane	Yield	ee	dr
1	A	$PhCH_2CH_2$	(S,S)-2.6	80%	--	1.4:1
2	A	$PhCH_2CH_2$	(S,S)-2.8	90%	27%	> 20:1
3	B	$PhCH_2CH_2$	(S,S)-2.1	56%	23%	> 20:1
4	B	$PhCH_2CH_2$	(S,S)-2.6	75%	17%	> 20:1
5	B	$PhCH_2CH_2$	(S,S)-2.8	45%	96%	> 20:1
6	B	c-Hex	(S,S)-2.8	54%	50%	> 20:1
7	B	c-HexCH$_2$	(S,S)-2.8	54%	3%	> 20:1
8	B	i-Bu	(S,S)-2.8	10%	27%	> 20:1
9	B	$PhCH_2$	(S,S)-2.8	55%	22%	> 20:1
10	C	$PhCH_2CH_2$	(S,S)-2.8	82%	85%	12:1
11	C	c-Hex	(S,S)-2.8	54%	--	2:1
12	C	Ph	(S,S)-2.8	NR	--	--

Unfortunately, the results presented in Table 2-1 clearly show that stereoselectivities

of the reactions were across the board without a particular trend. However, yields were in

moderate to good range in most cases. The pyrimidine motif for instance gave the best yields albeit with terrible stereoselectivities (Entries 1-2). The pyridazine motif showed a particular substrate dependency for its corresponding hydrocinnamaldehyde derived hydrazone in terms of selectivity, but it followed no trend in terms of yields or ee's for other substrates or silanes (Entries 3-9). While we could not unify this methodology by using a single *N*-heteroaryl motif, the most optimal result for the cinnamylation reaction with (*S,S*)-2.8 was observed for the chloropyridazyl hydrocinnamaldehyde-derived hydrazone which gave its cinnamylation product in 82% yield and 85% ee (entry 10). It seems as if the relative position of both the nitrogens and the chlorine atom in the heteroaryl motif play a crucial role for selectivity perhaps due to a stereoelectronic effect. We attempted to probe this by exchanging the chlorine atom in the quinoline series (heteroaryl B, Figure 2-2) for a methoxy group, but this dramatically affected the reactivity of the system and resulted in no reaction.

2.5. Tandem Cross-Metathesis/Cinnamylation of *N*-Heterocylic Hydrazones

We further explored the performance of chloropyridazyl-derived hydrazones in a previously established tandem cross-metathesis/cinnamylation protocol[12]. This protocol consists of generating cinnamyl-like silanes *in situ* by reacting allylsilane **2.1** with a styrene of choice and catalytic amounts of Grubbs-II catalyst in refluxing CH_2Cl_2, $CHCl_3$, or DCE. Subsequently, the hydrazone is added to the same reaction pot to proceed with the allyl transfer. One of the most attractive features of this protocol is that one can streamline the synthesis of more complex allylation reagents from simple and commercially available

starting materials in one step. This bypasses the need to design a *de novo* synthesis of the each desired allylation reagent, which in cases may be non-isolable. Thus, this protocol provides a great avenue to access a wide range of potentially useful chiral substituted homoallylic carbinamines.

In order to explore the previously mentioned protocol, we picked the hydrocinnamyl-pyridazyl-derived substrate (Table 2-1, entry 10) given that it performed best in the cinnamylation reaction with isolated silane (*S,S*)-**2.8**. In the tandem protocol; however, we found that the resulting hydrazide **2.9** was obtained in about a 2:1 ratio to its N-N bond oxidized diazine analogue **2.10** (Table 2-2). In addition, other aliphatic substrates underwent this protocol with considerably lower yields and selectivities.

Table 2-2: *N*-Heteroaryl Hydrazones in Tandem CM/Cinnamylation Reactions
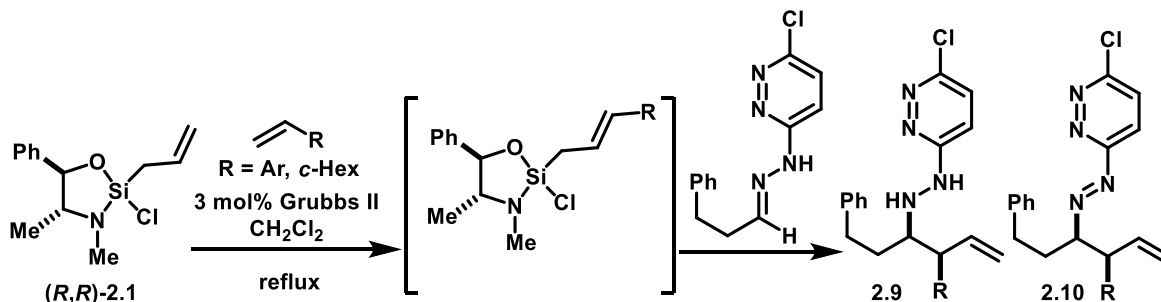
Entry	R	Yield (%)	ee (%)	2.9:2.10
1*	C$_6$H$_5$	82	85	1:0
2	C$_6$H$_5$	73	90	2:1
3	4-F-C$_6$H$_4$	44	79	1.6:1

*reaction run with isolated cinnamyl silane

While we rigorously attempted to suppress oxygen from the reaction and even added oxidant suppressants such as dimethylsulfide and triphenylphosphine, we still observed the

diazine product. Thus, we attributed the oxidation to be most likely due to ruthenium species remaining from the cross-metathesis as there is precedence that these species can catalyze N-N bond dehydrogenation[13]. We also noted that the added yields of **2.9** and **2.10** were comparable to the yield of the direct cinnamylation with (*S,S*)-**2.8** with unaltered stereoselectivities. Since it was cumbersome to isolate two different species as product, we decided to treat the entire reaction crude mixture under different oxidizing conditions to convert all of the hydrazide product to its diazine analogue (Table 2-3).

Table 2-3: Redox Conditions on Crude CM/Cinnamylation Reactions
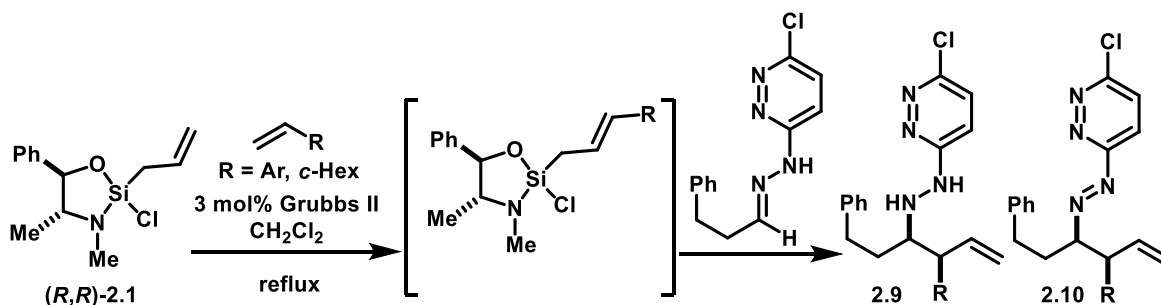
Entry	Conditions	Observations
1	3eq. Me$_2$S	mixture of 2.9 and 2.10
2	3eq. PPh$_3$	mixture of 2.9 and 2.10
3	xs. O$_2$ (g) on crude	Slow conversion to 2.10
4	H$_2$O$_2$ after w/up	Product loss, poor yield
5	2:1 CH$_2$Cl$_2$: H$_2$O$_2$ on crude	100% conv. to 2.10

We were pleased to find that upon stirring the CM/cinnamylation crude contents with a 2:1 mixture of dichloromethane and hydrogen peroxide (Table 2-3, entry 5), all of the hydrazide product was converted to its corresponding diazine. With these findings, we proceeded to explore this tandem reaction with other substituted styrenes (electron poor,

electron rich, heterocyclic, and hindered) and vinyl cyclohexane (Table 2-4). Reactions gave moderate yields and good to excellent stereoselectivities.

Table 2-4: Tandem CM/Cinnamylation of *N*-Heteroaryl Hydrazones
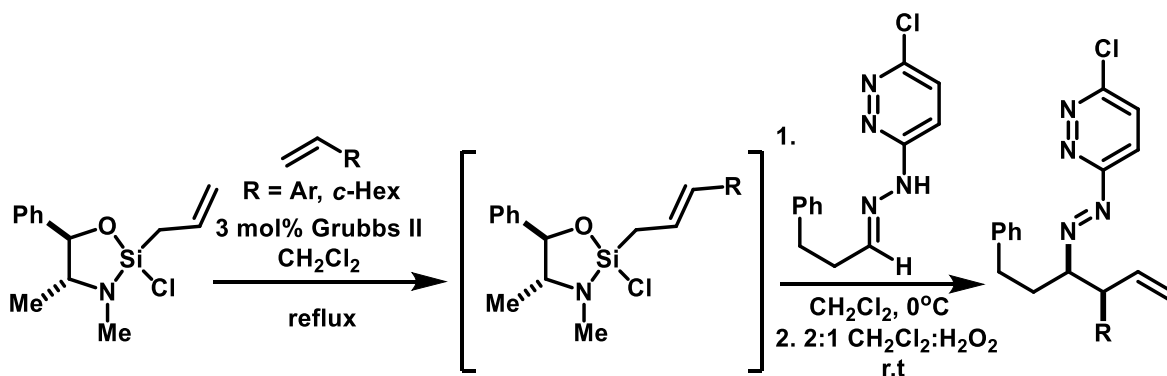
Entry	R	Yield	ee	dr
1	Ph	62%	90%	>20:1
2[a]	o-CH$_3$C$_6$H$_4$	71%	90%	>20:1
3[b]	p-CH$_3$C$_6$H$_6$	68%	86%	>20:1
4[a]	m-CF$_3$C$_6$H$_4$	62%	86%	>20:1
5	p-F-C$_6$H$_4$	66%	82%	>20:1
6[b]	c-Hex	72%	91%	5:1

[a] Reaction was run in CHCl$_3$.
[b] Imine addition/cinnamylation done at 23°C

2.6. Cleavage of the *N*-Heteroaryl Activating Group

Having established a reliable method for the tandem CM/Cinnamylation described above, we turned our attention to the cleavage of the N-N bond of the corresponding diazine products. While these diazines were susceptible to hydrogenation conditions with Pd(OH)$_2$, attempts to purify the resulting free amine were unsuccessful as we obtained instead the *N*-(4-aminopyridazyl) product **2.11**. This process is thought to happen via an S$_N$Ar reaction on

the chloropyridazyl motif, presumably with palladium serving as a Lewis acid to activate one of the nitrogens in the heterocycle (Scheme 2-8).

Scheme 2-8: Direct Cleavage of Diazine Products with Pd(OH)$_2$
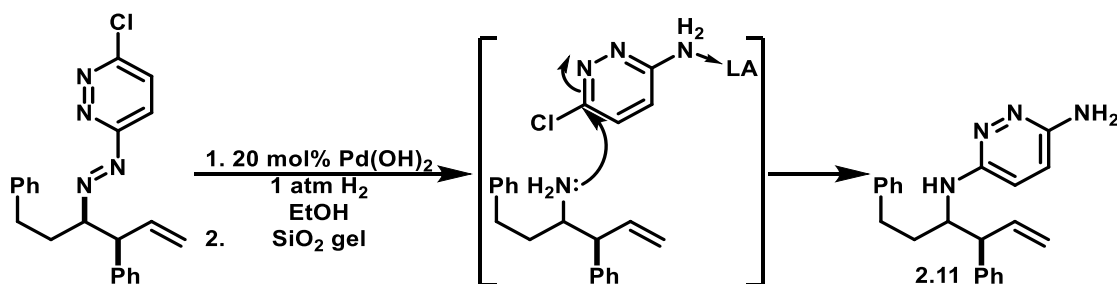
Attempts to protect the crude free amine with benzoyl chloride, acetyl chloride, di-*tert*-butyl dicarbonate, acetic anhydride, and trifluoroacetic anhydride, only afforded either the mono- and/or bis-acylated versions of **2.11**.

To circumvent this problem, we attempted to reduce and replace the chloride substituent on the heteroaryl motif since it was responsible to engage in the undesired S$_N$Ar pathway. Unfortunately, these attempts only gave the corresponding ketimine **2.12**, destroying the carbinamine stereocenter (Scheme 2-9)

Scheme 2-9: Nucleophilic Additions to Diazine Products
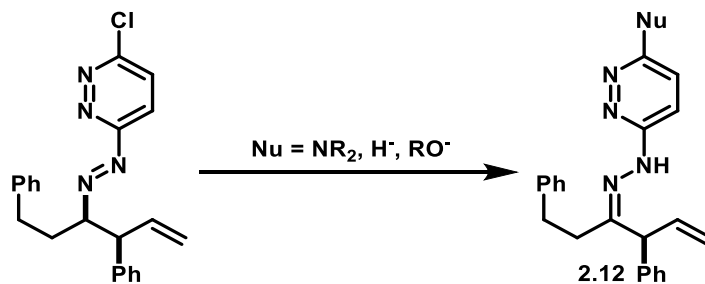
Interestingly, we found that hydrogenating the hydrazide products with Pd/C and NaOH reduces the chloride, albiet isomerizing the diazine to the ketimine **2.13** (Scheme 2-10)[14].

Scheme 2-10: Direct Reduction with Pd/C in Basic Conditions
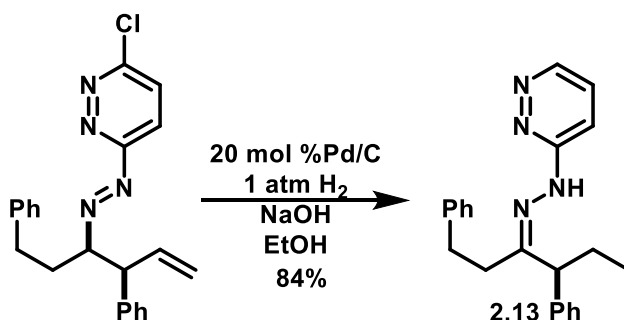
We found that sodium hydroxide was not necessary to reduce the chloride, so we removed it from the protocol above. This allowed us to carry the crude dehalogenated diazine into a second stage hydrogenation with Pearlman's catalyst to effect the desired N-N bond cleavage to obtain **2.14** in 89% yield over two steps (Scheme 2-11).

Scheme 2-11: Cleavage of the *N*-(4-chloropyridazyl) Motif
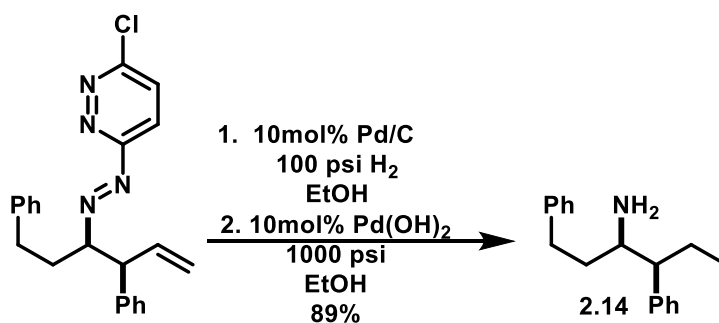
2.7. Stereochemical Proofs

The relative and absolute configuration of the compounds listed in Table 2-4 were determined by means of converging to known compounds in the literature. The enantiomer of cleaved cinnamylation product **2.14** was benzoylated to give benzamide **2.15**, which was directly compared to the analogous benzamide **2.16** obtained from the method of Loh and coworkers[15]. Absolute stereochemistry was determined by comparing the optical rotation of the two benzamide samples (Scheme 2-12).

Scheme 2-12: Stereochemical Proof for the CM/Cinnamylation Products
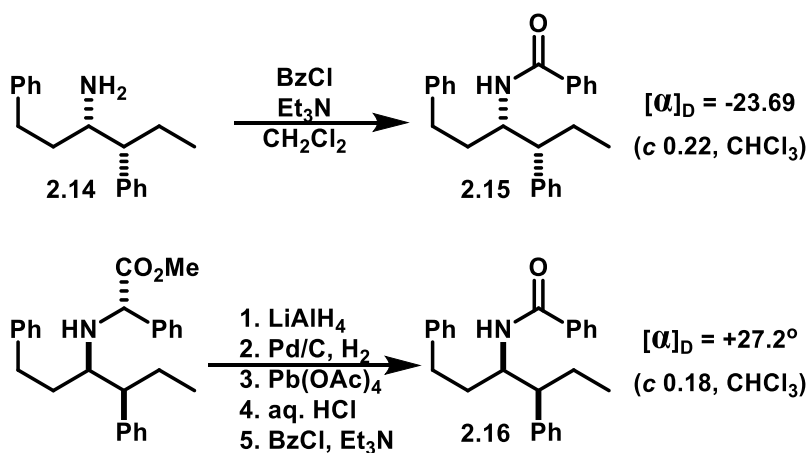
2.8. Stereochemical Rationale

Some mechanistic insights were obtained to rationalize the stereochemical outcome of the cinnamylation products. As expected, the *N*-heteroaryl motif on the hydrazone **2.17** serves as a protic nucleophile on the chlorosilane **2.18**. We can clearly observe by ^{1}H and ^{29}Si NMR the formation of a new single complex over time, presumably **2.19**. For instance, the N-Me signal from the pseudoephedrine backbone becomes a doublet, which is

indicative of N-Me protonation. This protonation can result from the hydrazone attacking the silicon, displacing the chloride and generating an equivalent of HCl which should be scavenged by the N-Me moiety[16]. Moreover, the ^{29}Si NMR spectrum shows a new single peak at -92 ppm, which corresponds to the chemical shift of a pentacoordinate silicon species[17]. This finding implies that the imine nitrogen is participating in coordination to the silicon to form the pentacoordinate species, which is consistent to the original reported crystal stucture for coodination of acyl hydrazones and silane **2.18**[18] (Scheme 2.13).

Scheme 2-13: *N*-**Heteroaryl Hydrazones and Complexation to Leighton Phenyl Silane**
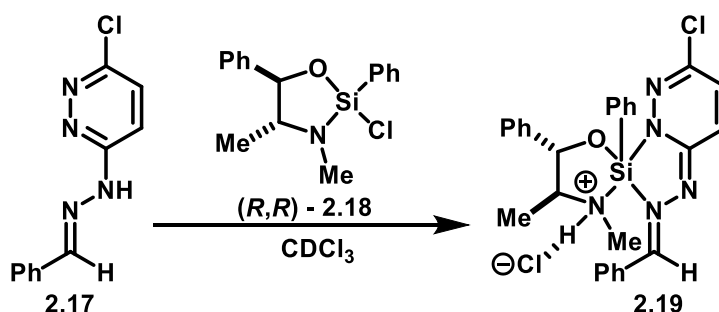
Using these clues along with the observed stereochemical outcomes of the reaction, we propose that a generic *N*-heteroaryl hydrazone **2.20** binds the chlorosilane **2.21**, providing a six-member closed transition state for the subsequent cinnamyl transfer (Scheme 2-14). While this is plausible based on the experimental stereochemical outcomes of the reaction, we cannot generalize this transition state for other substrates besides the hydrocinnamaldehyde-pyridazyl-derived hydrazones as the yields and stereoselectivities were across the board when varying substrate and/or aryl motifs. This observation is perhaps indicative of other competitive transition states which are relatively close in energy.

Scheme 2-14: Proposed Transition State for Cinnamylation of *N*-Heteroaryl
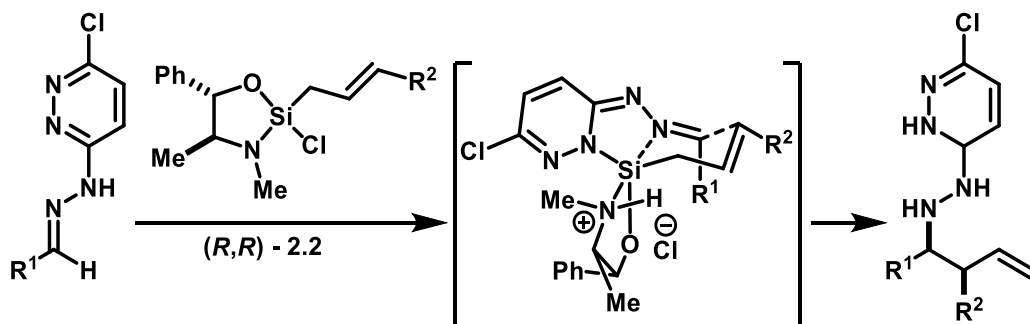
Hydrazones

2.9. Conclusions

We have developed a method for asymmetric allylation, crotylation, and cinnamylation of several aliphatic *N*-heteroaryl hydrazones. We have been able to introduce these substrates into a tandem cross-metathesis/cinnamylation/oxidation protocol which allowed for the synthesis of more diversely substituted cinnamyl products in moderate yields and good to excellent stereoselectivities. We have also demonstrated that these *N*-heteroaryl motifs on our products can be readily and efficiently cleaved by catalytic hydrogenation to unmask the corresponding free amine without the use of inefficient, expensive, or toxic multistep protocols. While these new methodologies have improved the scope and synthetic utility of the Leighton allylation, further studies should be devoted to the development of an even better activating group that is readily cleaved without the use of metals and in such a way as to preserve the synthetically valuable aryl halides and terminal olefin contained in the allylation products.

2.10. References

1. See current references on chiral amines in the Journal of Medicinal Chemistry:

a) Juknaitė, L.; Sugamata, Y.; Tokiwa, K.; Ishikawa, Y.; Takamizawa, S.; Eng, A.; Sakai, R.; Pickering, D. S.; Frydenvang, K.; Swanson, G. T.; Kastrup, J. S.; Oikawa, M. *Journal of Medicinal Chemistry* **2013**, *56*, 2283–2293.

b) Bryan, M. C.; Dillon, B.; Hamann, L. G.; Hughes, G. J.; Kopach, M. E.; Peterson, E. A.; Pourashraf, M.; Raheem, I.; Richardson, P. F.; Richter, D. T.; Sneddon, H. F. *Journal of Medicinal Chemistry* **2013**. Article just accepted.

c) Lorthiois, E.; Breitenstein, W.; Cumin, F.; Ehrhardt, C.; Francotte, E.; Jacoby, E.; Ostermann, N.; Sellner, H.; Kosaka, T.; Webb, R. L.; Rigel, D. F.; Hassiepen, U.; Richert, P.; Wagner, T.; Maibaum, J. *Journal of Medicinal Chemistry* **2013**, *56*, 2207–2217.

d) Addie, M.; Ballard, P.; Buttar, D.; Crafter, C.; Currie, G.; Davies, B. R.; Debreczeni, J.; Dry, H.; Dudley, P.; Greenwood, R.; Johnson, P. D.; Kettle, J. G.; Lane, C.; Lamont, G.; Leach, A.; Luke, R. W. A.; Morris, J.; Ogilvie, D.; Page, K.; Pass, M.; Pearson, S.; Ruston, L. *Journal of Medicinal Chemistry* **2013**, *56*, 2059–2073.

e) Mosberg, H. I.; Yeomans, L.; Harland, A. A.; Bender, A. M.; Sobczyk-Kojiro, K.; Anand, J. P.; Clark, M. J.; Jutkiewicz, E. M.; Traynor, J. R. *Journal of Medicinal Chemistry* **2013**, *56*, 2139–2149.

2. See discussion in Chapter 1, Section 1.1.2.

3. See references:

a) Berger, R.; Rabbat, P. M. A.; Leighton, J. L. *Journal of the American Chemical Society* **2003**, *125*, 9596–9597.

b) Berger, R.; Duff, K.; Leighton, J. L. *Journal of the American Chemical Society* **2004**, *126*, 5686–5687.

4. See references:

a) Rabbat, P. M. A.; Valdez, S. C.; Leighton, J. L. *Organic Letters* **2006**, *8*, 6119–6121.

b) Huber, J. D.; Leighton, J. L. *Journal of the American Chemical Society* **2007**, *129*, 14552–3.

5. These hydrazones have been only used as ligands for metal complexes:

a) Tupolova, Y. P.; Lukov, V. V; Kogan, V. A.; Popov, L. D. *Russian Journal of Coordination Chemistry* **2007**, *33*, 301–305.

b) Tang, J.; Sanchez Jose, C.; Pevec, A.; Kozlevcar, B.; Massera, C.; Roubeau, O.; Mutikainen, I.; Turpeinen, U.; Gamez, P.; Reedijk, J. *Crystal Growth & Design* **2008**, *8*, 1005–1012.

6. See discussion and X-ray structure displayed in Chapter 1, pp. 18-19.

7. Pozharskii, A. F. *Chemistry of Heterocyclic Compounds* **1985**, *21*, 717–749.

8. See references:

a) Hearn, M. J.; Chung, E. S. *Synthetic Communications* **1980**, *10*, 253–259.

b) Toti, A.; Frediani, P.; Salvini, A.; Rosi, L.; Giolli, C. *Journal of Organometallic Chemistry* **2005**, *690*, 3641–3651.

9. Cmoch, P. *Magnetic Resonance in Chemistry* **2002**, *40*, 507–516.

10. With Dr. Miriam Inbar Feske. Other motifs: oxazoles, triazoles, etc.

11. Feske, M. I.; Santanilla, A. B.; Leighton, J. L. *Organic letters* **2010**, *12*, 688–91.

12. Huber, J. D.; Perl, N. R.; Leighton, J. L. *Angewandte Chemie, International Edition* **2008**, *47*, 3037–3039.

13. Seems like Ru^{3+} species are better at catalyzing oxidation. See:

a) Field, L. D.; Li, H. L.; Dalgarno, S. J.; McIntosh, R. D. *Inorganic Chemistry* **2013**, *52*, 1570–1583.

b) Chen, W.; Wang, J. *Organometallics* **2013**, *32*, 1958–1963.

14. Rewcastle, G. W.; Gamage, S. A.; Flanagan, J. U.; Giddens, A. G.; Giddens, A. C.; Tsang, K. Y. Pyrimddinyl and 1,3,5-Triazinyl Benzimtoazole Sulfonamides and Their Use in Cancer Therapy. US Patent 831,128. September 30, 2010.

15. Kobayashi, S.; Ogawa, C.; Konishi, H.; Sugiura, M. *Journal of the American Chemical Society* **2003**, *125*, 6610–6611.

16. Berger, R.; Duff, K.; Leighton, J. L. *Journal of the American Chemical Society* **2004**, *126*, 5686–5687.

17. Marsmann, H. C. In *Encyclopedia of Magnetic Resonance*; John Wiley & Sons, Ltd, 2007.

18. See reference 16.

2.11. Experimental Section

All reactions were carried out under an atmosphere of nitrogen in flame- or oven-dried glassware with magnetic stirring unless otherwise indicated. Degassed solvents were purified by passage through an activated alumina column. Absolute ethanol was purchased from Pharmco Inc. and used without purification. 3,6-dichloropyridazine, (1*R*,2*R*)-pseudoephedrine and aldehyde reagents unless otherwise indicated were purchased from Aldrich. [1]Aldehydes were distilled before use and stored at -20 °C. ^{1}H NMR spectra were recorded on a Bruker spectrometer of the field strength indicated in the experimentals at 25°C and are reported in ppm from TMS internal standard (0.0 ppm). Data are reported as follows: (s=singlet, br s=broad singlet, d=doublet, t=triplet, q=quartet, quin=quintet, m=multiplet, dd=doublet of doublets, td= triplet of doublets; coupling constant(s) in Hz; integration; assignment). Proton decoupled ^{13}C NMR spectra were recorded on a Bruker spectrometer at the indicated field strength at 25 °C and are reported in ppm from CDCl3 internal standard (77.0 ppm). Infrared spectra were recorded on a Perkin Elmer Paragon 1000 FT-IR spectrometer. Mass spectra were recorded on a JEOL LCmate spectrometer. Optical rotations were recorded on a Jasco DIP-1000 digital polarimeter.

---

[1] Silane reagents and precursors were prepared according to previously reported procedures:
Tsuji, J.; Hara, M.; Ohno, K. *Tetrahedron* **1974**, 30, 2143-2146. (b) Furuya, N.; Sukawa, T. J. *Organomet. Chem*. **1975**, 96, C1-C3. (c) Kira, M.; Hino, T.; Sakurai, H. *Tetrahedron Lett*. **1989**, 30, 1099-1102. (d) Iseki, K.; Kuroki, Y.; Takahashi, M.; Kishimoto, S.; Kobayashi, Y. *Tetrahedron* **1997**, 53, 3513-3526. (e) Kinnaird, J. W. A.; Ng, P. Y.; Kubota, K.; Wang, X.; Leighton, J. L. *Journal of the American Chemical Society* **2002**, *124*, 7920–7921.

Typical Procedure for the preparation *N*-Heteroaryl Hydrazones. <u>Generation of the arylhydrazine</u>: To a stirring solution of the corresponding dichlorodiazine (6.71mmol) in absolute ethanol (20 mL) at room temperature, hydrazine hydrate (57.1 mmol) was added via syringe dropwise. The orginally brown solution starts yielding white precipitate in about 5 minutes. The reaction mixture was then cooled to 0°C, and the precipitate was collected via vacuum filtration and rinsed with chilled ethanol. The resulting white solid can be further azeotroped with toluene to remove any moisture and dried under high vacuum. The collected solid is the desired product and can be used without further purification.

      <u>Generation of the pyridazyl-derived hydrazone</u>: To a stirring suspension of the 6-chloro-3-hydrazinopyridazine (2.56 mmol) in absolute ethanol (12 mL) was added hydrocinnamaldehyde (2.56 mmol) dropwise at room temperature then heated to reflux for 4 h. After cooling to room temperature, the resulting precipitate was collected under vacuum filtration, dried, and used without further purification.

General procedure for the Cross-Metathesis/cinnamylation of pyridazylhydrazones: To a solution of the vinylarene or vinylalkane (2.150 mmol) in either chloroform ($CHCl_3$) or dichloromethane (CH_2Cl_2) (3 mL) is added (*R,R*)-allylsilane reagent (0.430 mmol) followed by the second generation Grubbs catalyst (11 mg, 3.0 mol% based on (*R,R*)-allylsilane). The resulting mixture is heated at reflux for 7 h (CH_2Cl_2) or 5 h ($CHCl_3$) and then cooled to room temperature. The pyridazylhydrazone (0.192 mmol) is then added. Depending on the vinylarene or vinylalkane of choice, the reaction is run at room temperature or at 0°C for 14 h and then quenched with methanol (2 mL). The resulting

mixture is concentrated down and rediluted in CH_2Cl_2 (10 mL) and hydrogen peroxide 30 wt. % solution in water (5 mL) and allowed to stir vigorously for 4 h at room temperature. The organic phase is separated. The aqueous layer is extracted with additional amounts of CH_2Cl_2 (10 mL). The combined organics are washed with brine (10 mL) and dried over magnesium sulfate, filtered, and concentrated. The residue is purified by column chromatography on silica gel to obtain the desired product.

3-chloro-6-(2-((3R,4S)-1,4-diphenylhex-5-en-3-yl)hydrazinyl)pyridazine **(2.9)**: The reaction was carried out in dichloromethane at 0^oC according to the general procedure with the exception of the oxidation step. The crude was directly purified without work up by flash chromatography in silica gel (0-40 % ethyl acetate/hexanes) to give 40 mg (55%) of the title compound. ^{1}H NMR (400 MHz, CDCl₃) δ 7.32 (t, J = 7.3 Hz, 2H, Ar-**H**), 7.28 – 7.22 (m, 4H, Ar-**H**), 7.22 – 7.07 (m, 5H, Ar-**H**), 6.95 (d, J = 7.1 Hz, 2H, Ar-**H**), 6.82 (s, 1H, ArN-**H**), 6.15 (dt, J = 17.1, 9.8 Hz, 1H, CH**CH**=CH₂), 5.32 – 5.19 (m, 2H, CH=**CH₂**), 4.14 (s, 1H, CH**NH**NHAr), 3.52 (t, J = 9.0 Hz, 1H, Ph**CH**CH=CH₂), 3.20 (dd, J = 12.0, 7.5 Hz, 1H, CH₂**CH**NH), 2.62 (tdd, *J* = 13.9, 10.4, 4.3 Hz, 2H, Ph**CH₂**), 1.82 – 1.49 (m, 2H, **CH₂**CHNH). ^{13}C NMR (400 MHz, CDCl₃) δ 162.37, 148.12, 142.01, 141.64, 139.28, 129.86, 129.29, 128.78, 128.65, 128.32, 127.30, 126.30, 117.99, 116.37, 77.75, 77.44, 77.12, 63.66, 53.61, 32.50, 31.50. IR (thin film): 3218.10 (m), 3060.29 (m), 3025.17 (m), 2921.02 (m), 1600.21 (s). HRMS (FAB+) calculated for $C_{22}H_{24}ClN_4$: 379.1689, observed: 379.1690 (M+H); $[\alpha]_D^{23}$ = -13 (c 3.00, CHCl₃).

3-chloro-6-((E)-((3R,4S)-1,4-diphenylhex-5-en-3-yl)diazenyl)pyridazine **(2.10):** The reaction was carried out in dichloromethane at 0^oC according to the general procedure. The

product was purified by flash chromatography in silica gel (0-10 % ethyl acetate/hexanes) to give 45 mg (62%) of the corresponding diazine. ^{1}H NMR (400 MHz, CDCl$_3$) δ 7.65 (d, J = 9.0 Hz, 1H, Ar-**H**), 7.52 (d, J = 9.0 Hz, 1H, Ar-**H**), 7.35 (t, J = 7.3 Hz, 2H, Ar-**H**), 7.28 – 7.18 (m, 5H, Ar-**H**), 7.18 – 7.10 (m, 1H, Ar-**H**), 7.04 (d, J = 7.0 Hz, 2H, Ar-**H**), 6.05 – 5.90 (m, 1H, CHC**H**=CH$_2$), 5.10 – 4.96 (m, 2H, CH=C**H$_2$**), 4.32 (td, J = 9.1, 3.1 Hz, 1H, C**H**N=NAr), 4.07 (t, J = 8.8 Hz, 1H, PhC**H**CH=CH$_2$), 2.50 (t, J = 7.6 Hz, 2H, PhC**H$_2$**), 2.38 – 1.93 (m, 2H, C**H$_2$**CHNNAr). ^{13}C NMR (400 MHz, CDCl$_3$) δ 164.33, 158.36, 141.44, 140.98, 139.16, 130.79, 129.30, 128.84, 128.77, 128.70, 127.44, 126.31, 119.22, 117.18, 82.57, 77.73, 77.42, 77.10, 54.41, 33.38, 32.60. IR (thin film): 3056.52 (w), 3026.62 (w), 2921.20 (m), 2850.84 (w). HRMS (FAB+) calculated for C$_{22}$H$_{22}$ClN$_4$: 377.1533, observed: 377.1541 (M+H); [α]$_D^{23}$ = -84 (c 1.00, CHCl$_3$).

3-chloro-6-((*E*)-((3*R*,4*S*)-1-phenyl-4-*o*-tolylhex-5-en-3-yl)diazenyl)pyridazine (Table 2-4, entry 2): The reaction was carried out in chloroform at 0°C according to the general procedure. The product was purified by flash chromatography in silica gel (0-10 % ethyl acetate/hexanes) to give 53 mg (71%) of the corresponding diazine. ^{1}H NMR (400 MHz, CDCl$_3$) δ 7.66 (d, J = 9.0 Hz, 1H, Ar-**H**), 7.56 (d, J = 9.0 Hz, 1H, Ar-**H**), 7.17 (dddd, J = 24.9, 23.2, 9.4, 6.8 Hz, 7H, Ar-**H**), 7.03 (d, J = 7.0 Hz, 2H, Ar-**H**), 5.87 (ddd, J = 16.7, 10.8, 8.3 Hz, 1H, CHC**H**=CH$_2$), 4.95 (dd, J = 11.4, 5.6 Hz, 2H, CH=C**H$_2$**), 4.47 – 4.31 (m, 2H, PhC**H**-C**H**N=NAr), 2.49 (t, J = 7.8 Hz, 2H, PhC**H$_2$**), 2.44 (s, 3H, Ar-C**H$_3$**), 2.49 – 1.97 (m, 2H, C**H$_2$**CHNNAr). ^{13}C NMR (400 MHz, CDCl$_3$) δ 164.30, 158.34, 141.36, 139.20, 139.03, 136.51, 131.32, 130.78, 128.88, 128.76, 127.70, 127.04, 126.93, 126.31, 119.37, 116.88, 82.48, 77.74, 77.42, 77.10, 49.22, 32.97, 32.68, 20.42. IR (thin film): 3062.01 (w) 3025.54

(w), 2921.82 (m), 1494.84 (m). HRMS (FAB+) calculated for $C_{23}H_{24}ClN_4$: 391.1689, observed: 391.1700 (M+H); $[\alpha]_D^{23} = -78$ (c 1.7, CHCl$_3$).

3-chloro-6-((*E*)-((3*R*,4*S*)-1-phenyl-4-*p*-tolylhex-5-en-3-yl)diazenyl)pyridazine (Table 2-4, entry 3): The reaction was carried out in dichloromethane at room temperature according to the general procedure. The product was purified by flash chromatography in silica gel (0-10 % ethyl acetate/hexanes) to give 51 mg (68%) of the corresponding diazine. ^{1}H NMR (400 MHz, CDCl$_3$) δ 7.64 (d, *J* = 9.0 Hz, 1H), 7.52 (d, *J* = 9.0 Hz, 1H), 7.22 (t, *J* = 7.3 Hz, 3H, Ar-**H**), 7.13 (dd, *J* = 20.1, 8.0 Hz, 5H, Ar-**H**), 7.04 (d, *J* = 7.0 Hz, 2H, Ar-**H**), 6.03 – 5.89 (m, 1H, CHC**H**=CH$_2$), 5.04 – 4.93 (m, 2H, CH=C**H$_2$**), 4.30 (td, *J* = 9.1, 3.1 Hz, 1H, C**H**N=NAr), 4.03 (t, *J* = 8.7 Hz, 1H PhC**H**CH=CH$_2$), 2.50 (t, *J* = 7.9 Hz, 2H, PhC**H$_2$**), 2.35 (s, 3H, Ar-C**H$_3$**), 2.34 - 1.95 (m, 2H, C**H$_2$**CHNNAr). ^{13}C NMR (300 MHz, CDCl$_3$) δ 164.30, 158.33, 141.50, 139.38, 137.90, 137.02, 130.80, 129.98, 128.84, 128.74, 128.51, 126.28, 119.21, 116.91, 82.69, 77.84, 77.61, 77.41, 76.99, 54.05, 33.36, 32.64, 21.45. IR (thin film): 3000.00 (m) 2924.93 (s), 2854.38 (m), 1698.77 (m). HRMS (FAB+) calculated for $C_{23}H_{24}ClN_4$: 391.1689, observed: 391.1678 (M+H); $[\alpha]_D^{23} = +121$ (c 0.50, CHCl$_3$).

3-chloro-6-((*E*)-((3*R*,4*S*)-1-phenyl-4-(3-(trifluoromethyl)phenyl)hex-5-en-3-yl)diazenyl)pyridazine (Table 2-4, entry 4): The reaction was carried out in chloroform at 0°C according to the general procedure. The product was purified by flash chromatography in silica gel (0-10 % ethyl acetate/hexanes) to give 25 mg (62%) of the corresponding diazine. ^{1}H NMR (400 MHz, CDCl$_3$) δ 7.66 (d, *J* = 9.0 Hz, 1H, Ar-**H**), 7.52 (d, *J* = 8.9 Hz, 2H, Ar-**H**), 7.42 (dd, *J* = 29.9, 5.2 Hz, 3H, Ar-**H**), 7.24 (t, *J* = 7.3 Hz, 2H, Ar-**H**), 7.17 (d, *J*

= 7.3 Hz, 1H, Ar-**H**), 7.05 (d, J = 7.0 Hz, 2H, Ar-**H**), 6.02 (ddd, J = 17.0, 10.2, 8.8 Hz, 1H, CHC**H**=CH$_2$), 5.10 (dd, J = 12.9, 11.5 Hz, 2H, CH=C**H$_2$**), 4.31 (td, J = 8.8, 3.3 Hz, 1H, C**H**N=NAr), 4.13 (t, J = 8.5 Hz, 1H, PhC**H**CH=CH$_2$), 2.61 – 2.46 (m, 2H, PhC**H$_2$**), 2.39 - 1.90 (m, 2H, C**H$_2$**CHNNAr). 13C NMR (400 MHz, CDCl$_3$) δ 164.23, 158.47, 142.10, 141.08, 137.93, 132.03, 130.81, 129.76, 128.86, 128.84, 126.47, 125.56, 124.34, 119.16, 118.27, 82.00, 77.74, 77.43, 77.11, 54.10, 33.25, 32.47. IR (thin film): 3082.61 (w) 3056.52 (w), 3026.09 (w), 2922.00 (m). HRMS (FAB+) calculated for C$_{23}$H$_{21}$ClN$_4$F$_3$: 445.1407, observed: 445.1393 (M+H); $[\alpha]_D^{23}$ = +91 (c 0.8, CHCl$_3$).

3-chloro-6-((*E*)-((3*R*,4*S*)-4-(4-fluorophenyl)-1-phenylhex-5-en-3-yl)diazenyl)pyridazine (Table 2-4, entry 5) : The reaction was carried out in dichloromethane at 0°C according to the general procedure. The product was purified by flash chromatography in silica gel (0-10 % ethyl acetate/hexanes) to give 50 mg (66%) of the corresponding diazine. ^{1}H NMR (400 MHz, CDCl$_3$) δ 7.65 (d, J = 9.0 Hz, 1H, Ar-**H**), 7.52 (d, J = 9.0 Hz, 1H, Ar-**H**), 7.23 (t, J = 7.3 Hz, 2H, Ar-**H**), 7.19 – 7.11 (m, 3H, Ar-**H**), 7.03 (t, J = 8.7 Hz, 4H, Ar-**H**), 5.95 (ddd, J = 16.9, 10.3, 8.7 Hz, 1H, CHC**H**=CH$_2$), 5.11 – 4.93 (m, 2H, CH=C**H$_2$**), 4.27 (td, J = 9.1, 3.1 Hz, 1H, C**H**N=NAr), 4.06 (t, J = 8.6 Hz, 1H, PhC**H**CH=CH$_2$), 2.65 – 2.42 (m, 2H, PhC**H$_2$**), 2.52– 1.85 (m, 2H, C**H$_2$**CHNNAr). ^{13}C NMR (300 MHz, CDCl$_3$) δ 164.25, 158.39, 141.28, 138.83, 136.69, 130.79, 130.17, 130.07, 128.81, 126.37, 119.19, 117.40, 116.26, 115.98, 82.45, 77.82, 77.40, 76.98, 53.52, 33.33, 32.55. IR (thin film): 3027.00 (w) 2921.82 (m), 2854.97 (w), 1601.99 (m), 1508.29 (s). HRMS (FAB+) calculated for C$_{22}$H$_{21}$ClN$_4$F: 395.1439, observed: 395.1435 (M+H); $[\alpha]_D^{23}$ = -18 (c 0.50, CHCl$_3$).

3-chloro-6-((*E*)-((3*R*,4*S*)-4-cyclohexyl-1-phenylhex-5-en-3-yl)diazenyl)pyridazine

(Table 2-4, entry 6): The reaction was carried out in dichloromethane at $0^{\circ}C$ according to the general procedure. The product was purified by flash chromatography in silica gel (0-10 % ethyl acetate/hexanes) to give 53 mg (72%) of the corresponding diazine in 5:1 dr (syn:anti). ^{1}H NMR (400 MHz, CDCl$_3$) δ 7.70 – 7.59 (m, 1H, Ar-**H**), 7.56 - 7.52 (m, 1H, Ar-**H**), 7.26 (d, *J* = 7.0 Hz, 2H, Ar-**H**), 7.22 – 7.06 (m, 3H, Ar-**H**), 5.85 (dt, *J* = 17.1, 10.2 Hz, 1H, CHC**H**=CH$_2$), 5.13 (ddd, *J* = 19.1, 13.7, 2.0 Hz, 2H, CH=C**H$_2$**), 4.22 (dt, *J* = 9.2, 4.8 Hz, 1H, C**H**N=NAr), 2.70 – 2.56 (m, 1H, CyC**H**CH=CH$_2$), 2.51 – 2.37 (m, 2H, PhC**H$_2$**), 2.29 - 2.15 (m, 2H, C**H$_2$**CHNNAr), 1.82 – 1.28 (m, 11H, Cy-**H**). ^{13}C NMR (300 MHz, CDCl$_3$) δ 164.40, 158.26, 141.77, 137.72, 130.78, 128.81, 126.32, 119.01, 118.20, 79.25, 77.84, 77.42, 76.99, 54.76, 38.48, 34.00, 32.74, 31.32, 30.80, 26.72, 1.40. IR (thin film): 3026.65 (w) 2924.85 (s), 2852.75 (s), 1589.77 (m). HRMS (FAB+) calculated for C$_{22}$H$_{28}$ClN$_4$: 383.2002, observed: 383.1997 (M+H); $[\alpha]_D^{23}$ = +179 (c 0.3, CHCl$_3$).

Chapter 3

Asymmetric Allylation of Aminomethylnaphthol-derived Imines

3.1 Introduction

As discussed in the previous chapter, chiral homoallylic amines can be very valuable in the pharmaceutical and synthetic world as they can be used as small chiral building blocks given that they possess two major reactive functionalities: the amine nitrogen and the terminal olefin. We have shown that developing versatile, efficient, and user-friendly methods to make this type of chiral amines has been a major research area within the Leighton group by means of using inexpensive chiral strained silane Lewis acids. We previously addressed the development of a novel method for the asymmetric allylation, crotylation, and cinnamylation of aliphatic *N*-heteroaryl hydrazones as well as a protocol to efficiently cleave the remaining heteroaryl motif from the resulting products. While this method had some attractive features, but it also had certain limitations: 1. It only works for aliphatic substrates, 2. Aryl halogens cannot be incorporated in the cleavage step as palladium is the hydrogenation catalyst, and 3. We were deleting the terminal olefin, which besides the newly acquired stereocenters is the next most valuable functionality in the product (Figure 3-1). Thus, our search for a more optimal activating group continued.

Figure 3-1: Limitations in the *N*-Heteroaryl Hydrazones Allylation/Cleavage

R = *only aliphatic*   Ar = *non-halogenated as*   *olefin deletion!*
                           incompatible with cleavage
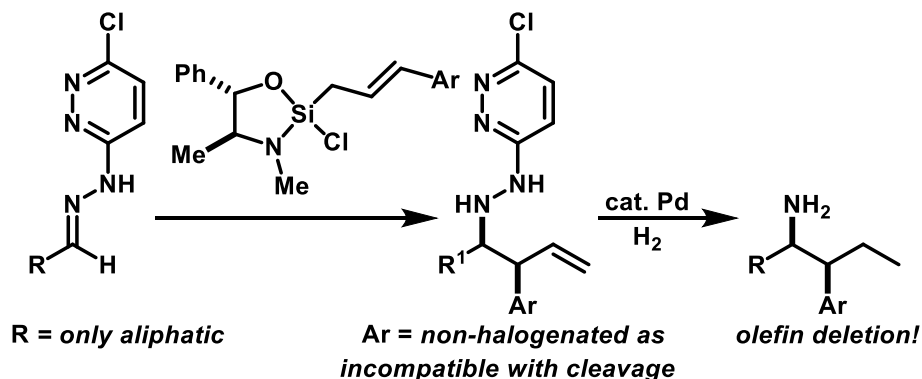
We decided to take a look back to the previously reported aminophenol and aminomethylphenol activating groups[1] (Figure 3-2), which had performed wonderfully in the asymmetric allylation of their corresponding imines with the Leighton allyl silanes. Our major goal to revisit this methodology was to fix its most important limitation, which was the lack of an efficient, mild, and functional group tolerant cleavage protocol of these activating groups from the products.

Figure 3-2: Aminophenol and Aminomethylphenol Activating Groups

3.1   **3.2**
aminophenol-derived imine   *aminomethylphenol-derived imine*
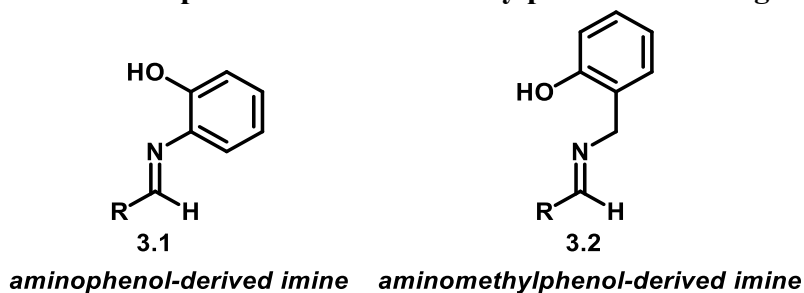
Overcoming that limitation would be crucial in order to fully access the valuable synthetic utility inherent to the resulting free homoallylic amines. A clear instance of this limitation can be seen in the work by Amgen Inc.[2] when they used the Leighton cross-metathesis/cinnamylation protocol with the *o*-aminomethylphenol-derived imines[3] to access chiral 1,2-diarylhomoallylic amines. However, in order to avoid the use of metal

hydrogenation conditions for the *N*-activating group cleavage due to the presence of aryl halides in the desired products, they had to resort to a four step sequence to obtain the free amines in low yields (Figure 3-3). Several calls from the pharmaceutical company have praised the academic and conceptual value of the allylation methodology, but it has also inquired about an efficient, mild, and orthogonal protocol for the *N*-activating group.

Figure 3-3: A Real Case of Method Limitation: The Amgen Inc. Case
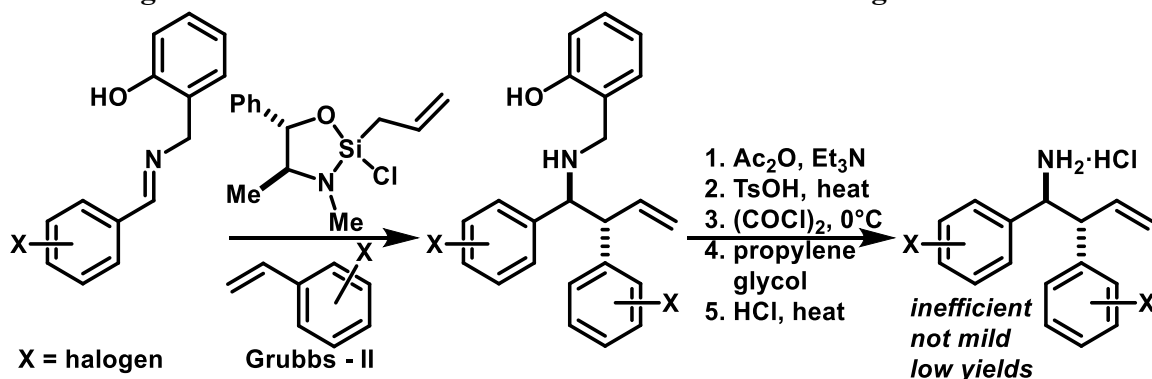
3.2. Cleavage of Aminophenol and Aminomethylphenol Activating Groups

Initial attempts to remove the aminophenol activating group by oxidative cleavage from allylation products **3.3**, prepared from imines **3.1**, only resulted in major decomposition and only trace amounts of desired product. Instead, a multistep protocol was necessary to obtain only fair yields of the boc-amine **3.4**[4]. This protocol required methylation of the phenol oxygen, reduction of the double of bond, followed by oxidation and in-situ protection of the resulting free amine (Scheme 3-1).

Scheme 3-1: Cleavage of Aminophenol-derived Homoallylic Amines
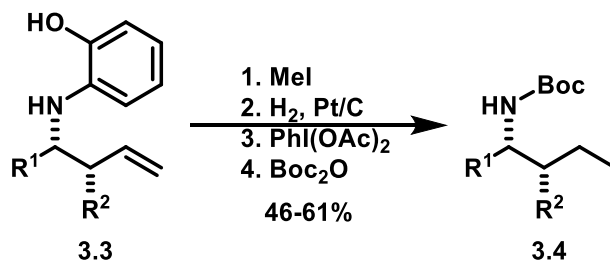
Similarly, attempts to oxidatively cleave the aminomethylphenol activating group from allylation products **3.5**, prepared from imines **3.2**, followed by action of strong acids just resulted in over oxidation of the product and overall decomposition, failing to provide any desired amine **3.6**[5] (Scheme 3-2).

Scheme 3-2: Attempted Cleavage of Aminomethylphenol-derived Homoallylic Amines
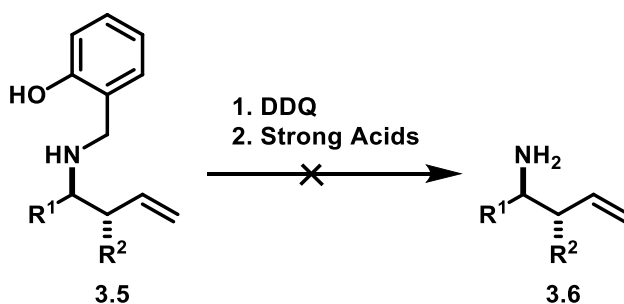
In order to ultimately cleave the aminomethylphenol activating group, it was required to hydrogenate **3.5** with Pd(OH)$_2$/C in order to obtain the free amines **3.7** in moderate yields[6] at the expense of sacrificing the synthetic utility of the olefin and excluding the use of halogenated/pseudo halogenated aromatic substrates which play an important role in pharmaceutical research (Scheme 3-3).

Scheme 3-3: Cleavage of Aminomethylphenol-derived Homoallylic Amines
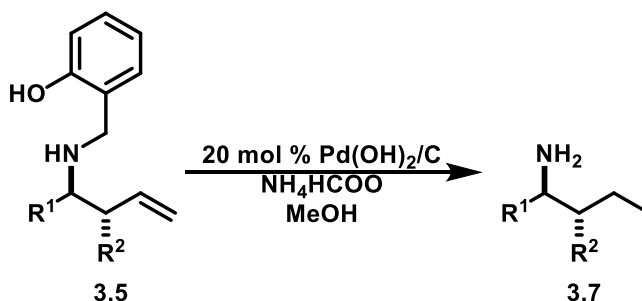
The limitations in these just mentioned methodologies left us with an ample range of variables to explore, but we took advantage of several experimental observations in order to

propose the next class of imine activating groups without having to redesign a whole new activating group from scratch. For instance, we noticed that in both attempts to oxidatively cleave the activating groups presented above, the existence of the double bond was always problematic. We believed that this olefin could potentially interact with highly reactive intermediates generated during oxidation such as *o*-quinone-methide monoimine[7] as in the case of **3.3** and *o*-quinone-methide[8] as in the case of **3.5**. Thus, we focused our efforts in the development of analogous activating groups that could generate similar lower energy intermediates under milder and more user-friendly conditions with the possibility of adding trapping species, so we could obtain the desired free amines without the need to use invasive oxidations or resorting to the use of metals to cleave these groups. This new class of activating groups will be directly related to the latter ones presented above only with minor structural changes but significantly different in reactivity: the *o*-aminomethylnaphthol and the *o*-aminonaphthol groups.

3.3. *o*-Aminomethylnaphthols as Activating Groups

Looking further at the allylation products of **3.5**, one can realize that the generation of the corresponding *o*-quinone methide **3.8** from that compound involves the disruption of aromaticity of a full benzene ring, requiring a high cost in energy. In fact, the generation of these species is well known to occur by means of high temperatures and photolysis protocols[9]. These conditions are not ideal given the presence of the olefin in the product and its suspected reactivity towards **3.8**. We could potentially lower the energy required to generate **3.8** turning the nitrogen into a better leaving group (i.e. structure **3.9**). However,

the highly reactive species **3.8** would still be an issue**.** A perhaps better alternative is to both lower the energy required to generate an analogous intermediate and attenuate that intermediate's reactivity. We envisioned that *o*-aminomethylnaphthol-derived amine **3.10** would require less energy to generate its corresponding *o*-aminomethylnaphthoquinone methide **3.11** since disruption of aromaticity would not be as prohibitive as it would still contain the resonance stabilization energy of a full benzene ring[10] (Scheme 3-4). For that same reason, reactivity of intermediate **3.11** would be expected to be lower. Thus, we could potentially utilize much milder conditions to generate **3.11** in the presence of a trapping species before it interacts with the terminal olefin of our products.

Scheme 3-4: *o*-Quinone Methide vs. *o*-Naphthoquinone Methide
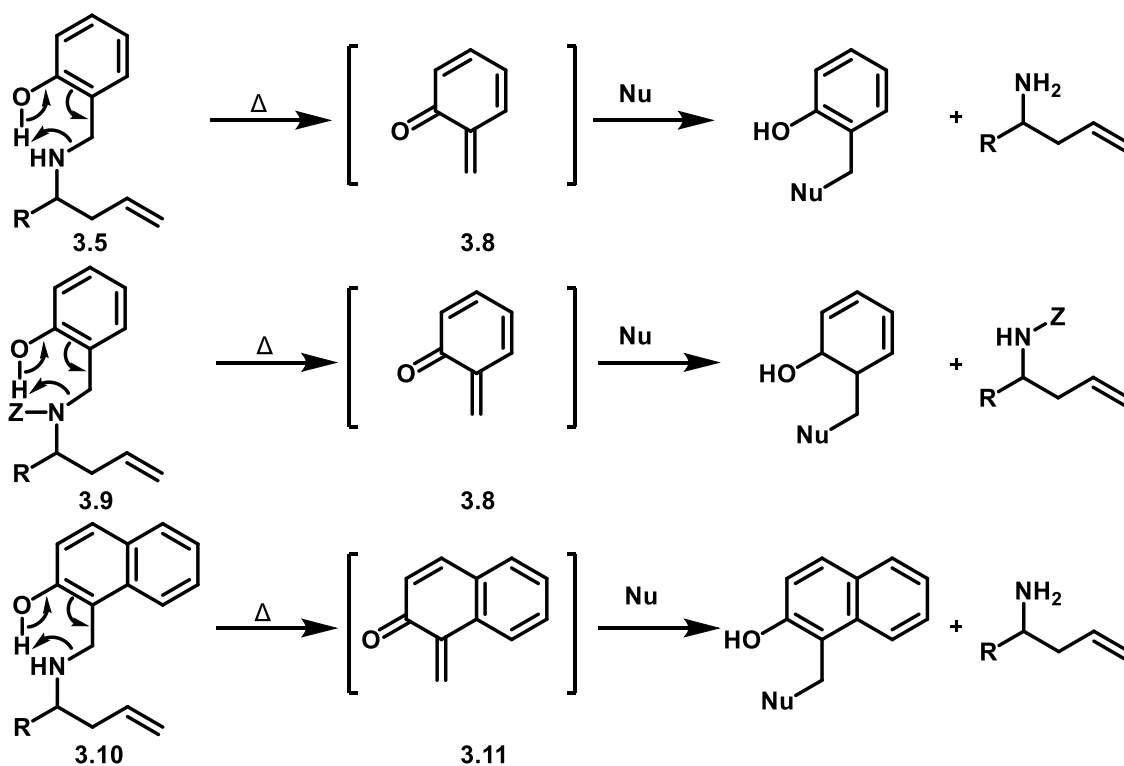
An advantageous feature of the required *o*-aminomethylnaphthol-derived imines is that they can be easily prepared from readily available and inexpensive starting materials in large scales and good yield by means of convenient if not trivial recrystallizations[11] (Scheme 3-5).

Scheme 3-5: Preparation of Aminomethylnaphthol-derived Imines
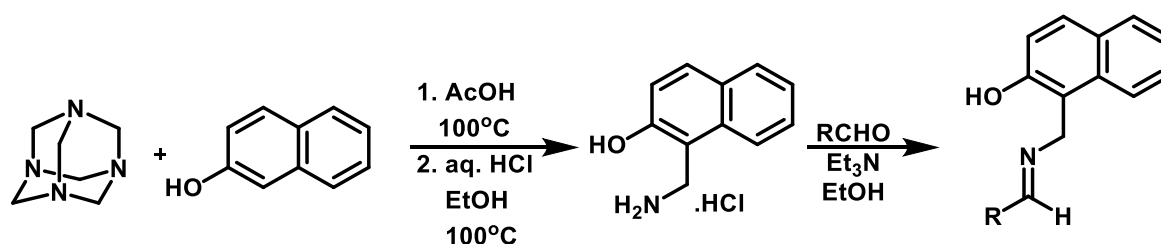
3.4. Asymmetric Crotylation of *o*-Aminomethylnaphthol-derived Imines

With the imines in hand, we turned our attention to their performance in the crotylation reaction with silane (*R,R*)-**3.12**, and we were pleased to find out that they can afford the corresponding crotylation products in good yields, and excellent stereoselectivities (Table 3-1). Unfortunately, this crotylation protocol was only suitable for aromatic imine substrates. Subjecting cyclohexyl-derived imine substrate to (*R,R*)-**3.12** afforded the corresponding homoallylic amine in only 27% yield albeit excellent diastereoselectivy >20:1 *dr*.

Table 3-1: Asymmetric Crotylation of *o*-Aminomethylnaphthol-derived Imines
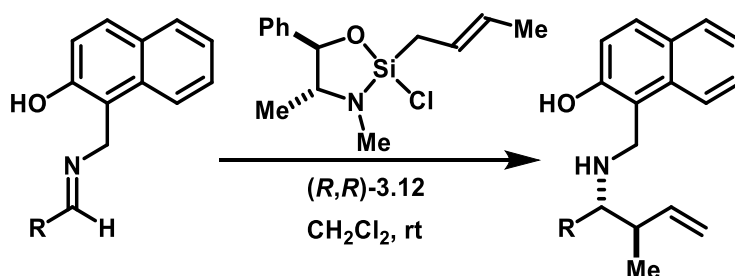
Entry	R	Yield (%)	ee (%)	dr
1	C_6H_5	86	99	>20:1
2	*p*-Br-C_6H_4	92	94	>20:1
3	*p*-OMe-C_6H_4	87	98	>20:1
4	*c*-Hex	27	---	>20:1

3.5. Asymmetric CM/Cinnamylation of *o*-aminomethylnaphthol-derived Imines

We found that these imines were also versatile substrates in the previously reported cross-metathesis/cinnamylation protocol[12] with silane (*R,R*)-**3.13**. Reactions with several substituted styrenes and vinyl cyclohexane afforded the corresponding cinnamylation products (**3.14 - 3.23**) in better yields and excellent stereoselectivities (Table 3-2). Unfortunately, just like in the crotylation reactions, the aliphatic substrates did not perform well in this protocol. When subjecting hydrocinnamyl-derived imine substrate to the above conditions, we only obtained the corresponding product in 34% yield although with good enantioselectivity (24% *ee*) and excellent diastereoselectivity (>20:1 *dr*). By monitoring the reaction progress in the aliphatic case, we observed several unidentifiable side products by ^{1}H NMR of the crude reaction mixture and also stronger fluorescence at the baseline by TLC analysis when compared to reactions with aromatic substrates. This comes as no

surprise since one potential issue with aliphatic imines in our protocol is that they could

tautomerize to the enamine aided by the presence of a Lewis acid such as **3.12**. As a result,

this enamine could then undergo other undesired reaction pathways.

Table 3-2: CM/Cinnamylation of *o*-Aminomethylnaphthol-derived Imines
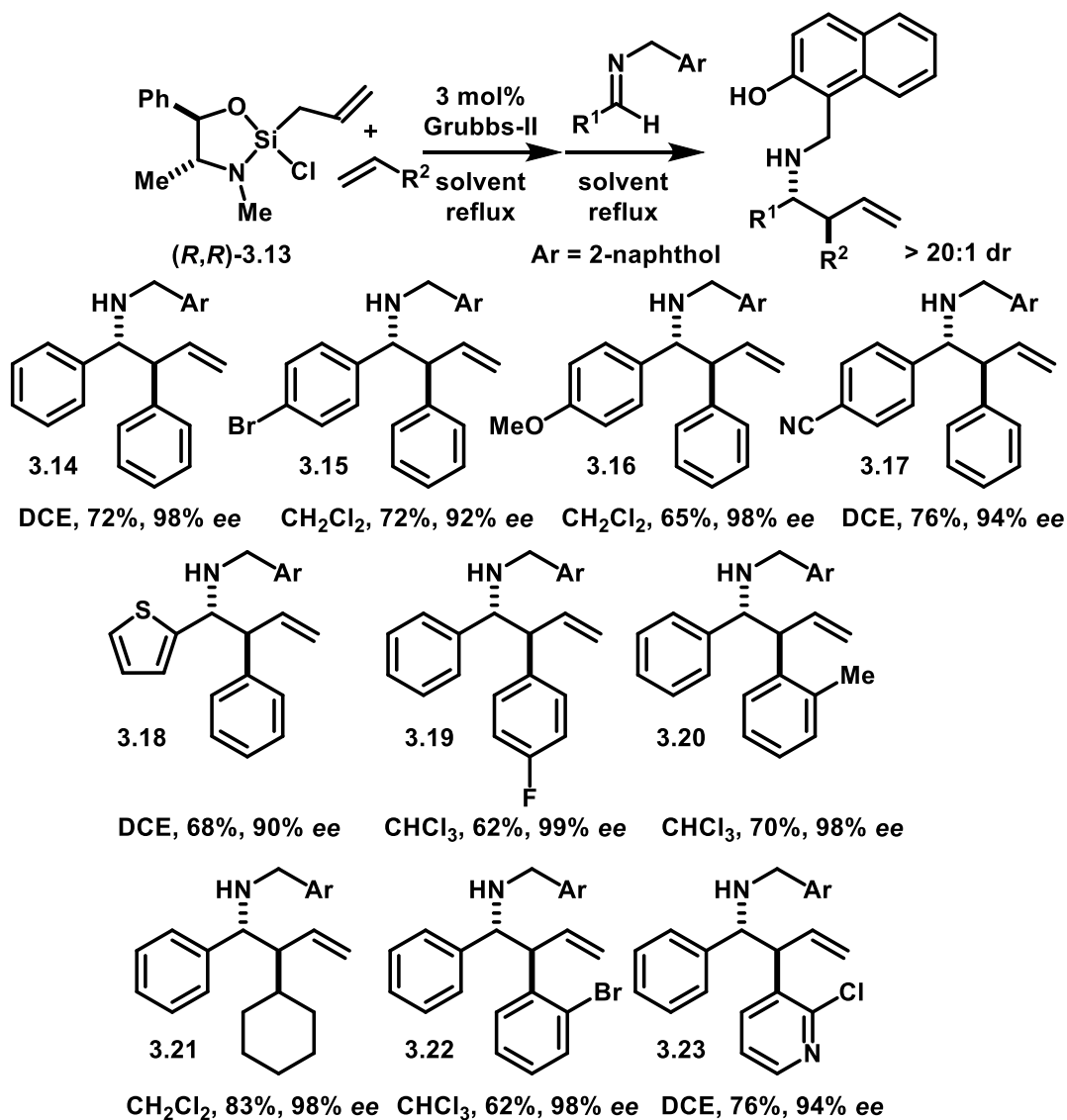
3.6. Cleavage of the *N*-(1-methyl-2-naphthol) Activating Group

We focused our efforts to provide a generally user-friendly method that would allow us to cleave this newly designed motif. Inspired on structure **3.9**, we hypothesized that we could lower the energy required to generate *o*-napthoquinone methide **3.11** by making the nitrogen on its homoallylic amine precursor **3.14** a better leaving group. Our initial attempts to generate **3.11** then consisted of refluxing the starting amines in the presence of strong acids. In this case, we were expecting that the protonated nitrogen would be a better leaving group. After screening several solvents, acids, and reaction conditions, we found no reaction other than the formation of the corresponding acid ammonium salt.

Scheme 3-6: Thermal *o*-Naphthoquinone Methide Generation from Ammonium Salts
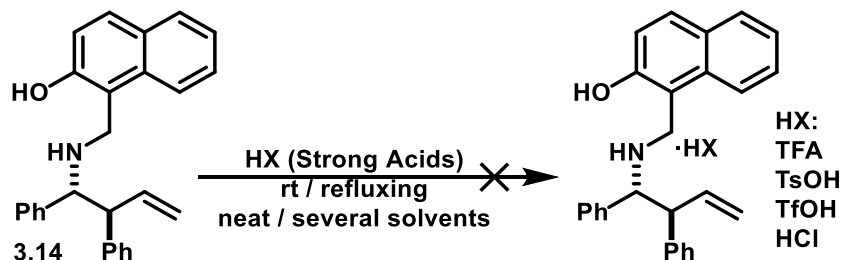
We also took a look at acylating the nitrogen to facilitate its ejection when refluxing in presence of strong acids, but this just led to trace amount of products and mostly recovered starting material (Scheme 3-7).

Scheme 3-7: Thermal *o*-Naphthoquinone Methide Generation from Amides
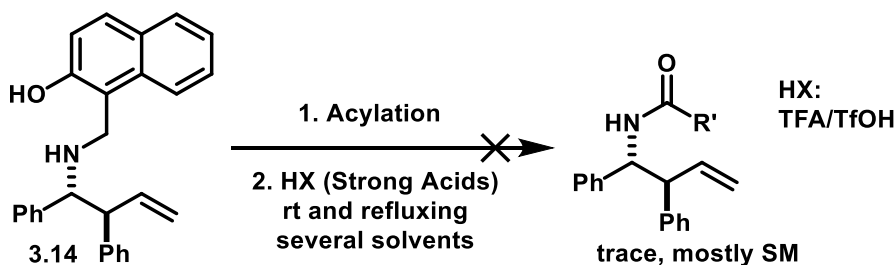
We also took a look at mild photolytic conditions[13] in the presence of ethanedithiol, mercapto ethanol and vinyl ethers as the trapping agents, but we observed mostly starting material, trace product, and decomposition (Scheme 3-8).

Scheme 3-8: Photolytic Generation of *o*-Naphthoquinone Methide
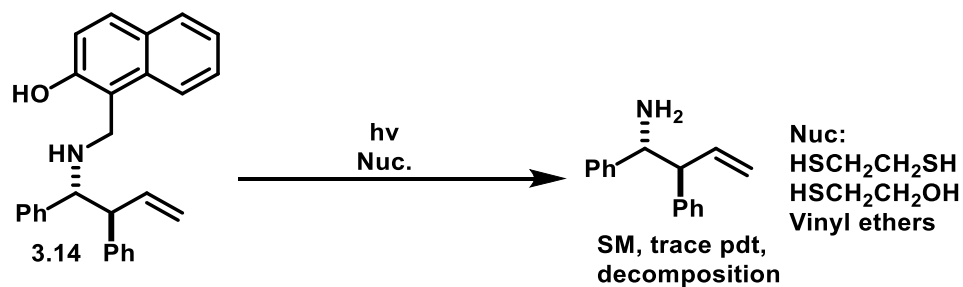
We decided to revisit the thermal conditions for the generation of **3.11** as we thought that the initial failures in Schemes **3.6** and **3.7** could be attributed to reversibility of the reaction[14]. One can imagine that once the amine is freed from the naphthol system, and the weakly nucleophilic counter ion of the acid attacks **3.11**, the resulting substituted naphthol can regenerate **3.11** even more readily than from **3.10** as this counter ion is also a good leaving group.

Next, we looked at thermal generation of **3.11** in the presence of strong nucleophiles[15] without activating the nitrogen (Scheme 3-9). A wide range of nucleophiles was explored including thiols, sulfides, alcohols, vinyl ethers, and 1,3-dienes as trapping agents for **3.11** in several solvents (polar, non-polar, protic, aprotic) and temperatures, but no fruitful results were obtained as we either observed no reaction or major decomposition of the starting material, especially at higher temperatures.

Scheme 3-9: Thermal Generation of *o*-Naphthoquinone Methide in Presence of Strong Nucleophiles
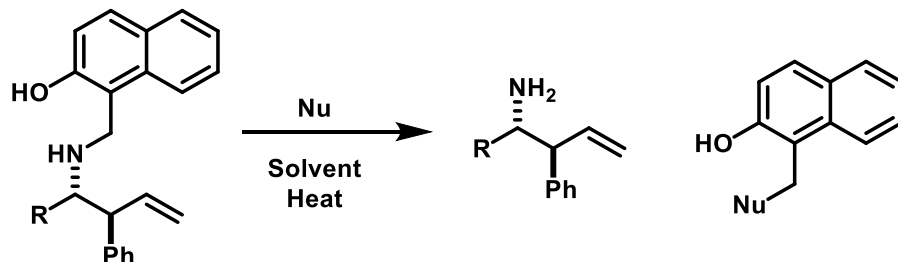
We then turned our attention to other amines as possible trapping agents for **3.11**. Page and coworkers reported that when **3.24** is refluxed in neat morpholine, it can afford the corresponding substituted *o*-phenol **3.26** in 51% yield[16] (Scheme 3-10). We obtained compound **3.25** from our CM/Cinnamylation protocol and subjected it the reported cleavage conditions, but major decomposition was observed as the vinyl pattern of the terminal olefin disappeared in the ^{1}H NMR spectrum. We also applied the reported conditions to **3.14**, and observed similar results as in the previous case. Since in our hands Page's cleavage of **3.24** was completely reproducible, we attributed that the change in reactivity between **3.24** and homoallylic amines **3.14** and **3.25** was the presence of the terminal olefin in the latter two. At such high temperatures required for Page's protocol, one can imagine that the rate of possible side reactions increases, resulting in major destruction of the desired product. Thus, we revisited our hypothesis that if *o*-naphthoquinone methide **3.11** was much more facile to generate, one could perhaps not require such high temperatures and infinitely large excess of the amine nucleophile.

Scheme 3-10: Page's Protocol for Thermal Cleavage in Morpholine
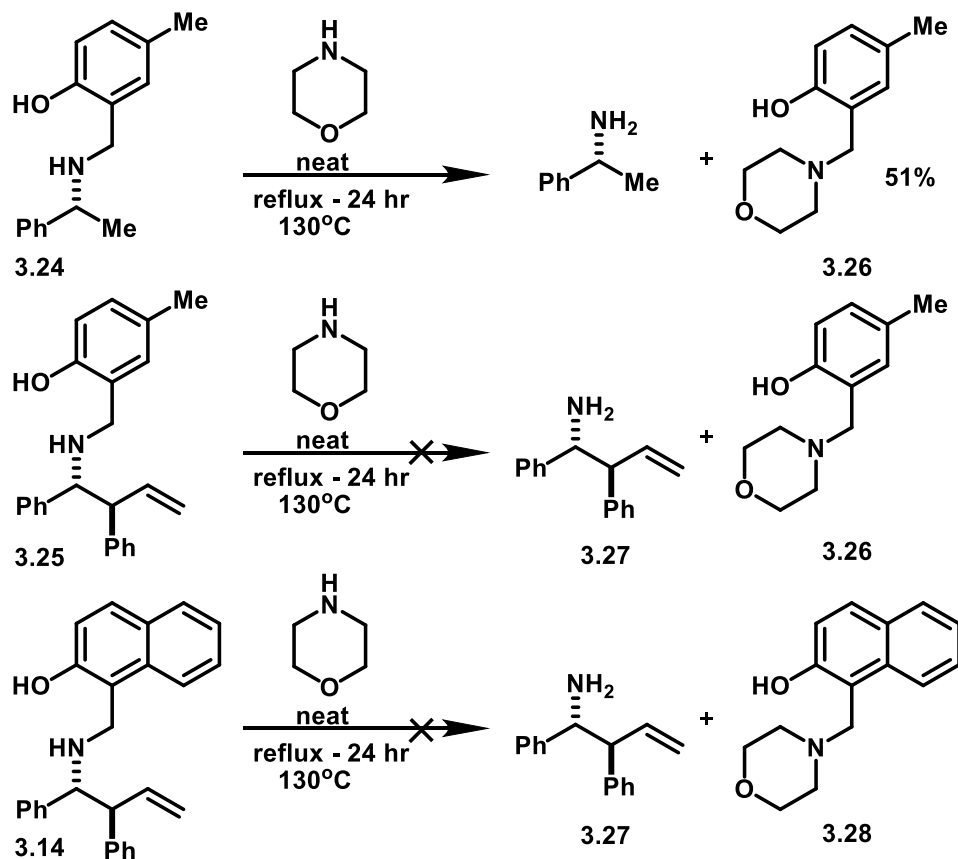
We then set for screening several conditions in which we tested solvents, concentration of the amine nucleophile, and temperature. Analyzing the reaction progress for the thermal cleavage of **3.14** by ^{1}H NMR, led us to find out that the best conversions to to **3.27** were in polar solvents (DCE, EtOAc, EtOH, CH$_3$CN), with at least five equivalents of morpholine, and temperatures between 60°C and 80°C (Scheme 3-10). We picked our best and most convenient result, which was 100% conversion to **3.27** by heating a 0.1 M solution of **3.14** in absolute ethanol at 60°C with five equivalents of morpholine. We further explored other commercially available amines, especially focusing on those with low boiling points for easier removal of their excess after reaction completion. We found that

secondary amines were optimal in all cases as they gave 100% conversion to the desired product by ^{1}H NMR with the exception of diisopropyl amine, which appeared to be too sterically hindered for our system (Scheme 3-11).

Scheme 3-11: Thermal Cleavage of the Aminomethylnaphtol Motif by 2° Amines
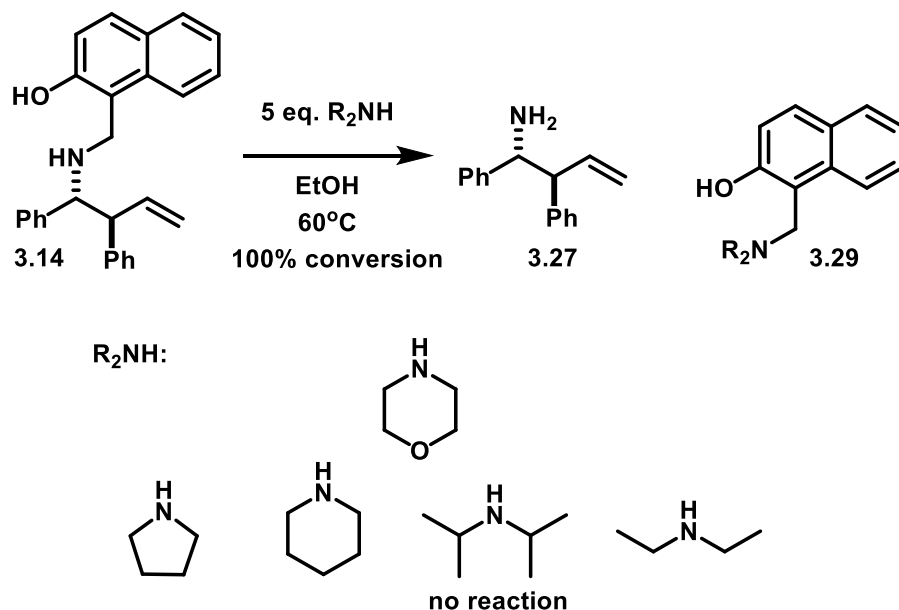
While these were promising results, the protocol turned out to be impractical as we struggled to cleanly isolate **3.27** either by acid/base extractions or chromatography. In most cases we obtained low yields of **3.27** and recovered starting material **3.14**. We attributed this result to reversibility of the reaction[17], aided by activation of **3.29** with Brønsted acids or silica gel. Neutralizing the silica gel or attempting to trap **3.27** in situ with several acylating agents failed to work any better (Scheme 3-12).

Scheme 3-12: Potential Reversible Pathway for the Cleavage Reaction
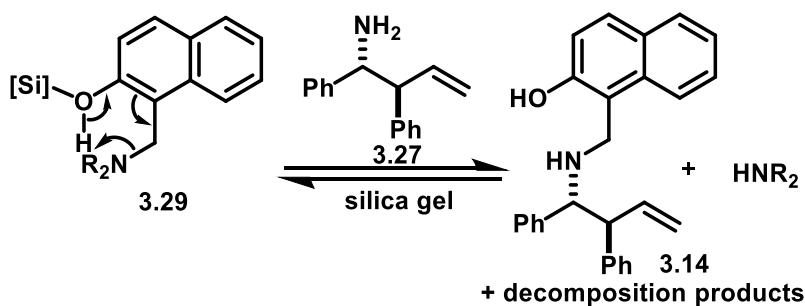
We turned our attention to a carbon nucleophile such as pyrrole as the resulting carbon-carbon bond in the naphthol substituted product **3.30** would be stronger than that of the carbon nitrogen bond in **3.29**. Indeed, we were pleased to find that pyrrole effected the cleavage cleanly as observed by ^{1}H NMR under the same reaction conditions shown in Scheme 3-11. However, we still ran into the problematic isolation of clean product, in which low yields persisted as well as recovery of starting material, which can be attributed to a retro electrophilic aromatic substitution aided by silica gel acting as a Lewis acid (Scheme 3-13).

Scheme 3-13: Pyrrole Cleavage of *o*-Aminomethylnaphthol Motif
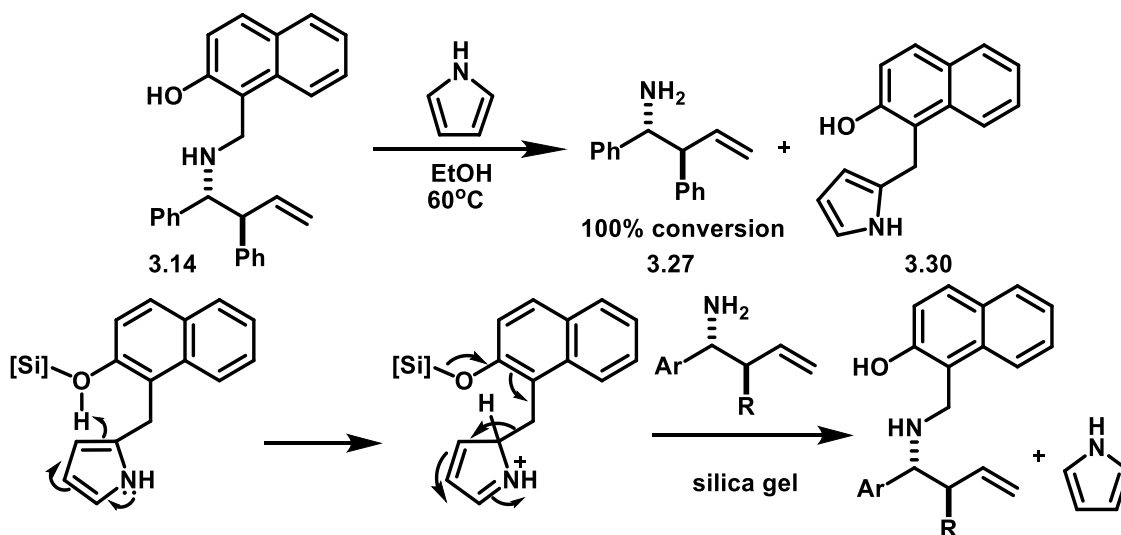
Attempts to optimize acid/base extraction work ups followed by chromatography only afforded **3.27** in 46% yield at most. Thus, we decided to explore *in situ* protection of **3.27**. After testing several acylating agents we found that di-*tert*-butyl dicarbonate was the best choice, affording the corresponding *N*-Boc protected homoallylic amines in good yields over two steps (Scheme 3-14). It is worth pointing out that this protocol is completely compatible with halogenated aromatic substrates and the terminal olefin in our products unlike methods utilizing transition metals, in which these functionalities could become labile[18].

Scheme 3-14: One-Pot Cleavage of *o*-Aminomethylnaphthol Motif
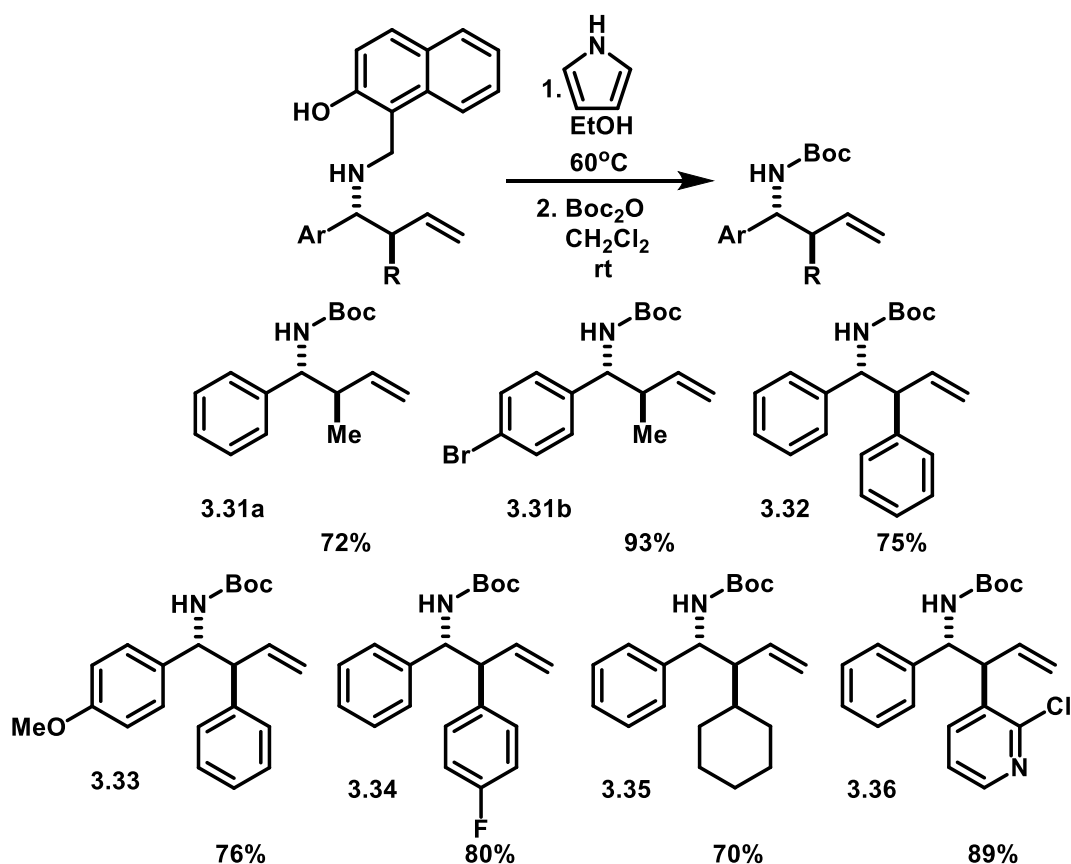
3.7. Stereochemical Proofs

In order to determine stereochemical outcome of the compounds listed in Scheme 3-14, compound **3.14** was cleaved to generate amine **3.27,** which by hydrogenation gave known compound **3.37**[19]. The ^{1}H NMR spectrum of **3.37** corresponded to the literature precedent, confirming the 1,2-*anti* relative stereochemistry. Similarly, the optical rotation of **3.37** was compared to the reported value, confirming the (1*R*,2*S*) absolute stereochemistry. (Scheme 3-15).

Scheme 3-15: Stereochemical Proof
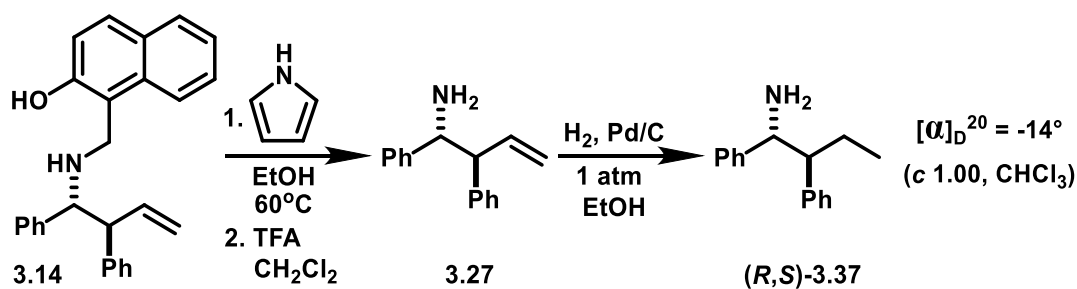
From the Literature[20]:
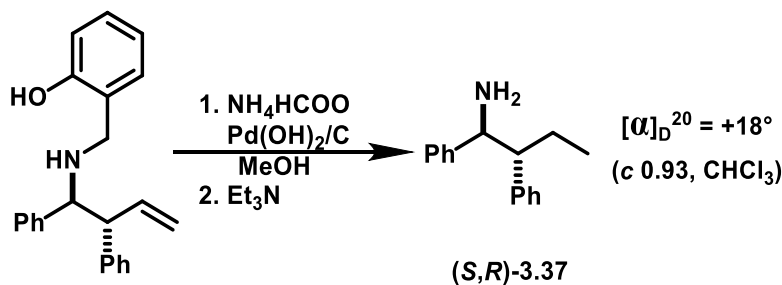
3.8. Stereochemical Rationale

Given that the stereochemical outcome of the cinnamylation products from imines **3.38** listed in Scheme 3-14 was similar to the reported cinnamylation products from imines **3.2**[21], we proposed that both types of imines are engaging in a similar closed transition state *cis*-**3.40** to deliver the corresponding *anti* diastereomer (Figure 3-4).

Figure 3-4: Proposed Transition State for the Cinnamylation of *o*-Aminomethylnaphthol –derived Imines
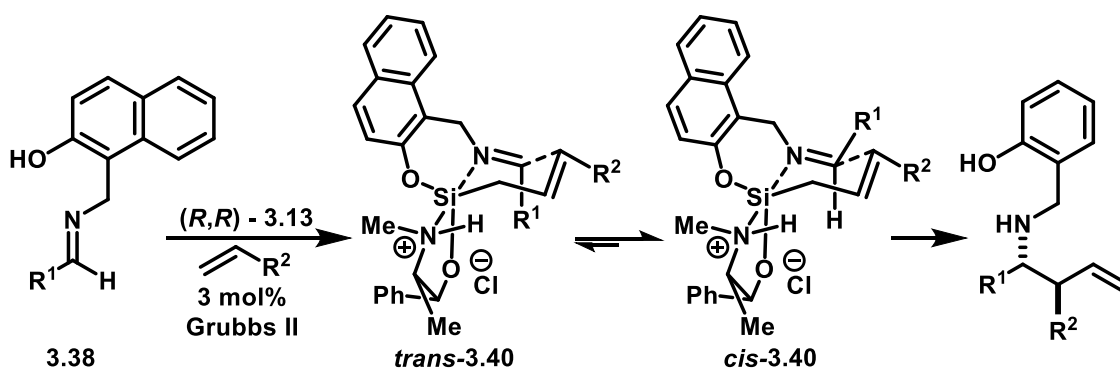
This proposed transition state minimizes steric interactions by placing R[1] in a pseudoequatorial position, which requires a *trans* to *cis* isomerization of the imine[22]. This process can be operative from addition/elimination of the chloride from the Si-bound imine or directly from opening its hemiaminal ether **3.41** by action of the silane as a Lewis acid (Figure 3-5). In fact, the starting material imines can be seen by ^{1}H NMR as a mixture ranging from 0 – 100% of hemiaminalether : imine depending on the solvent of choice, which leads us to believe that this process is even more facile in the presence of Lewis acids like our silanes, and it clearly did not affect our stereoselectivity results.

Figure 3-5: Silane Catalyzed Imine E/Z Isomerization from its Hemiaminal Ether
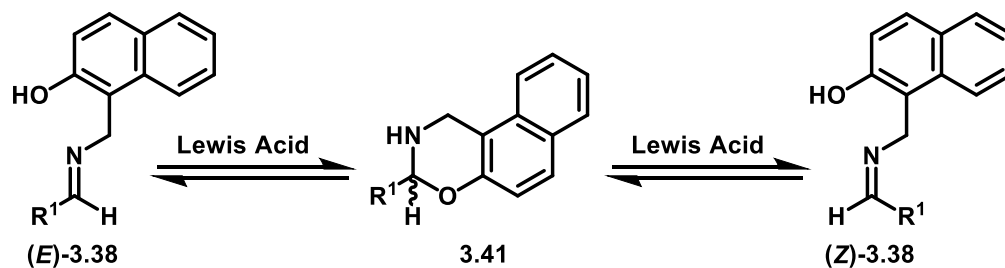
Using the rationale presented in Figure 3.3, we redesigned the imine *N*-bearing motif in order to obtain the *syn* diastereomer product (Figure 3-6).

Figure 3-6: Rationale for Proposed Imine *N*-bearing Motif Design
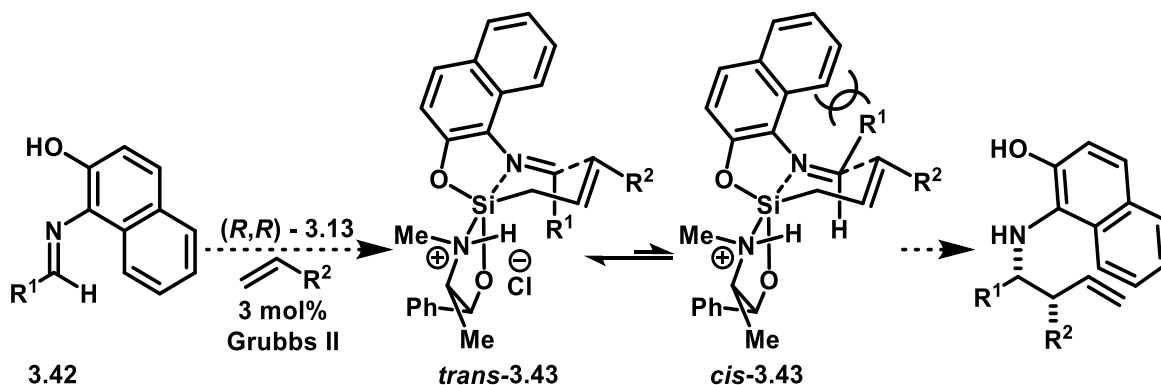
By increasing sterics at the carbon adjacent to the one bearing the nitrogen as in imines **3.42**, one can envision that proposed transition state *trans*-**3.43** would be more stable as it avoids severe steric interactions between the imine R^1 substituent and the naphthol ring system in transition state *cis*-**3.43**. We attempted to test this hypothesis by synthesizing a variety of 1-hydroxy-2-aminoarenes (Figure 3-7) and subjecting their resulting imines to the CM/cinnamylation protocol. However, in most cases the aromatic systems themselves, or once bound to the corresponding imine, or to their cinnamylation products were highly

labile to air oxidation and would decompose almost right away on standing. Unfortunately, these observations impeded us from further exploration into this new kind of substrates.

Figure 3-7: Aminoarenes Tested as Activating Groups
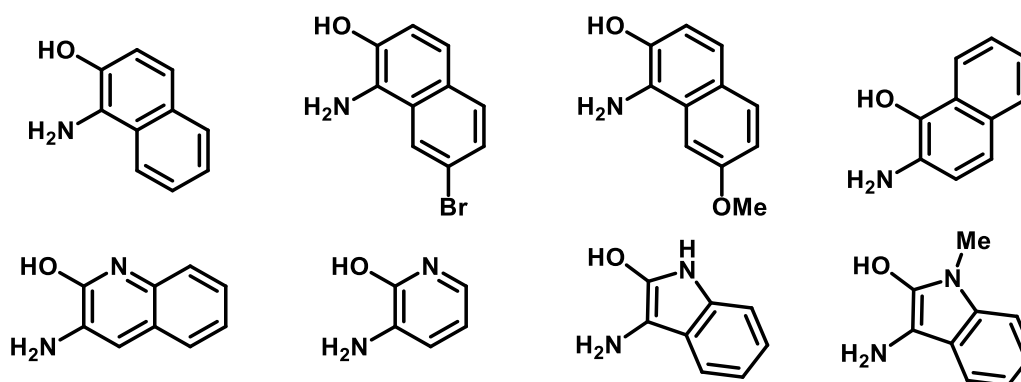
3.9. Conclusions

Overall, we have developed a method for the asymmetric crotylation and cinnamylation of a new class of *o*-aminomethylnaphthol-derived imines with the corresponding pseudoephedrine-derived Leighton silane reagents. The imines are trivially and economically synthesized in large quantities, and the corresponding homoallylic amine products are readily and smoothly cleaved and *in situ* protected to generate the desired boc-amines. Our method developed herein allows for taking advantage of the homoallylic amine products' inherent functionality by avoiding the use of metals, which are known to be incompatible with aryl halides and the terminal olefin; thus, placing this method in a more synthetically powerful perspective. Further efforts on these studies should be aimed at broadening the scope of substrates and products for this reaction methodology.

3.10. References

1. Huber, J. D.; Leighton, J. L. *Journal of the American Chemical Society* **2007**, *129*, 14552–3.

2. Bartberger, M. D.; Gonzalez Ana, B.; Beck, H. P.; Chen, X.; Connors, R. V.; Deignan, J.; Duquette, J.; Eksterowicz, J.; Fisher, B.; Fox, B. M.; Fu, J.; Fu, Z.; Gonzalez Felix, L. de T.; Gribble Jr., M. W.; Gustin, D. J.; Heath, J. A.; Huang, X.; Jiao, X.; Johnson, M.; Kayser, F.; Kopecky, D. J.; Lai, S.; Li, Y.; Li, Z.; Liu, J.; Low, J. D.; Lucas, B. S.; Ma, Z.; Mcgee, L.; Mcintosh, J.; Mcminn, D.; Medina, J. C.; Mihalic, J. T.; Olson, S. H.; Rew, Y.; Roveto, P. M.; Sun, D.; Wang, X.; Wang, Y.; Yan, X.; Yu, M.; Zhu, J. Piperidinone Derivatives as MDM2 Inhibitors and their Preparation and Use for the Treatment of Cancer. US Patent WO 2011/153509. December 08, 2011.

3. Huber, J. D.; Leighton, J. L. *Journal of the American Chemical Society* **2007**, *129*, 14552–3.

4. Huber, J. D. Enantioselective imine cinnamylation: Rapid construction of contiguous benzylic and carbinamine stereocenters, Columbia University: United States -- New York, 2007, p. 181.

5. Huber, J. D. Enantioselective imine cinnamylation: Rapid construction of contiguous benzylic and carbinamine stereocenters, Columbia University: United States -- New York, 2007, p. 181.

6. Huber, J. D.; Leighton, J. L. *Journal of the American Chemical Society* **2007**, *129*, 14552–3.

7. Verkade, J. M. M.; van Hemert, L. J. C.; Quaedflieg, P. J. L. M.; Alsters, P. L.; van Delft, F. L.; Rutjes, F. P. J. T. *Tetrahedron Letters* **2006**, *47*, 8109–8113.

8. Chiang, Y.; Kresge, A. J.; Zhu, Y. *Pure and Applied Chemistry* **2000**, *72*, 2299–2308.

9. Van De Water, R. W.; Pettus, T. R. R. *Tetrahedron* **2002**, *58*, 5367–5405.

10. Carey, F.; Sundberg, R. In *Advanced Organic Chemistry Part A: Structure and Mechanisms*; Springer US, 2007; pp. 713–770.

11. See references:

a) Duff, J. C.; Bills, E. J. *Journal of the Chemical Society (Resumed)* **1934**, 1305–1308.

b) Duff, J. C.; Furness, V. I. *Journal of the Chemical Society (Resumed)* **1951**, 1512–1515.

12. Huber, J. D.; Perl, N. R.; Leighton, J. L. *Angewandte Chemie, International Edition* **2008**, *47*, 3037–3039.

13. Nakatani, K.; Higashida, N.; Saito, I. *Tetrahedron Letters* **1997**, *38*, 5005–5008.

14. Page, P.; Heaney, H.; McGrath, M.; Sampler, E.; Wilkins, R. *Tetrahedron Letters* **2003**, *44*, 2965–2970.

15. Van De Water, R. W.; Pettus, T. R. R. *Tetrahedron* **2002**, *58*, 5367–5405.

16. Page, P.; Heaney, H.; McGrath, M.; Sampler, E.; Wilkins, R. *Tetrahedron Letters* **2003**, *44*, 2965–2970.

17. Page, P.; Heaney, H.; McGrath, M.; Sampler, E.; Wilkins, R. *Tetrahedron Letters* **2003**, *44*, 2965–2970.

18. Aryl halides can undergo oxidative additions with transition metals and further engage in other reaction pathways:

a) Zeni, G.; Larock, R. C. *Chemical Reviews* **2006**, *107*, 303.

b) Rendina, L. M.; Puddephatt, R. J. *Chemical Reviews* **1997**, *97*, 1735–1754.

c) Deutsch, P. P.; Eisenberg, R. *Chemical Reviews* **1988**, *88*, 1147–1161.

19. Huber, J. D.; Leighton, J. L. *Journal of the American Chemical Society* **2007**, *129*, 14552–3.

20. Huber, J. D.; Leighton, J. L. *Journal of the American Chemical Society* **2007**, *129*, 14552–3.

21. Huber, J. D.; Leighton, J. L. *Journal of the American Chemical Society* **2007**, *129*, 14552–3.

22. Berger, R.; Duff, K.; Leighton, J. L. *Journal of the American Chemical Society* **2004**, *126*, 5686–5687.

3.11. Experimental Section

General Information.

All reactions were carried out in flame-dried glassware under an inert atmosphere of nitrogen with magnetic stirring unless otherwise indicated. Methylene chloride and toluene were obtained from Fisher and purified by degassing with argon followed by passage through an activated neutral alumina column. Triethylamine was purchased from Alfa Aesar and purified by distillation from CaH_2 then stored under nitrogen. Pentane (HPLC grade) was purchased from Fisher and used as received. Anhydrous chloroform (stabilized with amylenes) and 1,2-dichloroethane were purchased from Aldrich and used as received. Pyrrole was purchased from Aldrich and redistilled under reduced pressure from CaH_2 then stored under nitrogen. The Grubbs second generation catalyst was obtained from Aldrich and used without further purification. Styrene was purchased from Alfa Aesar and used as received. Aldehydes and all other reagents were purchased from Aldrich and used as received. Allyl and (*E*)-crotyl chlorosilane reagents were prepared according to previously reported procedures[1]. ^{1}H NMR spectra were recorded on Avance III 400SL (400 MHz) or Avance III 500 Ascend (500 MHz) spectrometers. ^{1}H NMR chemical shifts (δ) are reported in parts per million (ppm) relative to tetramethylsilane internal standard (0 ppm) or DMSO-*d* internal standard (2.50 ppm). Data are reported as follows: (s = singlet, br s = broad singlet, d = doublet, br d =broad doublet, t = triplet, q = quartet, quint = quintet, dd =

---

[1] Silane reagents and precursors were prepared according to previously reported procedures:
Tsuji, J.; Hara, M.; Ohno, K. *Tetrahedron* **1974**, 30, 2143-2146. (b) Furuya, N.; Sukawa, T. J. *Organomet. Chem*. **1975**, 96, C1-C3. (c) Kira, M.; Hino, T.; Sakurai, H. *Tetrahedron Lett*. **1989**, 30, 1099-1102. (d) Iseki, K.; Kuroki, Y.; Takahashi, M.; Kishimoto, S.; Kobayashi, Y. *Tetrahedron* **1997**, 53, 3513-3526. (e) Kinnaird, J. W. A.; Ng, P. Y.; Kubota, K.; Wang, X.; Leighton, J. L. *Journal of the American Chemical Society* **2002**, *124*, 7920–7921.

doublet of doublets, dq = doublet of quartets, ddd = doublet of doublet of doublets, ddt = doublet of doublet of triplets, m = multiplet; integration; coupling constant in Hz; assignment). Proton decoupled ^{13}C NMR spectra were recorded on Avance III 400SL (100 MHz) or Avance III 500 Ascend (125 MHz) spectrometers and are reported in ppm from CDCl$_3$ internal standard (77.16 ppm) or DMSO-d internal standard (39.52 ppm). ^{29}Si NMR spectra were recorded on a Bruker DPX-300 (60 MHz) spectrometer and are reported with tetramethylsilane (0 ppm) as an internal standard. Infrared spectra were recorded on a Perkin Elmer Paragon 1000 FT-IR or Nicolet Avatar 370 DTGS spectrometers. Optical rotations were recorded on a Jasco DIP-1000 digital polarimeter; the concentration c is reported in g/100mL. Low resolution mass spectra were obtained on a JEOL HX100 mass spectrometer in the Columbia University Mass Spectrometry Laboratory.

General Procedure for the Synthesis of 1-(aminomethyl)-2-naphthol-derived Imines

To a suspension of 1-(aminomethyl)-2-naphthol hydrochloride (1.0 equiv) in ethanol (0.5M, 200 proof) is added anhydrous triethylamine (1.01 equiv.) followed by the corresponding aldehyde (1.0 equiv) and allowed to stir at room temperature for up to three hours. The resulting suspension is cooled to 0°C and filtered. The collected precipitate is rinsed with additional amounts of chilled ethanol and redissolved in CH$_2$Cl$_2$ and azeotroped with toluene under reduced pressure to remove any residual water. If needed the mother liquor can be further concentrated and chilled to collect a second or more crops of crystals. The resulting solid is further dried under vacuum and used without any further purification. Note: the isolated solid is a mixture of the corresponding imine and its hemiaminal closed

form and their ratio varies depending on the solvent and the electronic nature of the starting aldehyde.

For Imine thiophene-derived imine, crystallization from the reaction mixture was not observed. In this case, the ethanol was evaporated under reduced pressure, and the resulting residue was dissolved in ethyl acetate and extracted twice with water and then washed with brine. The organic layer was concentrated and azeotroped with toluene under reduced pressure to give the tittle compound as a crystalline solid.

General Procedure for the Imine Crotylation Reactions

To a solution of the imine (0.383 mmol) in CH_2Cl_2 (3.8 mL) is added (*R,R*)-**3.12** (0.575 mmol). The resulting solution is stirred at room temperature for 16 hr. The reaction mixture is diluted with ethyl acetate (20 mL) and extracted with brine (10 mL). The aqueous layer is reextracted with ethyl acetate (20 mL). The combined organic layers are dried (Na_2SO_4), decanted, and concentrated. The residue is purified by flash chromatography on silica gel (solvent gradient: 100% to 70% hexanes/ethyl acetate with 1% triethylamine).

General Procedure for the Cross-Metathesis/Imine Cinnamylation Reactions

To a solution of the vinylarene or vinylheteroarene (1.440 mmol) in either 1,2-dichloroethane (DCE), $CHCl_3$, or CH_2Cl_2 (1.9 mL) is added (*R,R*)-**3.13** (0.287 mmol) followed by the second generation Grubbs catalyst (9 mg, 3.0 mol% based upon (*R,R*)-**3.13**). The resulting mixture is heated at reflux for 3.5 h (DCE) or 5 h ($CHCl_3$) or 7 h

(CH$_2$Cl$_2$) and then cooled to room temperature. The imine (0.191 mmol) is then added. The reaction mixture is then heated at reflux for 14 h and then cooled to room temperature and quenched by the addition of ethanol (0.19 mL). The resulting mixture is diluted with ethyl acetate (10 mL) and extracted with brine (5 mL). The aqueous layer is reextracted with ethyl acetate (10 mL). The combined organic layers are dried (Na$_2$SO$_4$), decanted, and concentrated. The residue is purified by flash chromatography on silica gel (solvent gradient: 100% to 70% hexanes/ethyl acetate with 1% triethylamine).

General Procedure for the Cleavage of the *N*-(1-methyl)-2-hydroxynaphthyl Group

To a solution of the amine (0.166 mmol) in ethanol (1.7 mL, 200 proof) is added pyrrole (0.830 mmol), and the contents are then stirred at 60°C for 1.5 h. The resulting solution is cooled to room temperature and concentrated under reduced pressure. The residue is redissolved in dichloromethane (1.7 mL) followed by addition of di-*tert*-butyl dicarbonate (Boc$_2$O, 0.498 mmol) and triethylamine (0.332 mmol). The contents are allowed to stir at room temperature for 16 hrs. The reaction mixture is diluted in EtOAc (10 mL) and extracted with water (5 mL). The organic layer is dried (Na$_2$SO$_4$), decanted, and concentrated. The residue is purified via column chromatography on silica gel (solvent gradient: 100% to 70% hexanes/ethyl acetate).

Crotylation products

1-(((((1R,2R)-2-methyl-1-phenylbut-3-en-1-yl)amino)methyl)naphthalen-2-ol (Table 3-1, Entry 1): ^{1}H NMR (400 MHz, CDCl$_3$) δ 7.77 – 7.56 (m, 3H), 7.46 – 7.21 (m, 7H), 7.10 (d, J = 8.9 Hz, 1H), 5.81 (dt, J = 17.1, 9.5 Hz, 1H), 5.28 – 5.15 (m, 2H), 4.16 (dd, J = 93.4, 14.3 Hz, 2H), 3.46 (d, J = 9.1 Hz, 1H), 2.55 (q, J = 8.5 Hz, 1H), 0.87 (d, J = 6.8 Hz, 3H). ^{13}C NMR (126 MHz, CDCl$_3$) δ 156.59, 141.20, 140.50, 132.24, 129.09, 128.82, 128.76, 128.43, 127.97, 127.88, 126.19, 122.39, 121.10, 119.36, 117.00, 112.73, 67.82, 45.32, 45.21, 18.18. IR (neat): 3293, 3062, 2969, 2923, 1622, 1599, 1515, 1454, 1356, 1270, 1237, 1158, 999, 914, 814, 747, 701 cm^{-1}. HRMS (FAB+) calculated for C$_{22}$H$_{24}$NO: 318.1858, observed: 318.1865 (M+H). $[\alpha]_D^{21}$ = +74 (c 0.5, CHCl$_3$).

1-(((((1R,2R)-1-(4-bromophenyl)-2-methylbut-3-en-1-yl)amino)methyl)naphthalen-2-ol (Table 3-1, Entry 2): ^{1}H NMR (400 MHz, CDCl$_3$) δ 7.74 (d, J = 7.9 Hz, 1H), 7.68 (d, J = 8.9 Hz, 1H), 7.60 (d, J = 8.7 Hz, 1H), 7.56 – 7.48 (m, 2H), 7.38 (ddd, J = 9.4, 6.5, 1.3 Hz, 1H), 7.30 – 7.24 (m, 1H), 7.21 (d, J = 8.2 Hz, 2H), 7.10 (d, J = 8.8 Hz, 1H), 5.77 (ddd, J = 16.9, 10.1, 8.9 Hz, 1H), 5.33 – 5.18 (m, 2H), 4.16 (dd, J = 102.6, 14.3 Hz, 2H), 3.44 (d, J = 9.1 Hz, 1H), 2.50 (ddt, J = 15.6, 8.9, 6.8 Hz, 1H), 0.86 (d, J = 6.7 Hz, 3H). ^{13}C NMR (101 MHz, CDCl$_3$) δ 156.42, 140.68, 139.61, 132.16, 131.93, 129.61, 129.17, 128.77, 128.45, 126.24, 122.45, 121.67, 120.97, 119.26, 117.32, 112.48, 77.20, 67.31, 45.18, 18.01. IR (neat): 3291, 3063, 2972, 2927, 1621, 1597, 1517, 1485, 1467, 1406, 1373, 1336, 1270, 1236, 1163, 1073, 1163, 1141, 1073, 1009, 913, 856, 815, 733, 687, 649 cm^{-1}. HRMS (FAB+) calculated for C$_{22}$H$_{23}$BrNO: 396.0963, observed: 396.0955 (M+H). $[\alpha]_D^{21}$ = +107 (c 0.75, CHCl$_3$).

1-(((((1*R*,2*R*)-1-(4-methoxyphenyl)-2-methylbut-3-en-1-yl)amino)methyl)naphthalen-2-ol (Table 3-1, Entry 3): ^{1}H NMR (400 MHz, CDCl₃) δ 7.76 – 7.71 (m, 1H), 7.66 (d, *J* = 8.9 Hz, 1H), 7.62 (d, *J* = 8.5 Hz, 1H), 7.41 – 7.31 (m, 1H), 7.26 (dd, *J* = 8.1, 6.2 Hz, 3H), 7.10 (d, *J* = 8.8 Hz, 1H), 6.99 – 6.90 (m, 2H), 5.80 (dt, *J* = 17.0, 9.4 Hz, 1H), 5.28 – 5.14 (m, 2H), 4.16 (dd, *J* = 94.0, 14.4 Hz, 2H), 3.84 (s, 3H), 3.41 (d, *J* = 9.2 Hz, 1H), 2.58 – 2.44 (m, 1H), 0.86 (d, *J* = 6.8 Hz, 3H). ^{13}C NMR (101 MHz, CDCl₃) δ 159.19, 156.58, 141.34, 132.38, 132.22, 128.99, 128.96, 128.72, 128.40, 126.12, 122.33, 121.08, 119.33, 116.85, 114.18, 112.77, 67.20, 55.27, 45.42, 45.12, 18.16. IR (neat): 3289, 3063, 2961, 2930, 2836, 1609, 1512, 1465, 1416, 1355, 1303, 1249, 1178, 1034, 999, 912, 815, 746, 676 cm^{-1}. HRMS (FAB+) calculated for $C_{23}H_{26}NO_2$: 348.1964, observed: 348.1957 (M+H). $[\alpha]_D^{21}$ = +110 (c 0.5, CHCl₃).

Cinnamylation products

1-(((((1*R*,2S)-1,2-diphenylbut-3-en-1-yl)amino)methyl)naphthalen-2-ol   (3.14): The reaction was carried out in DCE according to the general procedure to give 53 mg (73%) of the tittle compound. ^{1}H NMR (400 MHz, CDCl₃) δ 7.75 (dd, *J* = 8.1, 1.4 Hz, 1H), 7.69 (d, *J* = 8.8 Hz, 1H), 7.66 – 7.53 (m, 1H), 7.36 (ddd, *J* = 8.5, 6.8, 1.5 Hz, 1H), 7.27 – 7.05 (m, 10H), 7.01 (dd, *J* = 6.9, 1.7 Hz, 2H), 6.22 (dt, *J* = 16.9, 9.7 Hz, 1H), 5.43 – 5.15 (m, 2H), 4.22 (dd, *J* = 86.7, 14.3 Hz, 2H), 4.00 (d, *J* = 9.4 Hz, 1H), 3.66 (t, *J* = 9.4 Hz, 1H). ^{13}C NMR (101 MHz, CDCl₃) δ 156.57, 140.69, 139.49, 138.93, 138.65, 132.26, 129.18, 128.78, 128.42, 128.37, 128.12, 128.04, 127.63, 127.32, 126.90, 126.58, 126.25, 122.47, 121.12, 119.39, 118.21, 117.40, 112.64, 77.40, 77.09, 76.77. IR (neat): 3291, 3061, 3029, 2962, 2920, 2852, 1621, 1599, 1518, 1493, 1467, 1453, 1412, 1266, 1235, 1161, 1093, 1014, 920,

815, 699 cm^{-1}.HRMS (FAB+) calculated for C$_{27}$H$_{26}$NO: 380.2014, observed: 380.2028 (M+H) . [α]$_D^{20}$ = +50 (c 1.7, CHCl$_3$).

1-(((((1*R*,2*S*)-1-(4-bromophenyl)-2-phenylbut-3-en-1-yl)amino)methyl)naphthalen-2-ol (3.15): ^{1}H NMR (400 MHz, CDCl$_3$) δ 7.82 – 7.75 (m, 1H), 7.71 (d, *J* = 9.0 Hz, 1H), 7.61 (d, *J* = 8.5 Hz, 1H), 7.46 – 7.34 (m, 2H), 7.33 – 7.25 (m, 2H), 7.20 (ddd, *J* = 7.6, 6.1, 1.7 Hz, 2H), 7.17 – 7.10 (m, 2H), 7.01 (ddt, *J* = 6.7, 4.5, 1.9 Hz, 4H), 6.20 (dt, *J* = 16.7, 9.8 Hz, 1H), 5.38 – 5.24 (m, 2H), 4.21 (dd, *J* = 99.5, 14.2 Hz, 2H), 3.99 (d, *J* = 9.4 Hz, 1H), 3.61 (t, *J* = 9.5 Hz, 1H). ^{13}C NMR (101 MHz, CDCl$_3$) δ 156.39, 140.22, 138.65, 138.26, 132.18, 132.01, 131.56, 129.68, 129.30, 128.89, 128.81, 128.53, 128.03, 126.80, 126.34, 122.55, 121.00, 119.32, 118.51, 112.39, 66.78, 57.97, 45.18.IR (neat): 3289, 3061, 3028, 2919, 2852, 1621, 1597, 1518, 1486, 1467, 1406, 1334, 1269, 1234, 1162, 1072, 1009, 911, 815, 701 cm^{-1}. HRMS (FAB+) calculated for C$_{27}$H$_{25}$BrNO: 458.1120, observed: 458.1119 (M+H). [α]$_D^{21}$ = +61 (c 0.5, CHCl$_3$).

1-(((((1*R*,2*S*)-1-(4-methoxyphenyl)-2-phenylbut-3-en-1-yl)amino)methyl)naphthalen-2-ol (3.16): ^{1}H NMR (500 MHz, Chloroform-d) δ 7.75 (d, *J* = 8.1 Hz, 1H), 7.70 (d, *J* = 8.9 Hz, 1H), 7.62 (d, *J* = 8.6 Hz, 1H), 7.40 – 7.33 (m, 1H), 7.28 – 7.25 (m, 1H), 7.21 – 7.08 (m, 4H), 7.08 – 6.96 (m, 4H), 6.77 (dt, *J* = 11.0, 2.6 Hz, 2H), 6.31 – 6.10 (m, 1H), 5.39 – 5.19 (m, 2H), 4.21 (dd, *J* = 111.3, 14.4 Hz, 2H), 3.96 (d, *J* = 9.4 Hz, 1H), 3.77 (d, *J* = 1.1 Hz, 3H), 3.64 (t, *J* = 9.4 Hz, 1H). ^{13}C NMR (126 MHz, CDCl$_3$) δ 158.89, 156.57, 140.82, 138.81, 132.25, 131.37, 129.10, 129.06, 128.76, 128.36, 128.13, 126.51, 126.20, 122.42, 121.11, 119.38, 118.05, 114.23, 113.80, 112.67, 66.58, 58.14, 55.16, 45.10. IR (neat): 3290,

3061, 3029, 3001, 2930, 2909, 2836, 1619, 1512, 1466, 1249, 1177, 1033, 911, 818, 733, 701 cm^{-1}. HRMS (FAB+) calculated for $C_{28}H_{28}NO_2$: 410.2129, observed: 410.2120 (M+H) . $[\alpha]_D^{21}$ = +33 (c 0.35, CHCl$_3$).

4-((1R,2S)-1-(((2-hydroxynaphthalen-1-yl)methyl)amino)-2-phenylbut-3-en-1-yl)benzonitrile (3.17): ^{1}H NMR (500 MHz, CDCl$_3$) δ 7.92 – 7.74 (m, 1H), 7.70 (d, J = 8.8 Hz, 1H), 7.58 (d, J = 8.5 Hz, 1H), 7.50 (d, J = 8.1 Hz, 2H), 7.39 (ddd, J = 8.3, 6.7, 1.3 Hz, 1H), 7.34 – 7.30 (m, 1H), 7.23 (d, J = 8.1 Hz, 2H), 7.21 – 7.10 (m, 4H), 7.01 – 6.88 (m, 2H), 6.20 (dt, J = 16.9, 9.7 Hz, 1H), 5.54 – 5.17 (m, 2H), 4.37 (d, J = 14.2 Hz, 1H), 4.22 – 3.96 (m, 2H), 3.59 (t, J = 9.5 Hz, 1H). ^{13}C NMR (126 MHz, CDCl$_3$) δ 156.22, 145.42, 139.69, 137.74, 132.15, 132.09, 129.47, 128.87, 128.74, 128.66, 128.55, 127.88, 127.03, 126.42, 122.66, 120.84, 119.22, 119.01, 118.54, 112.17, 111.54, 67.33, 57.96, 45.35. IR (neat): 3395, 3292, 3062, 3030, 2916, 2844, 2228, 1622, 1600, 1517, 1468, 1454, 1411, 1343, 1269, 1234, 1162, 1092, 1000, 911, 817, 733, 701 cm^{-1}. HRMS (FAB+) calculated for $C_{28}H_{25}N_2O$: 405.1953, observed: 405.1967 (M+H). $[\alpha]_D^{21}$ = +47 (c 0.5, CHCl$_3$).

1-(((((1R,2S)-2-phenyl-1-(thiophen-2-yl)but-3-en-1-yl)amino)methyl)naphthalen-2-ol (3.18): ^{1}H NMR (400 MHz, CDCl$_3$) δ 7.78 – 7.60 (m, 3H), 7.37 (ddd, J = 8.4, 6.8, 1.4 Hz, 1H), 7.29 – 7.23 (m, 1H), 7.23 – 7.16 (m, 3H), 7.16 – 7.10 (m, 2H), 7.10 – 7.02 (m, 2H), 6.79 (dd, J = 5.0, 3.5 Hz, 1H), 6.64 (dd, J = 3.5, 1.2 Hz, 1H), 6.18 (dt, J = 17.0, 9.8 Hz, 1H), 5.38 – 5.22 (m, 2H), 4.45 – 4.13 (m, 3H), 3.64 (t, J = 9.5 Hz, 1H). ^{13}C NMR (126 MHz, CDCl$_3$) δ 156.38, 143.88, 140.64, 138.41, 132.30, 129.25, 128.79, 128.53, 128.45, 127.97, 126.78, 126.75, 126.46, 126.28, 124.78, 122.51, 121.14, 119.36, 118.53, 112.52,

62.74, 59.03, 45.12. IR (neat): 3291, 3063, 3029, 2968, 2916, 1622, 1599, 1518, 1467, 1453, 1269, 1233, 1163, 1086, 955, 910, 814, 732, 699 cm^{-1}. LRMS (APCI+) calculated for C$_{25}$H$_{23}$NOS: 385.53, observed: 386.39 (M+H). $[\alpha]_D^{21}$ = +21 (c 0.7, CHCl$_3$).

1-(((((1*R*,2*S*)-2-(4-fluorophenyl)-1-phenylbut-3-en-1-yl)amino)methyl)naphthalen-2-ol (3.19): ^{1}H NMR (500 MHz, CDCl$_3$) δ 7.76 (d, *J* = 8.1 Hz, 1H), 7.70 (d, *J* = 8.8 Hz, 1H), 7.59 (d, *J* = 8.6 Hz, 1H), 7.37 (t, *J* = 7.7 Hz, 1H), 7.24 (dt, *J* = 13.4, 7.2 Hz, 4H), 7.13 (dd, *J* = 15.8, 8.1 Hz, 3H), 6.95 (dd, *J* = 8.3, 5.4 Hz, 2H), 6.85 (t, *J* = 8.5 Hz, 2H), 6.19 (dt, *J* = 17.0, 9.7 Hz, 1H), 5.48 – 5.17 (m, 2H), 4.22 (dd, *J* = 107.4, 14.3 Hz, 2H), 3.95 (d, *J* = 9.5 Hz, 1H), 3.64 (t, *J* = 9.5 Hz, 1H). ^{13}C NMR (75 MHz, CDCl$_3$) δ 156.58, 139.39, 138.59, 136.54, 132.32, 129.65, 129.54, 129.34, 128.90, 128.66, 128.58, 128.07, 127.88, 126.38, 122.62, 121.19, 119.44, 118.51, 115.45, 115.17, 112.66, 67.46, 57.40, 45.28. IR (neat): 3292, 3062, 2917, 1621, 1600, 1511, 1229, 1159, 748, 700 cm^{-1}. HRMS (FAB+) calculated for C$_{27}$H$_{25}$FNO: 398.1920, observed: 398.1932 (M+H). $[\alpha]_D^{20}$ = +25 (c 0.57, CHCl$_3$).

1-(((((1*R*,2*S*)-1-phenyl-2-(o-tolyl)but-3-en-1-yl)amino)methyl)naphthalen-2-ol (3.20): ^{1}H NMR (400 MHz, CDCl$_3$) δ 7.76 (d, *J* = 8.0 Hz, 1H), 7.71 (d, *J* = 8.8 Hz, 1H), 7.63 (d, *J* = 8.7 Hz, 1H), 7.44 – 7.33 (m, 1H), 7.29 – 7.24 (m, 3H), 7.24 – 7.08 (m, 6H), 7.06 – 6.99 (m, 1H), 6.95 (d, *J* = 7.6 Hz, 1H), 6.15 (dt, *J* = 16.8, 9.7 Hz, 1H), 5.41 – 5.19 (m, 2H), 4.37 (d, *J* = 14.4 Hz, 1H), 4.23 – 4.05 (m, 2H), 3.97 (t, *J* = 9.5 Hz, 1H), 2.10 (s, 3H). ^{13}C NMR (101 MHz, CDCl$_3$) δ 156.51, 139.61, 139.03, 138.95, 135.60, 132.22, 130.47, 129.16, 128.77, 128.46, 128.34, 127.86, 127.64, 127.08, 126.23, 125.99, 122.45, 121.10, 119.37, 118.04, 112.66, 66.90, 52.88, 45.27, 19.61. IR (neat): 3288, 3069, 3024, 2924, 2849, 1621, 1598,

1453, 1409, 1347, 1268, 1234, 1161, 1089, 1029, 993, 918, 857, 814, 749, 728, 700, 668, 522, 454. LRMS (APCI+) calculated for $C_{28}H_{27}NO$: 393.53, observed: 394.46 (M+H). $[\alpha]_D^{21}$ = +30 (c 0.4, CHCl$_3$).

1-(((((1R,2S)-2-cyclohexyl-1-phenylbut-3-en-1-yl)amino)methyl)naphthalen-2-ol (3.21):
^{1}H NMR (500 MHz, CDCl$_3$) δ 7.74 (d, *J* = 8.0 Hz, 1H), 7.67 (d, *J* = 8.8 Hz, 1H), 7.60 (d, *J* = 8.5 Hz, 1H), 7.43 (t, *J* = 7.4 Hz, 2H), 7.40 – 7.32 (m, 4H), 7.27 (dd, *J* = 12.7, 5.3 Hz, 1H), 7.12 (d, *J* = 8.8 Hz, 1H), 5.82 (dt, *J* = 16.9, 10.0 Hz, 1H), 5.42 – 5.05 (m, 2H), 4.15 (dd, *J* = 110.7, 14.3 Hz, 2H), 3.78 (d, *J* = 9.7 Hz, 1H), 2.39 – 2.21 (m, 1H), 1.85 – 1.49 (m, 5H), 1.49 – 1.36 (m, 1H), 1.25 – 0.90 (m, 5H). ^{13}C NMR (126 MHz, CDCl$_3$) δ 156.63, 140.93, 136.87, 132.23, 129.02, 128.83, 128.73, 128.39, 127.85, 127.78, 126.13, 122.33, 121.09, 119.72, 119.35, 112.77, 63.67, 56.98, 45.08, 37.99, 32.31, 27.54, 26.46, 26.41, 26.36. IR (neat): 3294, 3063, 3028, 2923, 2852, 1622, 1599, 1451, 1269, 1232, 1001, 911, 815, 732, 701 cm^{-1}. HRMS (FAB+) calculated for $C_{27}H_{32}NO$: 386.2470, observed: 386.2484 (M+H) ; $[\alpha]_D^{21}$ = +46 (c 0.9, CHCl$_3$).

1-(((((1R,2S)-2-(2-bromophenyl)-1-phenylbut-3-en-1-yl)amino)methyl)naphthalen-2-ol (3.22): ^{1}H NMR (500 MHz, CDCl$_3$) δ 7.76 (d, *J* = 8.0 Hz, 1H), 7.71 (d, *J* = 8.8 Hz, 1H), 7.60 (d, *J* = 8.6 Hz, 1H), 7.38 (dd, *J* = 22.1, 8.0 Hz, 2H), 7.28 – 7.18 (m, 8H), 7.15 (d, *J* = 8.8 Hz, 1H), 7.00 – 6.92 (m, 1H), 6.13 (dt, *J* = 17.0, 9.6 Hz, 1H), 5.52 – 5.16 (m, 2H), 4.39 (t, *J* = 9.3 Hz, 1H), 4.30 (d, *J* = 14.3 Hz, 1H), 4.17 – 4.09 (m, 2H). ^{13}C NMR (126 MHz, CDCl$_3$) δ 156.51, 139.99, 139.02, 137.46, 133.14, 132.23, 129.20, 129.15, 128.76, 128.41, 128.01, 127.91, 127.77, 127.40, 127.19, 126.21, 124.59, 122.44, 121.09, 119.34, 119.08,

112.56, 66.20, 55.11, 45.02. IR (neat): 3290, 3061, 3029, 2920, 2851, 1621, 1598, 1468, 1235, 1021, 911, 749, 730, 700 cm^{-1}. HRMS (FAB+) calculated for $C_{27}H_{25}BrNO$: 458.1117, observed: 458.1120 (M+). $[\alpha]_D^{21}$ = +64 (c 1.05, CHCl$_3$).

1-(((((1R,2S)-2-(2-chloropyridin-3-yl)-1-phenylbut-3-en-1-yl)amino)methyl)naphthalen-2-ol (3.23): ^{1}H NMR (400 MHz, CDCl$_3$) δ 8.28 – 8.01 (m, 1H), 7.81 – 7.63 (m, 2H), 7.63 – 7.46 (m, 2H), 7.43 – 7.32 (m, 2H), 7.28 – 7.18 (m, 5H), 7.19 – 7.09 (m, 2H), 6.13 (dt, J = 17.1, 9.6 Hz, 1H), 5.51 – 5.09 (m, 2H), 4.38 – 3.94 (m, 4H). ^{13}C NMR (126 MHz, CDCl$_3$) δ 156.42, 150.78, 149.08, 147.54, 138.67, 137.89, 136.33, 135.28, 132.23, 129.33, 128.78, 128.75, 128.16, 127.73, 126.28, 122.53, 122.40, 121.07, 120.03, 119.26, 112.41, 65.52, 52.99, 44.85. IR (neat): 3287, 3060, 3028, 2920, 2851, 1622, 1598, 1581, 1563, 1516, 1467, 1453, 1406, 1270, 1234, 1061, 911, 814, 732, 748, 701 cm^{-1}. HRMS (FAB+) calculated for $C_{26}H_{24}ClN_2O$: 415.1593, observed: 415.1577 (M+H). $[\alpha]_D^{21}$ = +69 (c 0.8, CHCl$_3$).

Cleavage Products

***tert*-butyl ((1R,2R)-2-methyl-1-phenylbut-3-en-1-yl)carbamate (3.31a):** ^{1}H NMR (400 MHz, CDCl$_3$) δ 7.38 – 7.28 (m, 2H), 7.25 – 7.18 (m, 3H), 5.71 (ddd, J = 16.5, 11.0, 7.3 Hz, 1H), 5.29 – 4.92 (m, 2H), 4.86 (s, 1H), 4.50 (s, 1H), 2.52 (s, 1H), 1.38 (s, 9H), 0.98 (d, J = 6.8 Hz, 3H). ^{13}C NMR (101 MHz, CDCl$_3$) δ 155.40, 139.57, 128.27, 126.97, 126.70, 116.10, 79.38, 58.92, 43.70, 28.33, 17.04. IR (neat): 3384, 3063, 3032, 2978, 2928, 1679, 1516, 1170, 701, 523 cm^{-1}. HRMS (FAB+) calculated for $C_{16}H_{24}NO_2$: 262.1807, observed: 262.1799. (M+H). $[\alpha]_D^{20}$ = +54 (c 0.80, CHCl$_3$).

***tert*-butyl ((1*R*,2*R*)-1-(4-bromophenyl)-2-methylbut-3-en-1-yl)carbamate (3.31b):** ^{1}H NMR (400 MHz, CDCl$_3$) δ 7.44 (d, *J* = 8.4 Hz, 2H), 7.11 (d, *J* = 8.4 Hz, 2H), 5.67 (ddd, *J* = 17.1, 10.5, 7.3 Hz, 1H), 5.25 – 5.00 (m, 2H), 4.84 (s, 1H), 4.43 (s, 1H), 2.47 (d, *J* = 11.2 Hz, 1H), 1.38 (s, 9H), 0.98 (d, *J* = 6.8 Hz, 3H). ^{13}C NMR (101 MHz, CDCl$_3$) δ 155.28, 139.08, 131.37, 128.44, 120.76, 116.58, 99.99, 79.64, 58.53, 43.48, 28.31, 16.98. IR (neat): 3376, 2985, 2968, 2931, 1680, 1518, 1165, 1008, 820, 602, 525 cm^{-1}. HRMS (FAB+) calculated for C$_{16}$H$_{23}$BrNO$_2$: 340.0912, observed: 340.0912 (M+H). $[\alpha]_D^{20}$ = +41 (c 0.95, CHCl$_3$).

***tert*-butyl ((1*R*,2*S*)-1,2-diphenylbut-3-en-1-yl)carbamate (3.32):** ^{1}H NMR (400 MHz, CDCl$_3$) δ 7.40 – 7.22 (m, 3H), 7.23 – 7.10 (m, 4H), 7.09 – 6.87 (m, 3H), 6.28 – 5.95 (m, 1H), 5.32 – 5.08 (m, 2H), 4.99 (s, 1H), 4.93 (s, 1H), 3.56 (t, *J* = 8.5 Hz, 1H), 1.40 (s, 9H). ^{13}C NMR (101 MHz, CDCl$_3$) δ 155.18, 140.48, 138.30, 128.37, 128.31, 128.01, 127.06, 126.63, 126.23, 126.17, 117.43, 79.59, 58.97, 57.14, 28.34. IR (neat): 3401, 3032, 2979, 1684, 1513, 1248, 1170, 756, 698 cm^{-1}. HRMS (FAB+) calculated for C$_{21}$H$_{26}$NO$_2$: 324.1964, observed: 324.1972 (M+H). $[\alpha]_D^{21}$ = +6.2 (c 0.80, CHCl$_3$).

***tert*-butyl ((1*R*,2*S*)-1-(4-methoxyphenyl)-2-phenylbut-3-en-1-yl)carbamate (3.33):** ^{1}H NMR (500 MHz, CDCl$_3$) δ 7.22 – 7.19 (m, 2H), 7.18 – 7.12 (m, 1H), 7.09 – 7.00 (m, 2H), 7.00 – 6.93 (m, 2H), 6.81 – 6.68 (m, 2H), 6.13 (ddd, *J* = 17.1, 10.4, 8.9 Hz, 1H), 5.27 – 5.09 (m, 2H), 4.93 (s, 2H), 3.76 (s, 3H), 3.57 (t, *J* = 8.7 Hz, 1H), 1.43 (s, 9H). ^{13}C NMR (126 MHz, CDCl$_3$) δ 158.46, 155.15, 140.59, 138.56, 128.41, 128.29, 128.12, 127.37, 126.56, 126.15, 113.40, 79.47, 57.18, 55.14, 29.70, 28.36. IR (neat): 3389, 2976, 2921, 1681, 1506,

1237, 1164, 1014, 918, 756, 556 cm^{-1}. HRMS (FAB+) calculated for C$_{22}$H$_{28}$NO$_3$: 354.2069, observed: 354.2084 (M+1). [α]$_D^{21}$ = +5.0 (c 0.43, CHCl$_3$).

tert-butyl ((1R,2S)-2-(4-fluorophenyl)-1-phenylbut-3-en-1-yl)carbamate (3.34): ^{1}H NMR (500 MHz, CDCl$_3$) δ 7.25 – 7.15 (m, 3H), 7.07 – 7.02 (m, 2H), 7.01 – 6.95 (m, 2H), 6.90 (t, J = 8.7 Hz, 2H), 6.12 (ddd, J = 17.0, 10.1, 8.6 Hz, 1H), 5.31 – 5.09 (m, 2H), 4.99 (s, 1H), 4.91 (s, 1H), 3.59 (t, J = 8.6 Hz, 1H), 1.42 (s, 9H).^{13}C NMR (101 MHz, CDCl$_3$) ^{13}C NMR (126 MHz, CDCl$_3$) δ 162.51, 160.56, 155.13, 140.73, 138.09, 136.26, 131.88, 129.81, 129.74, 128.59, 128.12, 127.64, 127.57, 127.26, 127.12, 127.01, 126.24, 125.37, 117.56, 115.45, 115.27, 115.20, 115.04, 79.66, 58.97, 56.29, 28.33 (Not ^{19}F decoupled). IR (neat): 3384, 3033, 3006, 2978, 2933, 1687, 1505, 1159, 701, 521 cm^{-1}. HRMS (FAB+) calculated for C$_{21}$H$_{25}$FNO$_2$: 342.1869, observed: 342.1875 (M+1). [α]$_D^{21}$ = +12 (c 0.95, CHCl$_3$).

tert-butyl ((1R,2S)-2-cyclohexyl-1-phenylbut-3-en-1-yl)carbamate (3.35): ^{1}H NMR (400 MHz, CDCl$_3$) δ 7.34 (dd, J = 8.6, 6.6 Hz, 2H), 7.25 (dd, J = 7.9, 5.9 Hz, 3H), 5.68 (dt, J = 17.0, 10.0 Hz, 1H), 5.17 (dd, J = 10.2, 2.0 Hz, 1H), 4.96 (dd, J = 17.1, 2.0 Hz, 1H), 4.86 (d, J = 7.7 Hz, 1H), 4.78 (s, 1H), 2.22 – 2.05 (m, 1H), 1.82 (d, J = 11.3 Hz, 1H), 1.70 (m, 2H), 1.61 (m, 2H), 1.40 (s, 9H), 1.24 – 1.04 (m, 5H), 1.04 – 0.91 (m, 1H). ^{13}C NMR (101 MHz, CDCl$_3$) δ 155.28, 136.44, 128.28, 126.87, 126.77, 118.61, 79.31, 56.53, 37.69, 31.96, 28.54, 28.34, 27.69, 26.50, 26.42, 26.38. IR (neat): 3425, 3068, 2975, 2931, 2853, 1692, 1505, 1168, 702 cm^{-1}. HRMS (FAB+) calculated for C$_{21}$H$_{32}$NO$_2$: 330.2433, observed: 330.2418 (M+1). [α]$_D^{21}$ = +9.8 (c 1.15, CHCl$_3$).

***tert*-butyl ((1*R*,2*S*)-2-(2-chloropyridin-3-yl)-1-phenylbut-3-en-1-yl)carbamate (3.36):**

^{1}H NMR (400 MHz, CDCl$_3$) δ 8.37 – 8.10 (m, 1H), 7.62 (dd, *J* = 7.8, 1.9 Hz, 1H), 7.27 – 7.24 (m, 3H), 7.24 – 7.10 (m, 4H), 6.06 (ddd, *J* = 17.0, 10.2, 8.2 Hz, 1H), 5.26 (dt, *J* = 10.2, 1.0 Hz, 1H), 5.18 (d, *J* = 17.0 Hz, 1H), 5.10 (d, *J* = 8.5 Hz, 1H), 5.03 (d, *J* = 9.0 Hz, 1H), 4.28 (t, *J* = 8.2 Hz, 1H), 1.41 (s, 9H). ^{13}C NMR (101 MHz, CDCl$_3$) δ 155.08, 151.11, 147.61, 140.03, 137.95, 135.94, 135.32, 128.49, 127.55, 126.80, 122.43, 119.02, 79.89, 57.68, 51.87, 28.29. IR (neat): 3277, 2978, 2930, 1697, 1165, 753, 701 cm^{-1}. HRMS (FAB+) calculated for C$_{20}$H$_{24}$ClN$_2$O$_2$: 359.1526, observed: 359.1521 (M+1). [α]$_D^{21}$ = +48 (c 0.8, CHCl$_3$).

Chapter 4

Bi(OTf)₃ – PyBox Catalyzed Asymmetric Allylation of Aldehydes via Strained Silanes

4.1. Introduction

In a similar manner that the asymmetric allylation of the imino group is important for the synthesis of chiral amines, the asymmetric allylation of aldehydes is one the most valuable transformation for the synthesis of chiral alcohol building blocks. A substantial amount of literature precedent on stoichiometric and catalytic systems developed for this chemical reaction has been reported.[1] Here at Columbia University, the Leighton group has largely made its contribution to this field inspired on the idea of methodology efficacy, efficiency, and scalability. In doing so, the Leighton group has developed several methods for the allylation and crotylation of aldehydes and ketones[2] by utilizing readily and inexpensively synthesized strained silane Lewis acids (Figure 4-1).

Figure 4-1: The Leighton Allylation of the Carbonyl Group
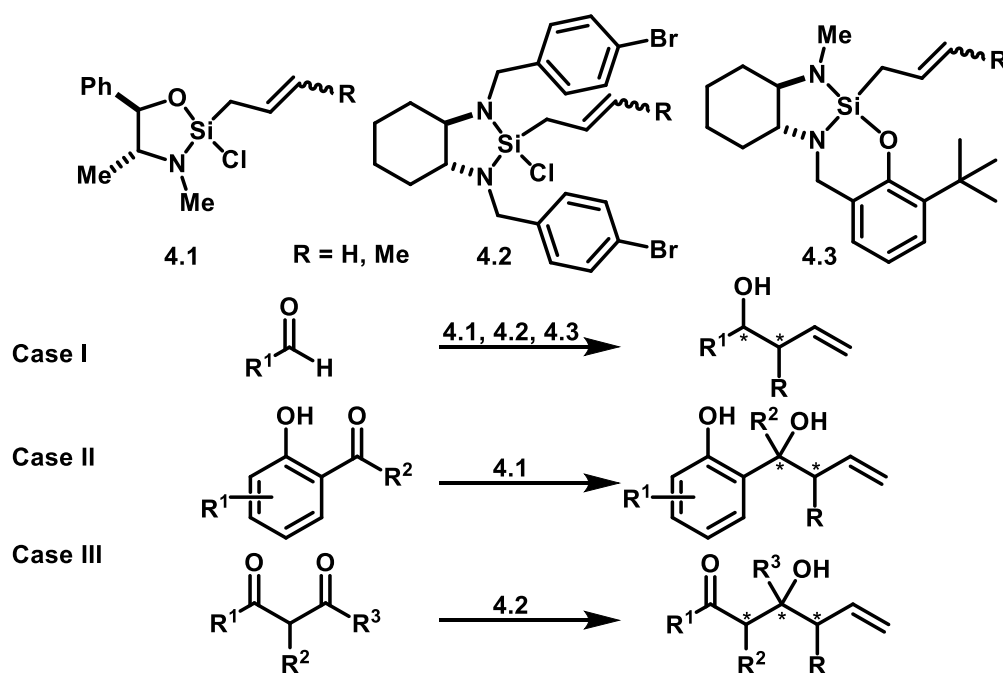
Unlike the imino group, in which a protic nucleophile (XH) is required as an activating group to boost its reactivity with the Leighton strained silane reagents, aldehydes typically do not require this extra feature. Mainly, this is due to the fact that they are inherently more electrophilic and less hindered than *N*-substituted imines; therefore, the silacycle strain release is sufficient to drive reactivity (Figure 4-1, Case I and Figure 4-2).

Figure 4-2: Imines vs. Aldehyde Allylation with Strained Silanes
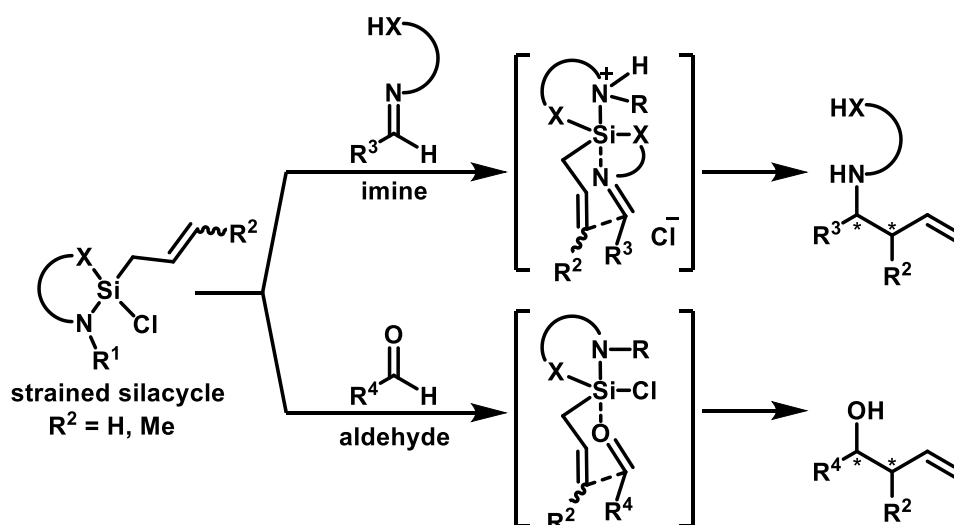
While aldehydes are the simplest and most reactive carbonyl species towards asymmetric allylation, ketones are much harder to allylate given that they are typically less electrophilic and more sterically hindered (Figure 4-1, Cases II and III). However, invoking the concept of activating groups as exemplified in imine allylations, the Leighton group has demonstrated a powerful approach to the asymmetric allylation of phenolic ketones[3] and β-diketones which are substrates that inherently contain a protic nucleophile as an activating group: the phenolic and the enol oxygens, respectively[4] (Figure 4-3). These reactions have been demonstrated to occur with high levels of enantio and diastereoselectivities.

Figure 4-3: Generic Allylation of Phenolic Ketones and β-Diketones
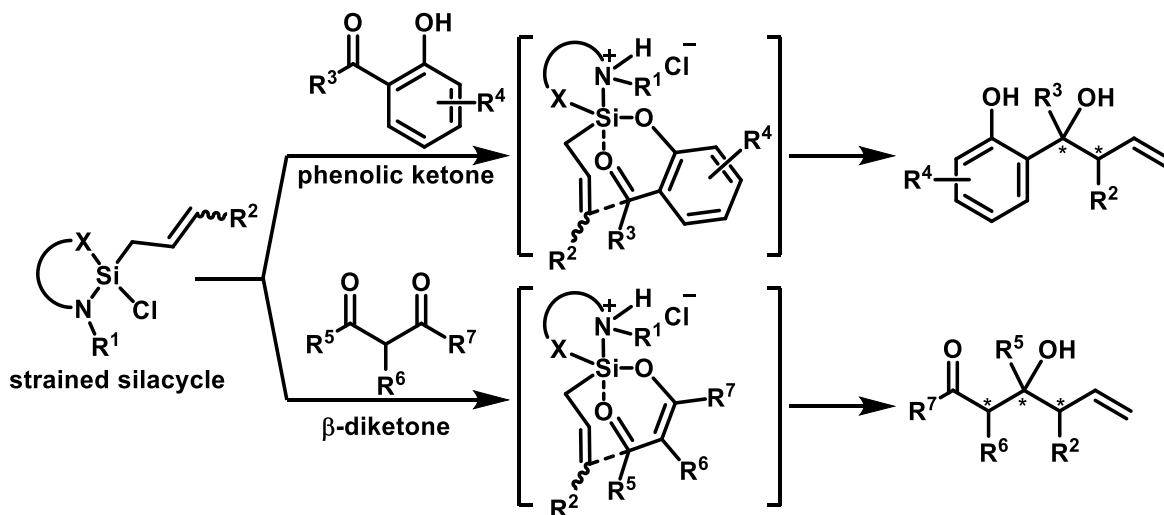

On the other hand, there are cases in which stubborn aldehyde substrates do not perform well in the Leighton allylation protocols given that they are severely hindered. For these aldehydes, the Leighton group has shown that catalytic amounts of an external Lewis acid, such as scandium (III) triflate, can dramatically accelerate the rate of allylation and crotylation reactions of standard to sterically congested aldehydes with chiral diamine-derived allylsilane reagents **4.2**[5]. This combination is also commercially known as the EZ allyl and crotyl mixes for allylation and crotylation, respectively (Figure 4-4).

Figure 4-4: EZ-Allylation of Aldehydes
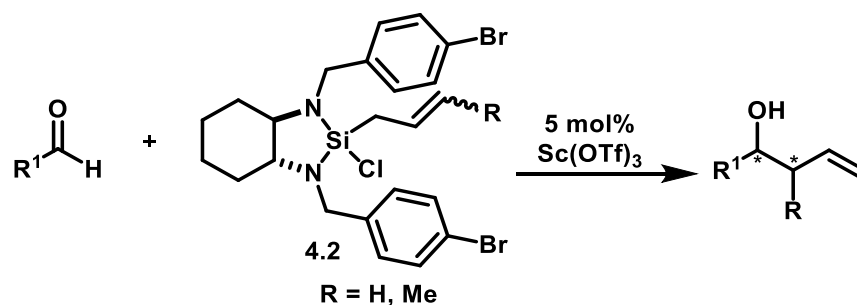
The role of scandium triflate in this methodology is thought to be analogous to that of the protic nucleophile available in imine activating groups. In imines, this protic nucleophile displaces the chloride of the reagent, generating one equivalent of HCl, which protonates the nitrogen adjacent to silicon; thus, decreasing its electron density and enhancing its Lewis acidity (Figure 4-2). In the case of scandium triflate, it can be envisioned that coordination with one of the nitrogens adjacent to the silicon will cause the same effect (Figure 4-5).

Figure 4-5: Sc(OTf)₃ Catalyzed Asymmetric Allylation of Aldehydes
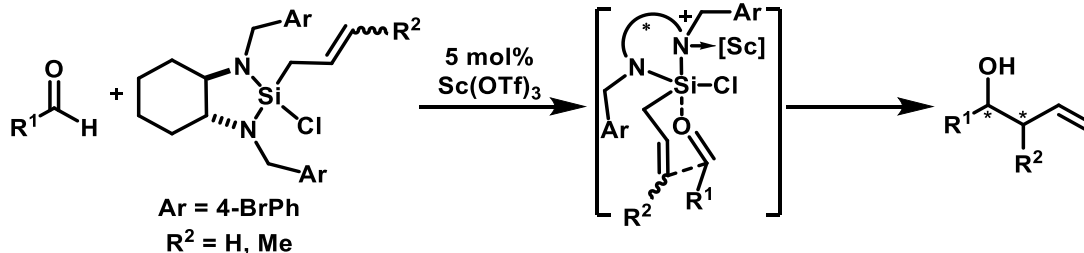
While all the previous methodologies reported have so far proved to be effective, efficient, and convenient, we wanted to further explore the catalysis avenue for the asymmetric allylation of aldehydes so that the use of stoichiometric chiral reagents could be avoided. Unlike silanes **4.1**, for which optically pure pseudoephedrine precursor can be inexpensively purchased in kilo amounts, the diamine precursor to the EZ-allyl and EZ-crotyl mixes requires a chiral resolution to reduce cost and achieve high optical purity plus a synthetic step. We envisioned that if instead an achiral strained silane **4.4** could be both activated and chirally differentiated by external catalytic amounts of either a chiral Brønsted acid[6], hydrogen-bond donor, or Lewis acid[7] species Z*, the enantioselective allylation of aldehydes could also be feasible (Figure 4-6).

Figure 4-6: Proposed Catalytic Asymmetric Allylation of Aldehydes
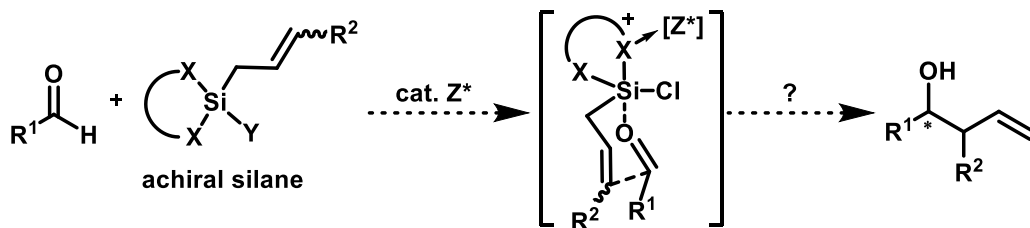
4.2. Initial Catalytic Design: Brønsted Acids as Possible Catalysts

With the idea of using achiral silanes as reagents in mind, we promptly synthesized allyl chlorosilanes derived from several commercially available achiral diols and diamines in order to study their background reactivity with aldehydes in the absence of added catalysts (Scheme 4-1).

Scheme 4-1: Synthesis of Achiral Chlorosilane Reagents
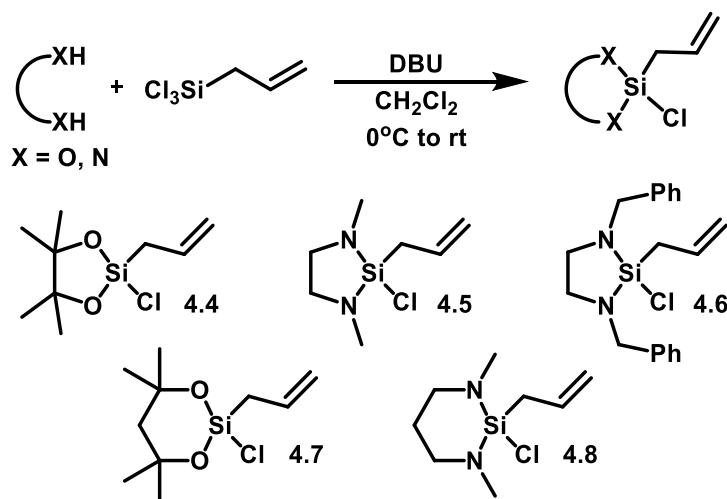
The reactivity of silanes **4.4**, **4.7**, and **4.8** towards benzaldehyde was indeed already precedented in our group. Silanes **4.7** and **4.8** were inactive even at 50°C with the exception of silane **4.4** which was active at room temperature albeit at high concentration (1.0M). Indeed, the reactivity of **4.4** was perhaps the major breakthrough discovery in the allylation

of aldehydes within the Leighton group since it represents a proof of concept for silicon strain release Lewis acidity in the oxasilacyclopentane series[8]. This seminal discovery led to the development of all of our chiral silane reagents. In agreement with that discovery, we also found that silanes **4.5** and **4.6** were also active and even more reactive as they fully converted benzaldehyde to its homoallylic alcohol at room temperature and at more dilute concentrations.

Next, we subjected benzaldehyde and hydrocinnamaldehyde to these silanes in presence of catalytic amounts of chiral Brønsted acids as potential catalysts[9] (Table 4-1). Based on the results on this table, we noticed that systems in which there was no background reaction (entries 1, 8, and 14), addition of the Brønsted acids did not afford any conversion to desired product. Conversely, systems with active background reactions (entries 5 and 11), addition of Brønsted acids did not improve the reaction rate or gave any enantioselectivity even at lower reaction temperatures (entries 6 and 7). Moreover, attempts to suppress the rate of the background reaction by introducing a hindered aldehyde only resulted in shutdown of the reaction overall (entries 8-10).

**Table 4-1: Screen of Silanes and Added Chiral Catalysts**
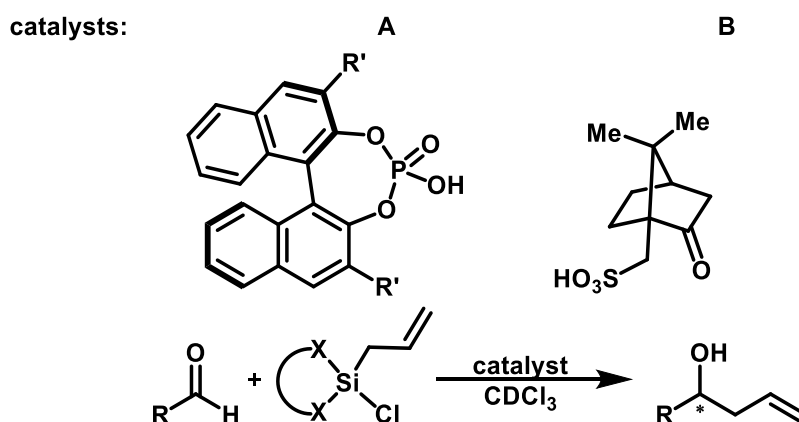
Entry	R	Silane	Catalyst	T	Time	Observations
1	Ph	4.4	no catalyst	rt	> 24 h	no reaction
2	Ph	4.4	10 mol% A, R' = H	rt	> 24 h	no reaction
3	Ph	4.4	10 mol% A, R' = H	45°C	> 24 h	no reaction
4	Ph	4.4	10 mol% B	rt	> 24 h	no reaction
5	Ph	4.5	no catalyst	rt	2 h	100% conversion
6	Ph	4.5	10 mol% A, R' = H	-10°C	> 24 h	74%, 0% ee
7	Ph	4.5	10 mol% B	-10°C	> 24 h	74%, 0% ee
8	(E)-PhCHC(CH₃)	4.5	no catalyst	rt	> 8 h	no reaction
9	(E)-PhCHC(CH₃)	4.5	10 mol% A, R' = H	rt	> 16 h	no reaction
10	(E)-PhCHC(CH₃)	4.5	10 mol% B	rt	> 24 h	no reaction
11	Ph	4.6	no catalyst	rt	4 h	****
12	Ph	4.6	10 mol% A, R' = H	rt	4 h	11%, 0% ee
13	Ph	4.6	10 mol% B	rt	4 h	38%, 0% ee
14	Ph	4.8	no catalyst	rt	> 24 h	no reaction
15	Ph	4.8	10 mol% A, R' = H	rt	> 24 h	no reaction
16	Ph	4.8	10 mol% A, R' = 3,5-CF₃Ph	rt	> 24 h	no reaction
17	Ph	4.8	10 mol% A, R' = 3,5-CF₃Ph	reflux	12 h	decomposition

4.3. Initial Catalytic Design: Chiral Lewis Acids as Potential Catalysts

We turned our attention to studying the effect of chiral Lewis acid complexes to the allylation systems reported above[10]. We initially chose scandium triflate as the Lewis acid since it has been shown to enhance the rate of aldehyde allylation with chiral diamine-derived Leighton reagents. Also, chiral complexes of scandium triflate with

pyridinebisoxazoline ligands (PyBOX) complexes are well precedented as Lewis acid catalysts in several asymmetric transformations[11] (Table 4-2).

Recalling that silane **4.4** does not display uncatalyzed background reactions with benzaldehyde or hydrocinnamaldehyde at 0.1M, the data collected on Table 4-2 reveals that only this silane is participating in the allylation catalysis by uncomplexed $Sc(OTf)_3$ (Entries 1 and 7). When $Sc(OTf)_3$ is complexed with chiral PyBOX ligands; however, the allylation is shut down for both aldehydes, in different solvents, at room temperature and at 45°C (entries 1-8). Silanes **4.5** and **4.6** had displayed uncatalyzed background allylation reactions with benzaldehyde at room temperature, so we attempted to cool down the reaction to -10°C when adding complexed $Sc(OTf)_3$ to see if we could obtain any enantioselectivity. While the yields were good, the reactions underwent a completely racemic pathway (entries 9-13). One possible explanation is that the complexed $Sc(OTf)_3$ loses catalytic activity with our silanes, as observed with silane **4.4**, allowing the racemic background allylation reaction of benzaldehyde and **4.5** and/or **4.6** to proceed. Conversely, silanes **4.7** and **4.8** do not display any reactivity with benzaldehyde or hydrocinnamaldehyde with or without any catalyst added even at higher temperatures. This is probably due to the fact that these silanes are not as strained as the five member ring silacycles; thus, they are inherently less reactive as Lewis acids.

Table 4-2: Effect of Sc(OTf)$_3$·PyBOX Complexes

PyBOX Ligands:

(R)-iPrPyBOX

(R)-PhPyBOX
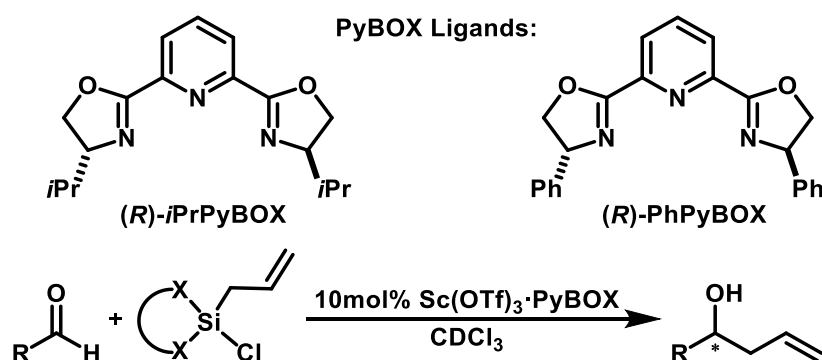
Entry	R	Silane	Catalyst	T	Solvent	Time	Observations
1	Ph	4.4	10 mol% Sc(OTf)$_3$	rt	CDCl$_3$	1 h	50% conversion
2	Ph	4.4	10 mol% Sc(OTf)$_3$ 10 mol% (R)-iPrPyBOX	rt	CDCl$_3$	> 24 h	no reaction
3	Ph	4.4	10 mol% Sc(OTf)$_3$ 10 mol% (R)-iPrPyBOX	45°C	CDCl$_3$	> 24 h	no reaction
4	Ph	4.4	10 mol% Sc(OTf)$_3$ 10 mol% (R)-iPrPyBOX	rt	Toluene	> 24 h	no reaction
5	Ph	4.4	10 mol% Sc(OTf)$_3$ 10 mol% (R)-iPrPyBOX	45°C	Toluene	> 24 h	no reaction
6	Ph	4.4	10 mol% Sc(OTf)$_3$ 10 mol% (R)-PhPyBOX	rt	CDCl$_3$	> 24 h	no reaction
7	PhCH$_2$CH$_2$	4.4	10 mol% Sc(OTf)$_3$	rt	CDCl$_3$	3 h	100% conversion
8	PhCH$_2$CH$_2$	4.4	10 mol% Sc(OTf)$_3$ 10 mol% (R)-iPrPyBOX	rt	CDCl$_3$	> 24 h	no reaction
9	Ph	4.5	10 mol% Sc(OTf)$_3$	rt	CDCl$_3$	2 h	100% conversion
10	Ph	4.5	10 mol% Sc(OTf)$_3$ 10 mol% (R)-PhPyBOX	rt	CDCl$_3$	2 h	100%, 0% ee
11	Ph	4.5	10 mol% Sc(OTf)$_3$ 10 mol% (R)-PhPyBOX	-10°C	CDCl$_3$	1 h	89%, 0% ee
12	Ph	4.6	10 mol% Sc(OTf)$_3$	rt	CDCl$_3$	2 h	100% conversion
13	Ph	4.6	10 mol% Sc(OTf)$_3$ 10 mol% (R)-PhPyBOX	rt	CDCl$_3$	2 h	93%, 0% ee
14	(E)-PhCHC(CH)$_3$	4.6	10 mol% Sc(OTf)$_3$	rt	CDCl$_3$	> 24 h	no reaction
15	Ph	4.7	10 mol% Sc(OTf)$_3$	rt	CDCl$_3$	> 24 h	no reaction
16	Ph	4.7	10 mol% Sc(OTf)$_3$	45°C	CDCl$_3$	> 24 h	no reaction
17	PhCH$_2$CH$_2$	4.7	10 mol% Sc(OTf)$_3$	rt	CDCl$_3$	> 24 h	no reaction
18	PhCH$_2$CH$_2$	4.7	10 mol% Sc(OTf)$_3$	45°C	CDCl$_3$	> 24 h	no reaction
19	Ph	4.8	10 mol% Sc(OTf)$_3$	rt	CDCl$_3$	> 24 h	no reaction
20	Ph	4.8	10 mol% Sc(OTf)$_3$ 10 mol% (R)-iPrPyBOX	rt	CDCl$_3$	> 24 h	no reaction

4.4. Changing Strategy: Modifying Silane Structure and Electronics

While we could continue screening for different backbones on allyltrichlorosilane and/or chiral Lewis acids, we decided instead to derivatize the pinacol-derived silane **4.4** since this silane showed rate acceleration and reaction completion with benzaldehyde when Sc(OTf)$_3$ was added. In addition, the Leighton group had previously shown that when benzaldehyde is subjected to allyl siloxane **4.9**, it undergoes a tandem aldol – allylation reaction to give diol **4.10** and a minor allylation product **4.11**[12] (Scheme 4-2).

Scheme 4-2: The Leighton Tandem Aldol – Allylation Reaction
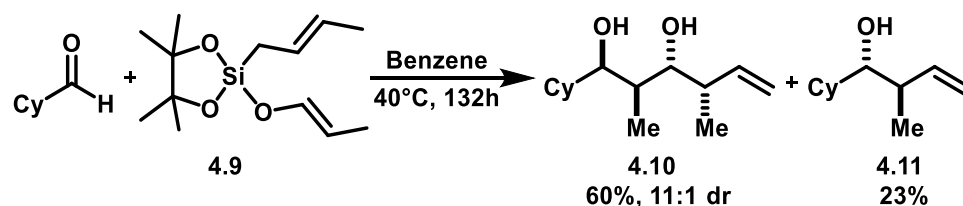
Interestingly, when catalytic amounts of Sc(OTf)$_3$ were added to the above reaction, overall rate acceleration was observed along with an increased ratio of direct allylation product **4.11** to tandem product **4.10**[13]. Presumably, this is due to coordination of the silyl enol ether oxygen to Sc(OTf)$_3$, which could decrease its inherent nucleophilicity to effect the aldol reaction; therefore, allowing direct allylation to occur more facile (Scheme 4-3).

Scheme 4-3: Effect of Sc(OTf)$_3$ on Tandem Aldol – Allylation Reaction
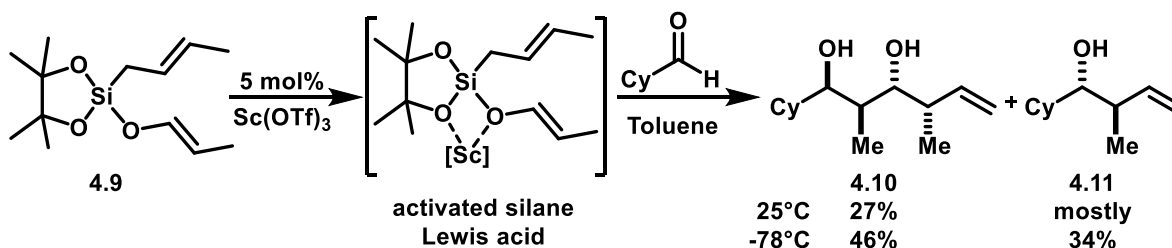
While this observation was perhaps detrimental for the purposes of the tandem aldol-allylation methodology, it served as a model to redesign our catalytic system. For simplicity, we substituted the chloride in **4.4** with a methoxy group. This transformation was easily achieved by stirring **4.4** with DBU and methanol from 0°C to room temperature to obtain **4.12** in 74% yield[14] (Scheme 4-4).

Scheme 4-4: Preparation of 1-allyl-1-methoxy-1,1'-pinacol silane
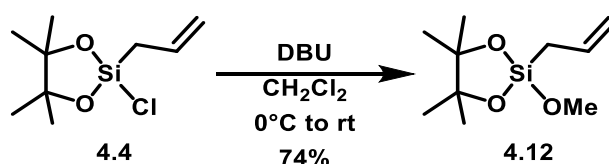
With silane **4.12** in hand, we tested its performance in allylation reactions with benzaldehyde in presence of the previously discussed Brønsted acids and Lewis acid catalysts (Table 4-3).

Table 4-3: Probing the Reactivity of Allylsiloxane
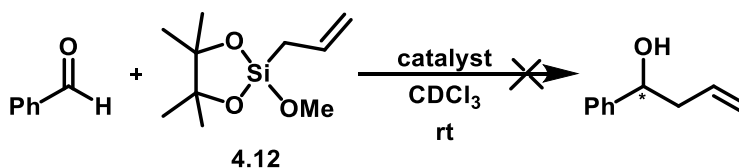
Entry	Catalyst
1	no catalyst
2	10 mol% A, R = H*
3	10 mol% Bi*
4	10 mol% Sc(OTf)$_3$
5	10 mol% Sc(OTf)$_3$ 15 mol% (*R*)-PhPyBOX

* Refer to Table 4-1 catalysts

While the results presented on Table 4-3 were not encouraging, we decided to screen other Lewis acids with this latter system since we had changed the silane electronics

by going from **4.4** to **4.12**, and hard and soft acid-base interactions could play an important role. We chose among several metal triflates to perform the screen: $Sc(OTf)_3$, $In(OTf)_3$, $La(OTf)_3$, $Bi(OTf)_3$, $Y(OTf)_3$, $Yb(OTf)_3$, $Zn(OTf)_2$, and $Cu(OTf)_2$. We were glad to find out that both indium (III) triflate and bismuth (III) triflate were able to catalyze the allylation of benzaldehyde with **4.12** at room temperature while the other metal triflates were virtually inert to the reaction conditions. With these findings, we complexed both $In(OTf)_3$ and $Bi(OTf)_3$ to commercially available chiral BOX and PyBOX ligands and used these complexes as chiral Lewis acid catalysts (Table 4-4).

Table 4-4: Chiral In(OTf)₃/Bi(OTf)₃ – BOX/PyBOX Complexes as Catalysts
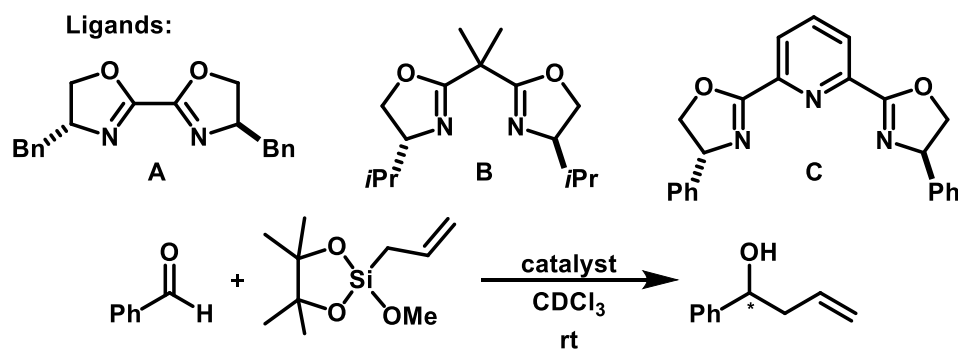
Entry	Catalyst	% Yield, % ee	Observations
1	10 mol% In(OTf)₃ 15 mol% A	no reaction	---
2	10 mol% In(OTf)₃ 15 mol% B	no reaction	---
3	10 mol% In(OTf)₃ 15 mol% C	no reaction	---
4	10 mol% Bi(OTf)₃ 15 mol% A	75%, 16% ee	---
5	10 mol% Bi(OTf)₃ 15 mol% B	84%, 0% ee	---
6	10 mol% Bi(OTf)₃ 15 mol% C	96%, 46% ee	---
7	10 mol% Bi(OTf)₃ 15 mol% C	15%*, 68% ee	with 4 ÅMS
8	10 mol% Bi(OTf)₃ 15 mol% C	20%*, 9% ee	with 50 mol% iPr₂NEt
9	10 mol% Bi(OTf)₃ 15 mol% C	100%*, 35% ee	1 h complexation
10	10 mol% Bi(OTf)₃ 15 mol% C	72%*, 0% ee	from silane 4.4

* %conversion

While we found that In(OTf)$_3$ complexes with either BOX or PyBOX ligands were not active catalysts (Entries 1-3), we were glad to discover that Bi(OTf)$_3$ complexes do catalyze the allylation of benzaldehyde. Among the three ligands tested, (*R*)-PhPyBOX gave the best results in terms of yield (96%) and enantioselectivity (46% ee) for the corresponding homoallylic alcohol **4.13** (Table 4-4, Entry 6). We screened a few additional conditions with the same ligand in order to study their impact on catalysis and selectivity. We found that by running the reaction with activated molecular sieves, or adding Hunig's base as a scavenger for adventitious acid, or doubling the time of the metal – ligand complexation did not improve the originally obtained results. We also applied our best conditions (Entry 6) using silane **4.4**, but we found that while the reaction is in fact catalyzed, we observed no enantioselectivity. Presumably, this is an indication that the methoxy oxygen on silane **4.12** does not only play an important role for reactivity, but also for enantioselectivity.

4.5. Bi(OTf)$_3$·PyBOX Catalyzed Asymmetric Allylation of Aldehydes

With goals now set on reaction optimization, we screened several other PyBOX ligands under our best behaved conditions (Table 4-5). The best enantioselectivities for benzaldehyde allylation were observed when using chiral phenethyl PyBox **B** and IndaPyBOX **D** (Entries 2 and 4). Using chiral PyBox **C** resulted in lower enantioselectivity and much slower reactions times (Entry 3). Finally, using chiral PyBOX **A** completely shut down the reaction. Based on the results from Tables 4-4 and 4-5, it seems like the reaction rate is sensitive to the ligand's denticity and steric bulk since the larger these two parameters become, the slower the reaction proceeds. Also, ligand denticity seems to

drastically affect the reaction selectivity since bidentate BOX ligands gave much lower selectivities than the tridentate PyBOX ligands. This might be partly due to further projection of the chiral groups from the ligand towards the metal center and tighter binding of the bismuth as the ligand denticity increases.

Table 4-5: PyBOX Ligand Screen
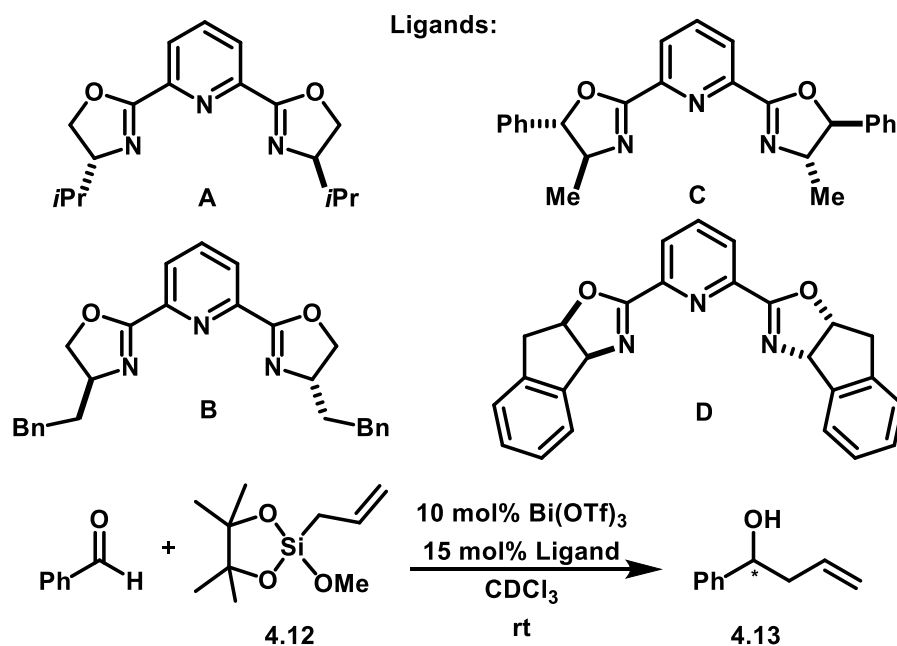
Entry	Catalyst	% ee
1	10 mol% Bi(OTf)₃ 15 mol% A	No reaction
2	10 mol% Bi(OTf)₃ 15 mol% B	89.5% ee
3	10 mol% Bi(OTf)₃ 15 mol% C	29% ee
4	10 mol% Bi(OTf)₃ 15 mol% D	92% ee

Given that the IndaPyBOX ligand provided the best selectivity, we proceeded to screen solvents for continuing our reaction optimization. We found that dichloromethane and 1,2-dichloroethane were the most optimal for both yield and selectivity for the

asymmetric allylation of benzaldehyde (Scheme 4-5). The reactions were run at room temperature and took 48 hours for full conversion.

Scheme 4-5: Optimized Catalytic Asymmetric Allylation of Benzaldehyde
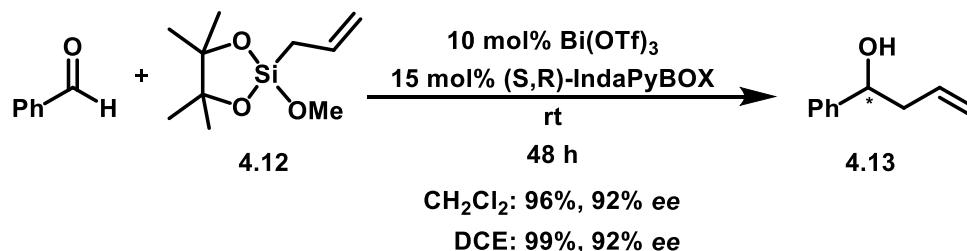
In order to further explore the catalytic power of our chiral Bi(OTf)$_3$·IndaPyBOX complex, we attempted to lower the catalyst loading. However, this just led to much longer reaction times (»48 hours). In addition, attempts to speed the rate of the reaction by heating led to complete shutdown of the reaction. This is presumably due to catalyst decomposition[15] or change in its coordination state to an inactive species since the starting materials remain intact. Finally, attempts to speed the reaction rate by increasing the concentration of the starting materials only resulted in lower enantioselectivities and variable reaction times. While we tried to study the reaction behavior over time by ^{1}H NMR at higher concentrations, the spectral analysis became much more complicated as other unidentifiable species besides starting materials and product were observed.

In order to explore the performance of other aldehydes in the protocol shown in Scheme 2-3, we subjected hydrocinnamaldehyde and *trans*-α-methylcinnamaldehyde as representative examples of aliphatic and hindered substrates, respectively (Table 4-6). We were delighted to find out that reactions with these aldehydes afforded the corresponding

homoallylic alcohols in excellent enantioselectivity albeit in moderate yield in the case of *trans*-α-methylcinnamaldehyde. However, this comes as no surprise since this aldehyde has been shown to be a difficult substrate due to its steric hindrance in previous Leighton allylation methodologies[16].

Table 4-6: Substrate Scope of the Bi(OTf)₃·IndaPyBOX Catalyzed Allylation

RCHO	% Yield	% ee
Ph (benzaldehyde)	99%	92%
Ph—CH₂CH₂—CHO	97%	94%
Ph—CH=C(Me)—CHO	60%	96%
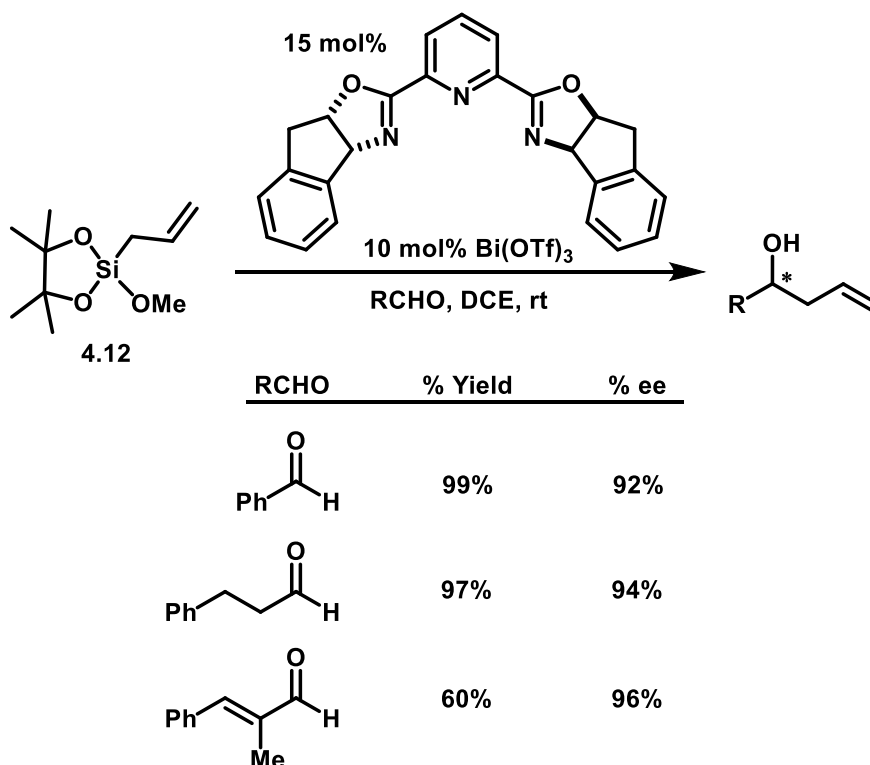
4.6. Experimental Challenges

After studying the substrates shown in Table 4-6, we wanted to test the silane's performance with more synthetically valuable aldehydes such as chiral β-silyloxy and β-alkoxy aldehydes. With the former types of aldehydes, we found that reaction progress was similar to the previously shown substrates, but regardless of silyl group size and stability and work up conditions tried, we observed cleavage of the silyl group. Further, the β-*p*-

methoxybenzyl aldehydes proved incompatible with our allylation conditions as major decomposition was observed, presumably because of the Lewis acidic bismuth species and/or silane[17]. Moreover, with the β-benzyloxy-derived Roche aldehyde, we observed lower reaction yields and low diastereoselectivities (Scheme 4-6).

Scheme 4-6: Allylation of β-benzyloxy Chiral Aldehyde
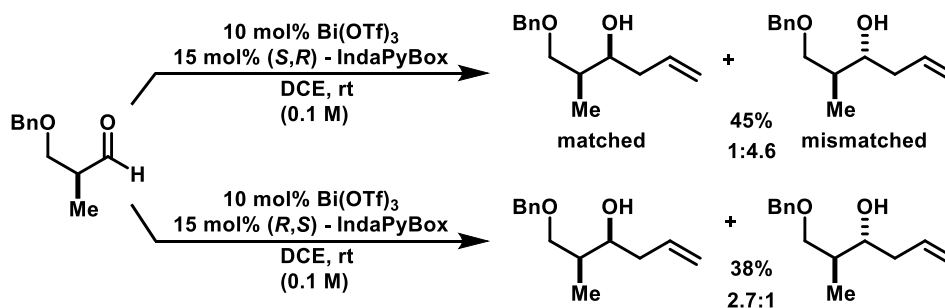
We originally thought that we had perhaps reached within the limits of our methodology given that chiral aldehydes of this sort are well behaved substrates with chiral diamine-derived strained allylsilanes. For control purposes, we decided to test the reagent and catalyst quality, so we attempted to reproduce the allylation of benzaldehyde with our current method, and we observed significant erosion of enantioselectivity (45% *ee* compared to 92% *ee* initially reported). Given that triflic acid does catalyze the allylation of benzaldehyde with silane **4.12**, we suspected that trace amounts of the acid were responsible for activating a racemic pathway for the reaction; thus, resulting in erosion of enantioselectivity. In order to test this hypothesis, we added 5 mol% of 2,6-di*tert*-butyl-4-methyl pyridine as part of the complexation stage of Bi(OTf)$_3$ and (*S,R*)-IndaPyBOX, and we were glad to find out that the enantioselectivity was even higher than initially reported (96% *ee*, see Table 4-7). We were successfully able to reproduce this result under identical

conditions and also at twice the scale and at twice the concentration, separately. While we were glad to find a way to circumvent the racemic pathway triggered by triflic acid, we also found that the rate of the reaction was significantly depressed by its absence. For instance, conversions of 20% were observed at 48 hours with the base additive versus 100% conversion at the same reaction time without it, suggesting that small amounts of acid also play an important role in the reaction rate. At first sight, these observations lead us to believe that perhaps with quantitatively controlled amounts of acid, we could find a balance between the reaction rate and enantioselectivity. This could be a possible explanation for the original high yielding and enantioselective results observed in Table 4-6 where no base additives were used. However, given that we initially used 5 mol% of the base additive, which is already half of the $Bi(OTf)_3$ loading in the reaction, we envisaged that any excess base remaining after scavenging the partially hydrolyzed $Bi(OTf)_3$ could be responsible of inhibiting the unhydrolized $Bi(OTf)_3$ ability to generate the active chiral complex catalyst with the PyBOX ligand. In order to test this hypothesis, we treated the $Bi(OTf)_3$•PyBOX mixture with different loadings of the base additive (Table 4-7). We found that when lower base loading (3 mol%) was used, the reaction proceeded relatively faster and with equally high enantioselectivity. Conversely, when higher loading (15 mol%) of the base was used, the reaction was significantly slower yet still highly enantioselective. These experimental results reconfirmed our hypothesis that triflic acid was the cause of enantioselectivity erosion as it can catalyze the racemic background allylation reaction. Moreover, these results also confirm that there is indeed a negative effect towards active catalyst formation by having excess base additive present in the reaction. While the nitrogen in 2,6-di*tert*-

butyl-4-methylpyridine is known to be very sterically hindered and just capable of accepting a proton[18], we believe that such negative effect that this base poses in our chemistry is due to its binding to Bi(OTf)$_3$, which inhibits the formation of the chiral active catalyst. This binding seems to be slowly reversible since the reaction still proceeds even in excess of the base additive relative to the total loading of Bi(OTf)$_3$. Other alternatives to circumvent the rate depression problem could involve exploring other basic and non-nucleophilic systems, and/or increasing the concentration of the reaction, and/or further modifying silane structure and electronics to render it more Lewis acidic. Future work for further optimization of this procedure should definitely be the focus of this project.

Table 4-7: Effect of 2,6-di*tert*-butyl-4-methylpyridine

MDTBP X mol%	sm : pdt 48 h	% ee
3	~3:1	96
5	~4:1	96
15	~7:1	96
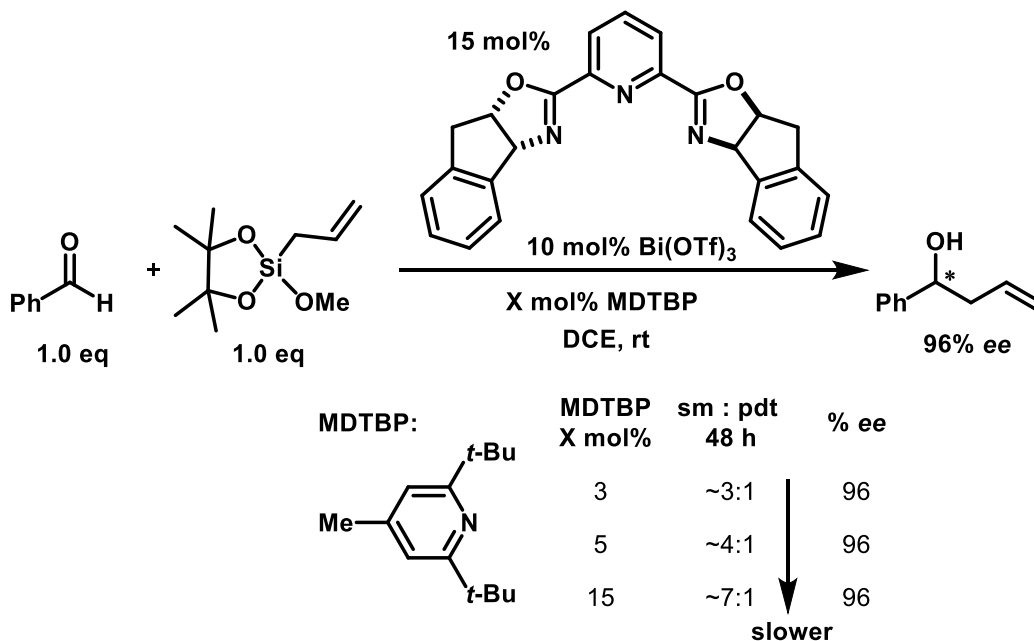
4.7. Mechanistic Insights

Having shown the proof of concept that external chiral Lewis acids can catalyze enantioselective allylation of aldehydes, we turned our attention to obtain information about

how the reaction works. In particular, we were interested in the role of the methoxy group in silane **4.12** and its presumed coordination with the chiral Lewis acid species as it was hypothesized in the Tandem aldol-allylation case with Sc(OTf)$_3$. In order to do this, we changed a few features of the silane. We synthesized silanes **4.14** and **4.15** and subjected them to the reaction conditions in Table 4-5. We found out that the reactions with these silanes proceeded much more slowly and were also much less selective than with silane **4.12** (Scheme 4-7).

Scheme 4-7: Comparison of Rate and Selectivity between Silanes
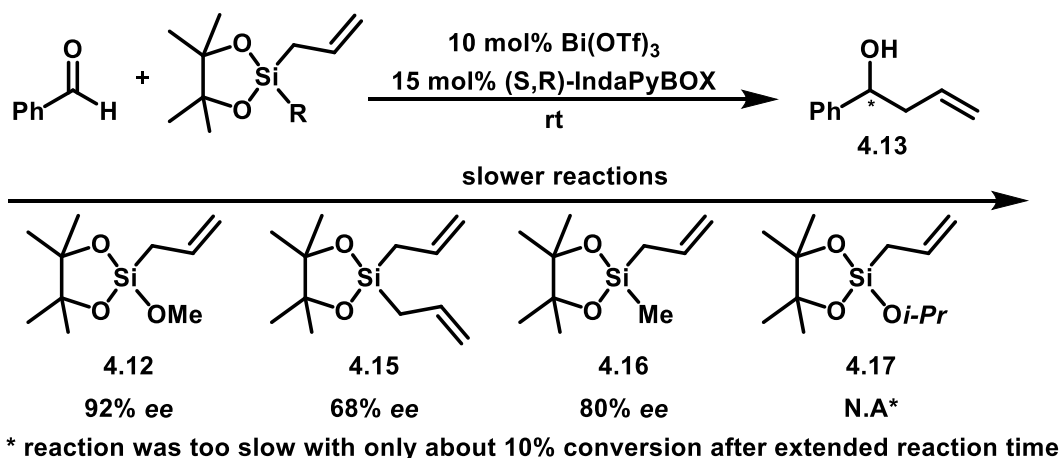
The silanes shown in scheme 4-7 do not exhibit racemic background allylation reactions with benzaldehyde under the conditions shown. The fact that these reactions even occur with addition of the chiral Lewis acid complex is highly suggestive that one of the oxygens in the pinacol backbone is involved in coordination with the chiral Lewis acid for activation. While one could claim that the chiral Lewis acid is activating the aldehyde for allyl transfer in a Sakurai Type II allylation reaction[19], the siloxanes shown above are not nucleophilic as the prototypical trialkylallylsilanes required in these reactions. In addition,

the slower reaction rates observed in absence of the methoxy substituent could be indicative that this group might also be involved in the transition state by coordinating to the chiral Lewis acid. It is noteworthy to point out that when the methoxy group is changed to isopropoxy in silane **4.17**, the reaction barely gives any conversion, which could be attributed to the inability of the alkoxy oxygens to bind the Lewis acid due of sterics. Moreover, since the reactions also display a drop in enantioselectivity, it could further suggest that the methoxy group participates in the enantio-determining step, providing a more highly organized transition state. These observations are consistent with that of the effect of scandium triflate in the tandem aldol-allylation of aldehydes presented in section 4.4 and in the crotylation of aldehydes with chiral diamine-derived allylsilanes referred to in section 4.1.

4.8. Conclusions

We have developed a catalytic enantioselective approach to the asymmetric allylation of aldehydes using chiral Bi(OTf)$_3$.PyBOX in combination with achiral strained allyl silane reagents. Representative allylation examples of aromatic, aliphatic, and hindered aldehydes have been demonstrated in this methodology, affording the corresponding homoallylic alcohols in good yields and high enantioselectivities. Progress remains to be done to better understand the mechanism of this reaction so that its full potential can be exploited. In doing so, one could more efficiently expand the substrate scope to more elaborate and synthetically valuable aldehydes. This method is by far, to the best of our knowledge, the first reported Lewis acid-catalyzed allylation of aldehydes using achiral strained allyl silane reagents[20].

4.9. References

1. See discussion in Chapter 1, section 1.1.1.

2. See references:

a) Kinnaird, J. W. A.; Ng, P. Y.; Kubota, K.; Wang, X.; Leighton, J. L. *Journal of the American Chemical Society* **2002**, *124*, 7920–7921.

b) Kubota, K.; Leighton, J. L. *Angewandte Chemie (International ed. in English)* **2003**, *42*, 946–8.

c) Hackman, B. M.; Lombardi, P. J.; Leighton, J. L. *Organic letters* **2004**, *6*, 4375–7.

d) Burns, N. Z.; Hackman, B. M.; Ng, P. Y.; Powelson, I. A.; Leighton, J. L. *Angewandte Chemie, International Edition* **2006**, *45*, 3811–3813.

e) Kim, H.; Ho, S.; Leighton, J. L. *Journal of the American Chemical Society* **2011**, *133*, 6517–6520.

f) Chalifoux, W. A.; Reznik, S. K.; Leighton, J. L. *Nature* **2012**, *487*, 86–89.

g) Reznik, S. K.; Marcus, B. S.; Leighton, J. L. *Chemical Science* **2012**, *3*, 3326–3330.

h) Suen, L. M.; Steigerwald, M. L.; Leighton, J. L. *Chemical Science* **2013**.

3. Burns, N. Z.; Hackman, B. M.; Ng, P. Y.; Powelson, I. A.; Leighton, J. L. *Angewandte Chemie, International Edition* **2006**, *45*, 3811–3813.

4. Chalifoux, W. A.; Reznik, S. K.; Leighton, J. L. *Nature* **2012**, *487*, 86–89.

5. Kim, H.; Ho, S.; Leighton, J. L. *Journal of the American Chemical Society* **2011**, *133*, 6517–6520.

6. See references:

a) Yu, S. H.; Ferguson, M. J.; McDonald, R.; Hall, D. G. *Journal of the American Chemical Society* **2005**, *127*, 12808–9.

b) Jain, P.; Antilla, J. C. *Journal of the American Chemical Society* **2010**, *132*, 11884–11886.

7. See references:

a) Kennedy, J. W. J.; Hall, D. G. *Journal of the American Chemical Society* **2002**, *124*, 11586–11587.

b) Lachance, H.; Lu, X.; Gravel, M.; Hall, D. G. *Journal of the American Chemical Society* **2003**, *125*, 10160–1.

c) Rauniyar, V.; Hall, D. G. *Angewandte Chemie (International ed. in English)* **2006**, *45*, 2426–8.

d) Rauniyar, V.; Zhai, H.; Hall, D. G. *Journal of the American Chemical Society* **2008**, *130*, 8481–90.

8. See references:

a) Zacuto M. J.; Leighton, J. L. *Journal of the American Chemical Society* **2000**, *122*, 8587–8588.

b) Kinnaird, J. W. A.; Ng, P. Y.; Kubota, K.; Wang, X.; Leighton, J. L. *Journal of the American Chemical Society* **2002**, *124*, 7920–7921.

9. Jain, P.; Antilla, J. C. *Journal of the American Chemical Society* **2010**, *132*, 11884–11886.

10. Lachance, H.; Lu, X.; Gravel, M.; Hall, D. G. *Journal of the American Chemical Society* **2003**, *125*, 10160–1.

11. Desimoni, G.; Faita, G.; Quadrelli, P. *Chemical Reviews* **2003**, *103*, 3119–3154.

12. See references:

a) Wang, X.; Meng, Q.; Nation, A. J.; Leighton, J. L. *Journal of the American Chemical Society* **2002**, *124*, 10672–10673.

b) Wang, X.; Meng, Q.; Perl, N. R.; Xu, Y.; Leighton, J. L. *Journal of the American Chemical Society* **2005**, *127*, 12806–12807.

13. Wang, X. Strained silacycles in organic synthesis: The Tandem Aldol-Allylation/Aldol-Aldol Reactions and their Asymmetric Variations. Columbia University: United States -- New York, 2005. Ch. 3, pp. 33-38.

14. See attached ^{1}H NMR spectrum in the Appendix.

15. While Bi(OTf)$_3$ has been reported to decompose above 100°C when uncomplexed, it may be more susceptible when complexed:

    Suzuki, H.; Komatsu, N.; Ogawa, T.; Murafuji, T.; Ikegami, T.; Matano, Y. *Organobismuth Chemistry*; Elsevier, 2001. Chapter 2.

16. Kim, H.; Ho, S.; Leighton, J. L. *Journal of the American Chemical Society* **2011**, *133*, 6517–6520.

17. *p*-Methoxybenzyl groups have been shown to be a bit problematic in our silane allylation methodologies using Sc(OTf)$_3$ as a Lewis acid in the diamine series. Presumably, this is due facilitation for the formation of the highly reactive *p*-quinone methide intermediate.

    Kim, H.; Ho, S.; Leighton, J. L. *Journal of the American Chemical Society* **2011**, *133*, 6517–6520.

18. Brown, H.C.; Kanner, B. *Journal of the American Chemical Society* **1953**, *75*, 3865

19. See discussion in the introduction of Chapter 1

20. Also, chiral Bi^{3+} complexes as catalysts are rare in the literature. A recent example of chiral Bi(OTf)$_3$·BiPy has been reported to asymmetrically catalyze Mukaiyama aldol reactions of silyl enol ethers and aldehydes with water as a co-solvent.

a) Kobayashi, S.; Ogino, T.; Shimizu, H.; Ishikawa, S.; Hamada, T.; Manabe, K. *Organic Letters* **2005**, *7*, 4729–4731.

4.10. Experimental Section

All reactions were carried out in flame-dried glassware under an inert atmosphere of nitrogen with magnetic stirring unless otherwise indicated. Methylene chloride and toluene were obtained from Fisher and purified by degassing with argon followed by passage through an activated neutral alumina column. Triethylamine was purchased from Alfa Aesar and purified by distillation from CaH_2 then stored under nitrogen. Pentane (HPLC grade) was purchased from Fisher and used as received. Anhydrous chloroform (stabilized with amylenes) and 1,2-dichloroethane were purchased from Aldrich and used as received. Aldehydes and all other reagents were purchased from Aldrich and used as received. ^{1}H NMR spectra were recorded on Avance III 400SL (400 MHz) or Avance III 500 Ascend (500 MHz) spectrometers. ^{1}H NMR chemical shifts (δ) are reported in parts per million (ppm) relative to tetramethylsilane internal standard (0 ppm) or DMSO-*d* internal standard (2.50 ppm). Data are reported as follows: (s = singlet, br s = broad singlet, d = doublet, br d =broad doublet, t = triplet, q = quartet, quint = quintet, dd = doublet of doublets, dq = doublet of quartets, ddd = doublet of doublet of doublets, ddt = doublet of doublet of triplets, m = multiplet; integration; coupling constant in Hz; assignment). Proton decoupled ^{13}C NMR spectra were recorded on Avance III 400SL (100 MHz) or Avance III 500 Ascend (125 MHz) or Bruker DPX-300 (75 MHz) spectrometers and are reported in ppm from $CDCl_3$ internal standard (77.16 ppm) or DMSO-*d* internal standard (39.52 ppm). HPLC Analysis was performed using an Agilent 1200 Seriers HPLC.

Preparation of Silane 4.12

In a flame-fried 500 mL reound bottom flask, dissolved allyltrichlorosilane (14 mL, 96.6 mmol) in CH_2Cl_2 (220 mL). The solution was stirred and cooled to 0°C and added DBU (28 mL, 187 mmol) slowly. Pinacol (11 g, 92.8 mmol) was then slowly added at 0°C as a solution in CH_2Cl_2 (30 mL) via addition funnel. The ice bath was allowed to expire to room temperature overnight (or in about 2-3 hours – check ^{1}H NMR). The resulting pale yellow solution was cooled to 0°C and added DBU (14 mL, 93.6 mmol), followed by anhydrous methanol (4 mL, 98.6 mmol). The reaction can be left overnight to reach room temperature or stopped after completion in about 2-3 hours (check ^{1}H NMR). The solvent was concentrated under vacuum and the residue was triturated with diethyl ether. Vigorous stirring is required as the DBU salts tend to glue to the bottom of the flask. After the salts were nicely suspended and freely stirring in the flask, the mixture was filtered using an air-free frit. The filtrate was evaporated under vacuum, and the residue was purified by vacuum distillation (40°C, 0.2-0.5 mm Hg) to give a colorless clear oil (14.8 g, 74% yield). ^{1}H NMR (300 MHz, CDCl$_3$) δ 5.80 (ddt, $J = 17.7$, 10.0, 7.8 Hz, 1H), 5.13 − 4.83 (m, 2H), 3.58 (s, 3H), 1.73 (dt, $J = 7.7$, 1.4 Hz, 2H), 1.25 (d, $J = 12.8$ Hz, 12H). ^{13}C NMR (75 MHz, CDCl$_3$) δ 131.78, 115.42, 81.27, 51.16, 25.81, 25.75, 19.09. ^{29}Si NMR (60 MHz, CDCl$_3$) δ -30.54. The reagent is stored under nitrogen at -20°C. The reagent has a stable shelf life over several months.

General Procedure for the Catalytic Asymmetric Allylation of Aldehydes (Table 4-6):

A *Fisherbrand*[®] disposable culture tube (borosilicate glass, 13 x 100 mL) was equipped with a stir bar, flame-dried under vacuum, and backfilled with dry nitrogen gas once at room temperature. The tube above was charged with bismuth triflate (14 mg, 10 mol%) and (*S,R*)-IndaPyBOX (13 mg, 15 mol%), followed by anhydrous dichloromethane or DCE at room temperature. The contents were well mixed for 30 minutes[1]. The starting heterogeneous mixture became homogeneous in the first 5-10 minutes. Silane **4.12** (0.226 mmol) was then added to the above mixture at room temperature and stirred for additional 10 minutes. A yellow coloring was observed a few minutes later. Finally, the aldehyde was added at room temperature and allowed to stir for 48 hours. The reaction was cooled to 0°C and quenched with TBAF (0.45 mL, 2 equiv., 1.0M in THF) and allowed to reach room temperature while stirring. Solvents were evaporated under vacuum, and the reaction crude was purified via silica gel chromatography (solvent gradient: 100% to 80% hexanes/ethyl acetate). The resulting products in Table 4-6 have been previously synthesized and characterized before in our group, so absolute stereochemistry was obtained by comparing with originally reported HPLC traces[2].

Modified Procedure for the Catalytic Asymmetric Allylation of Aldehydes (high *ee*):

The reaction vessel (3-dram vial or base bathed round bottom flask) was equipped with a stir bar, flame-dried under vacuum, and backfilled with dry nitrogen gas once at room temperature. The tube above was charged with bismuth triflate (14 mg, 10 mol%), (*S,R*)-

---

[1] According by ^{1}H NMR of a 1:1 mixture of $Bi(OTf)_3$ and IndaPyBOX, there are no observable changes in chemical shifts after 10 minutes. Originally, reactions were run after thirty minutes of complexation.

[2] Kinnaird, J. W. A.; Ng, P. Y.; Kubota, K.; Wang, X.; Leighton, J. L. *Journal of the American Chemical Society* **2002**, *124*, 7920–7921.

IndaPyBOX (13 mg, 15 mol%), and 2,6-di*tert*-butyl-4-methyl pyridine (10 mg, 5 mol%), followed by anhydrous dichloromethane or DCE at room temperature. The contents were well mixed for 30 minutes. Silane **4.12** (0.226 mmol) was then added to the above mixture at room temperature and stirred for additional 10 minutes, followed by addition of the aldehyde at room temperature and allowed to stir for 48 hours (for *ee* measurement purposes, reaction takes longer time for completion). The reaction was cooled to 0°C and quenched with TBAF (0.45 mL, 2 equiv., 1.0M in THF) and allowed to reach room temperature while stirring. Solvents were evaporated under vacuum, and the reaction crude was purified via silica gel chromatography (solvent gradient: 100% to 80% hexanes/ethyl acetate).

Appendix

I.   NMR Spectra
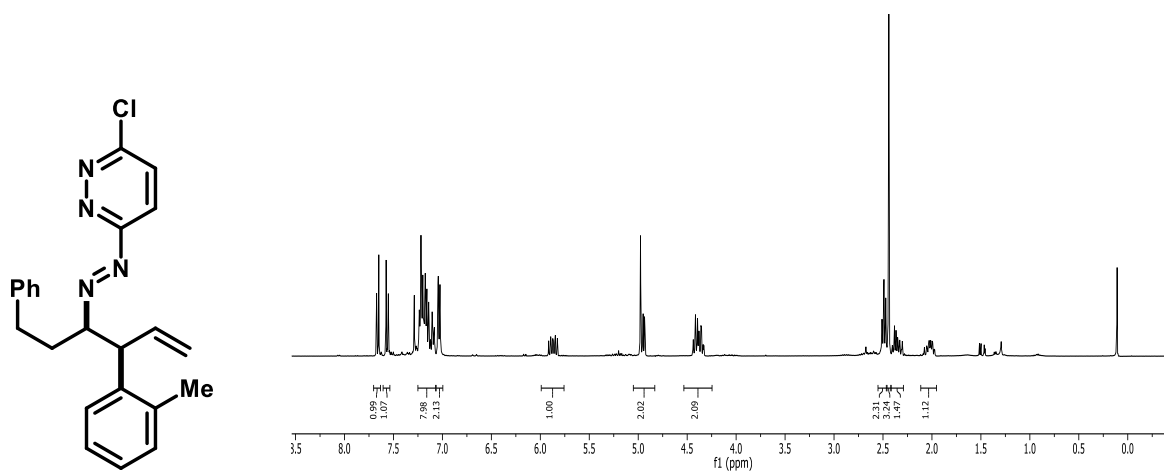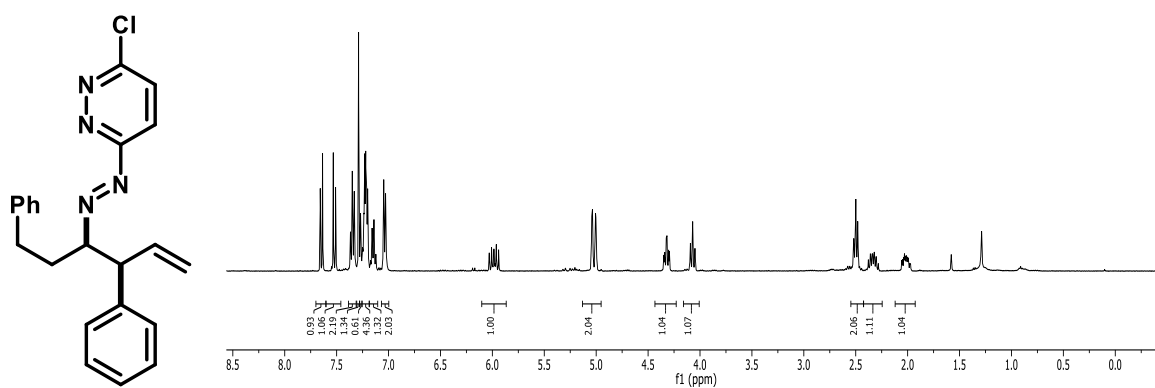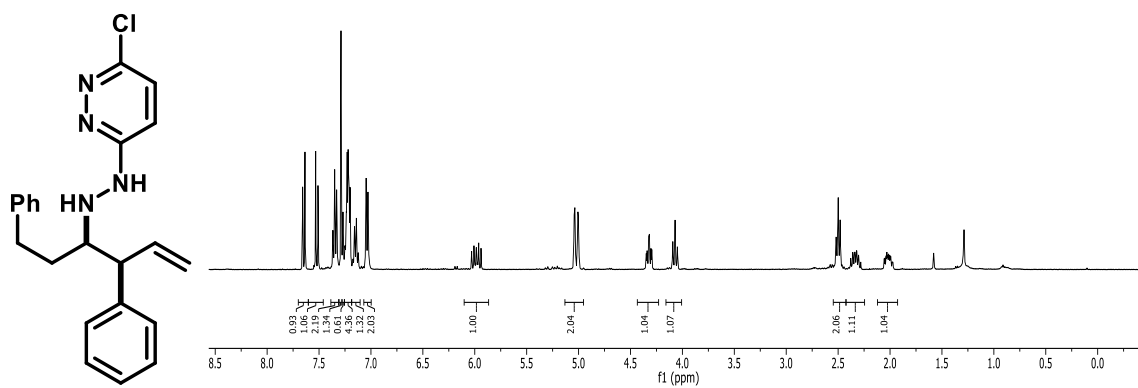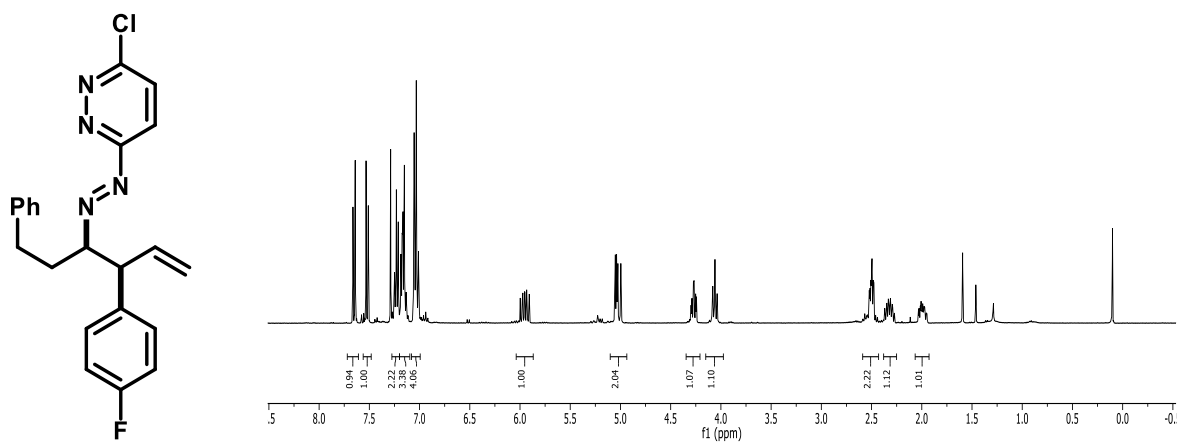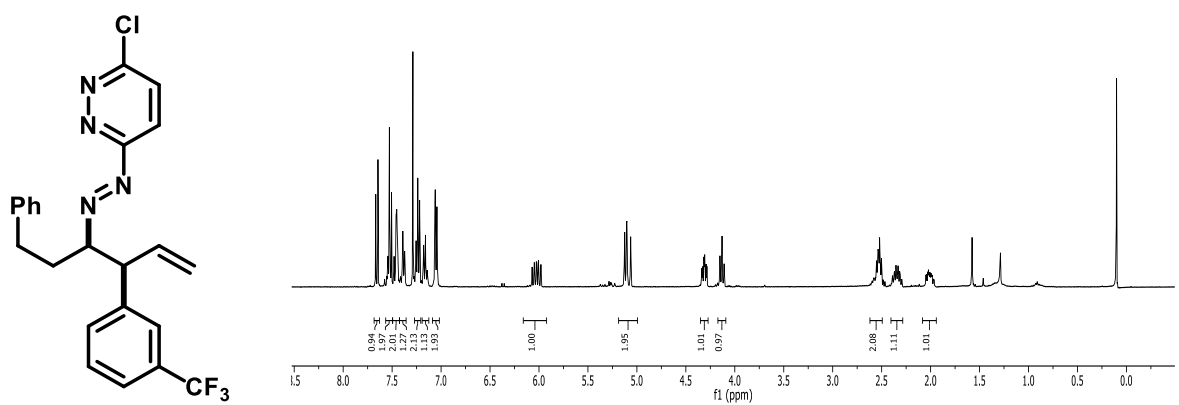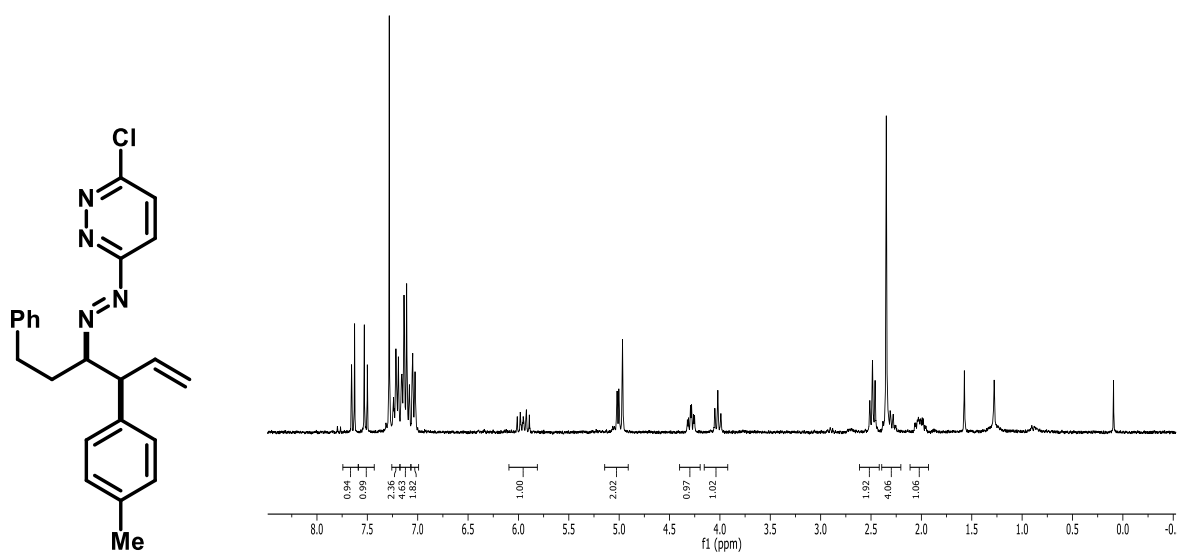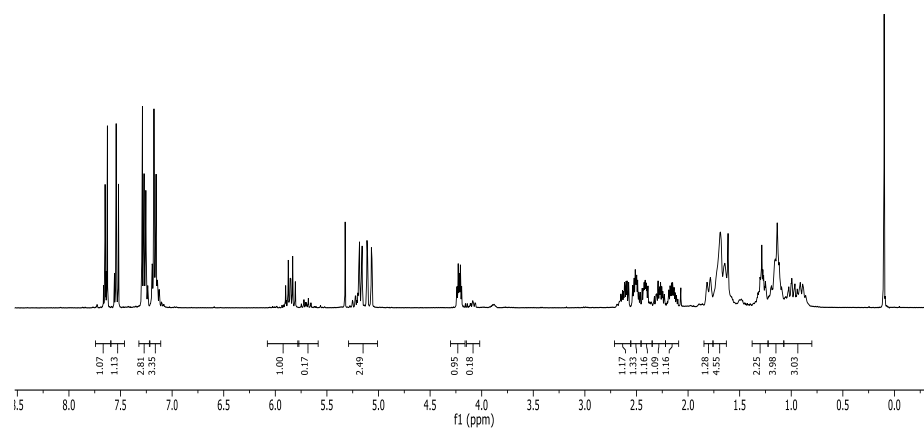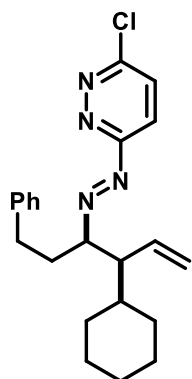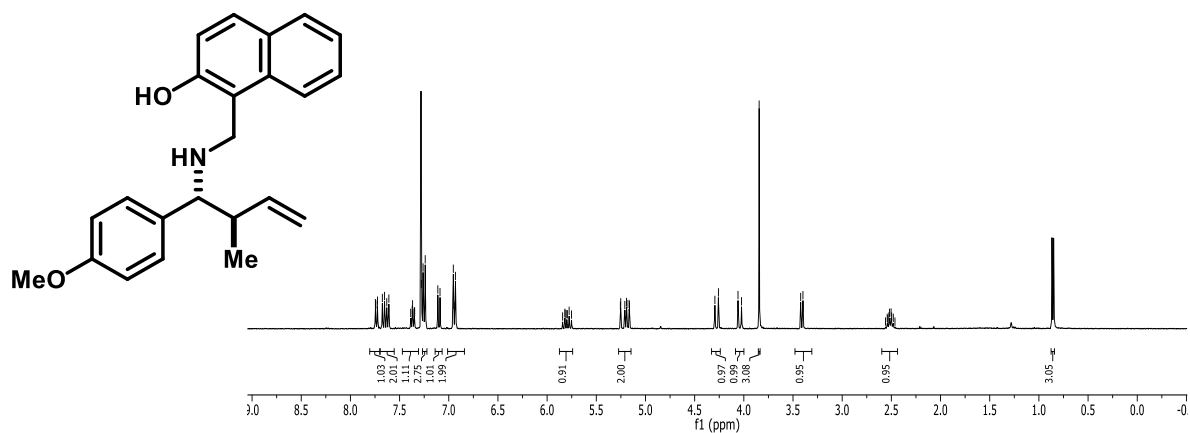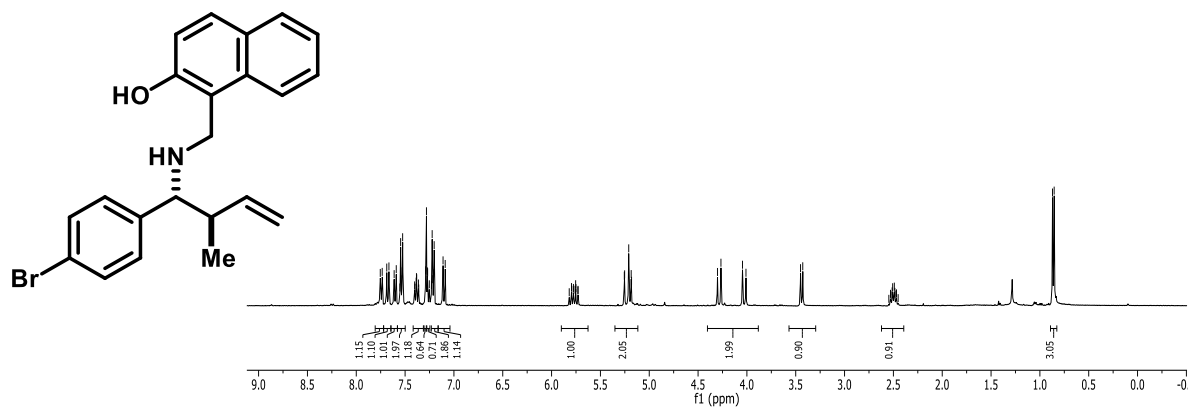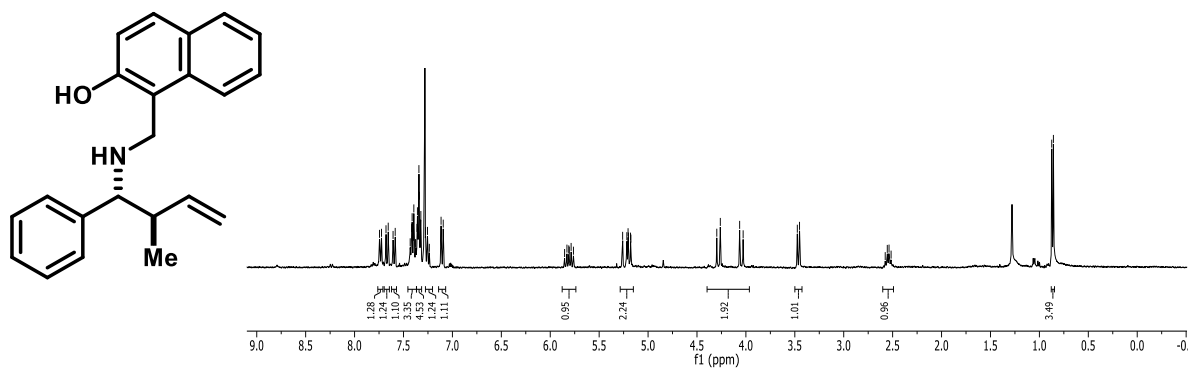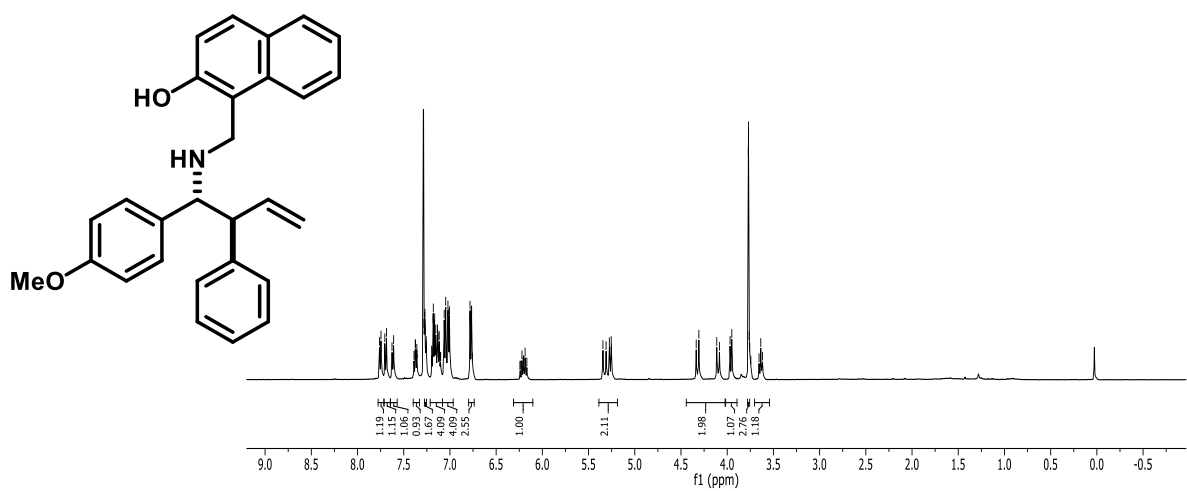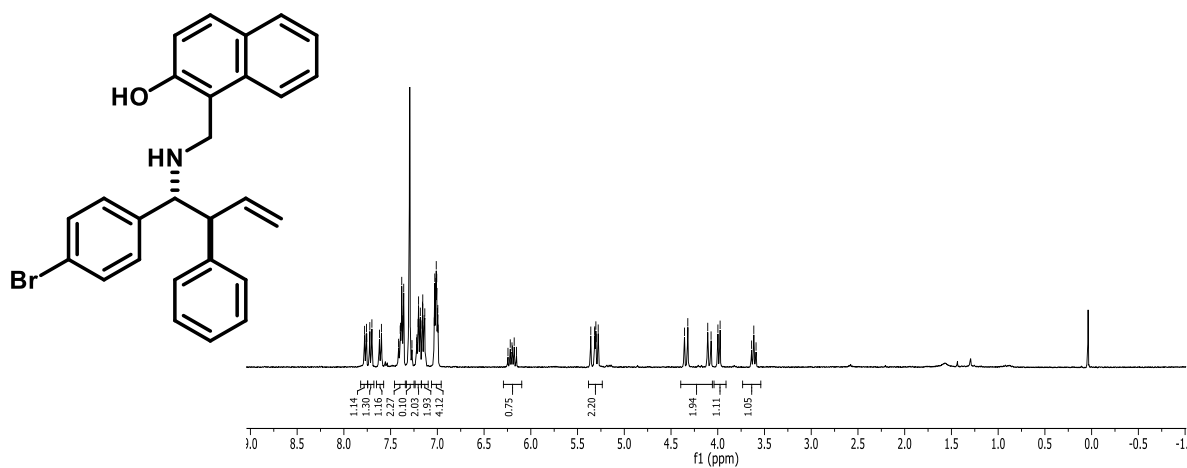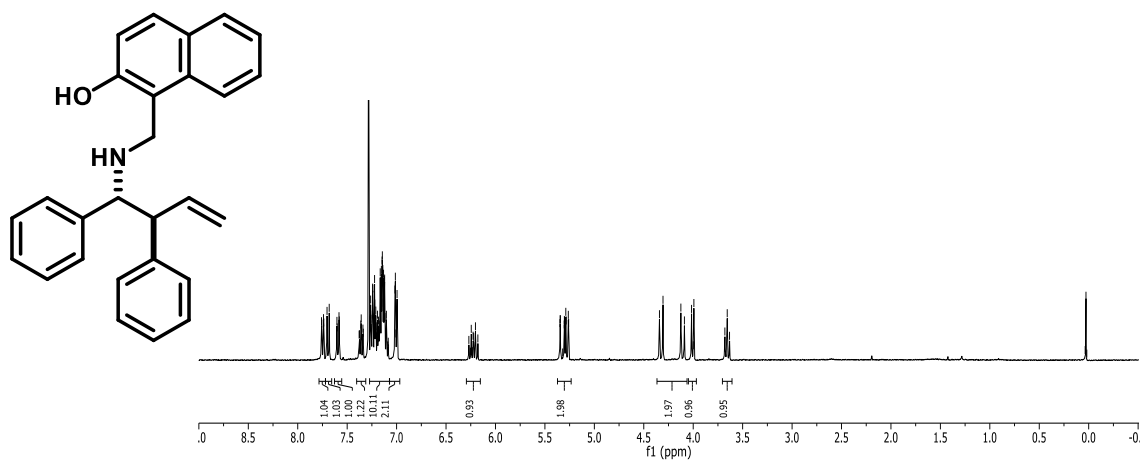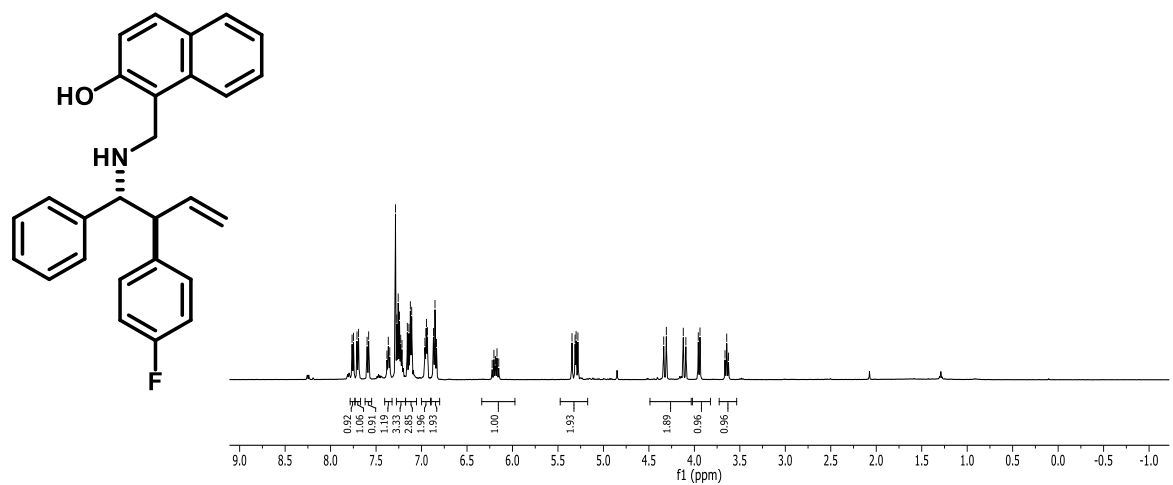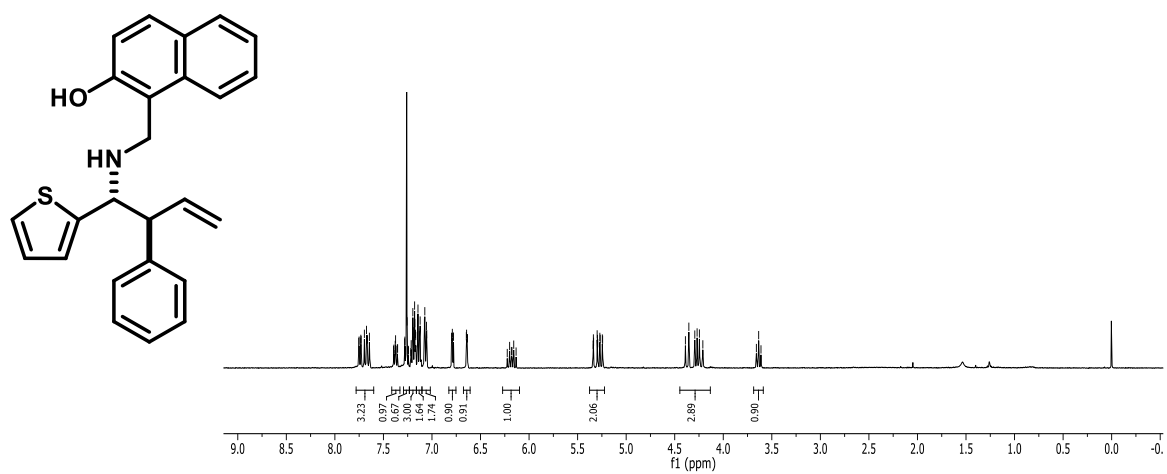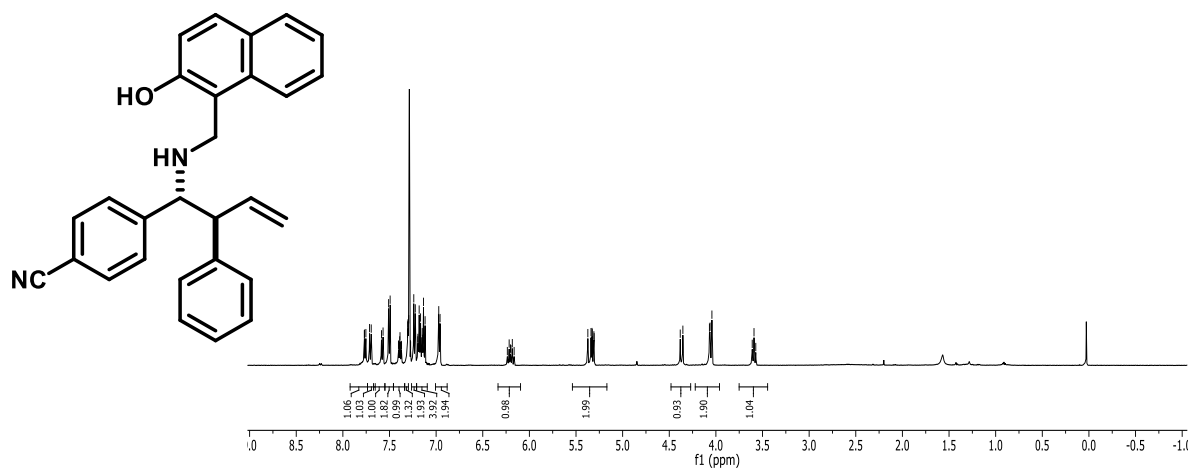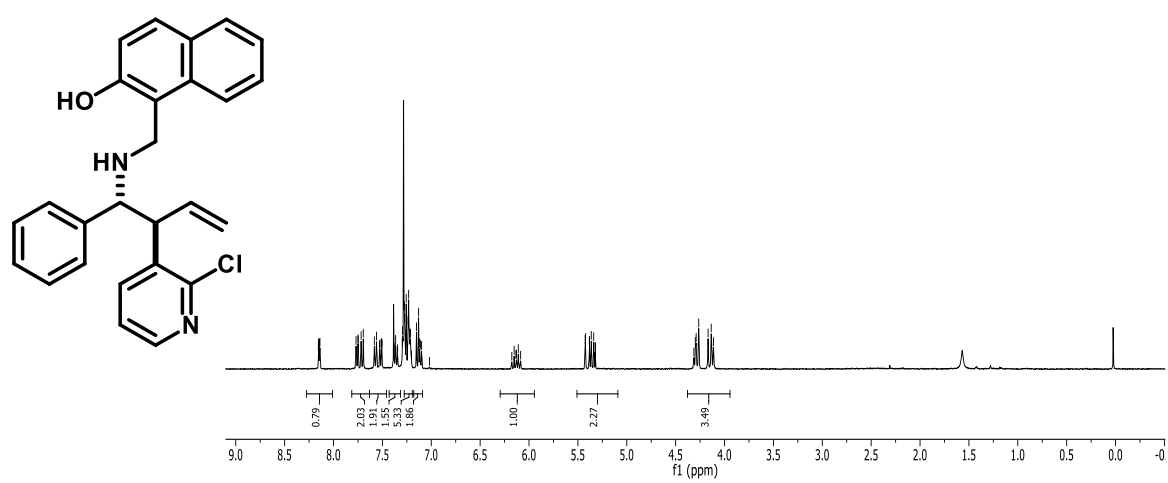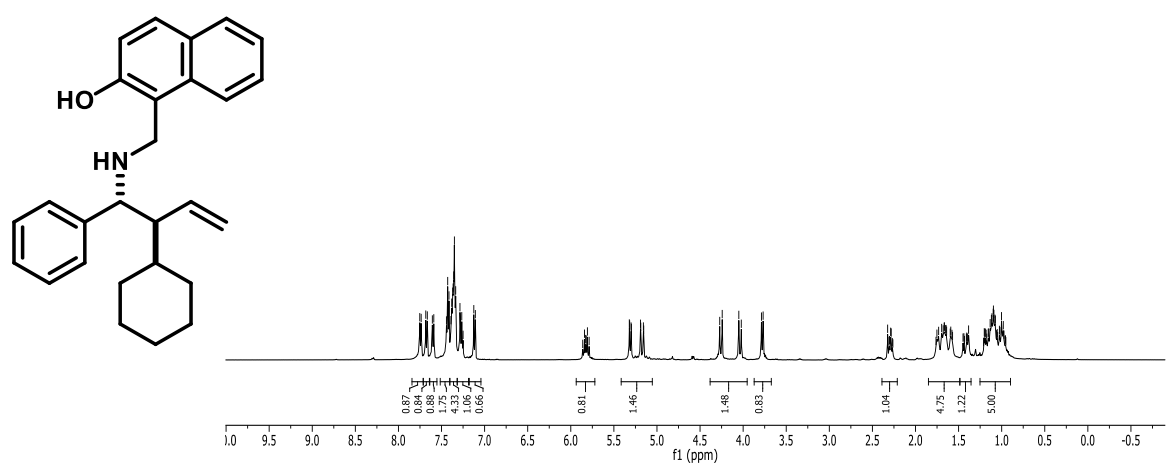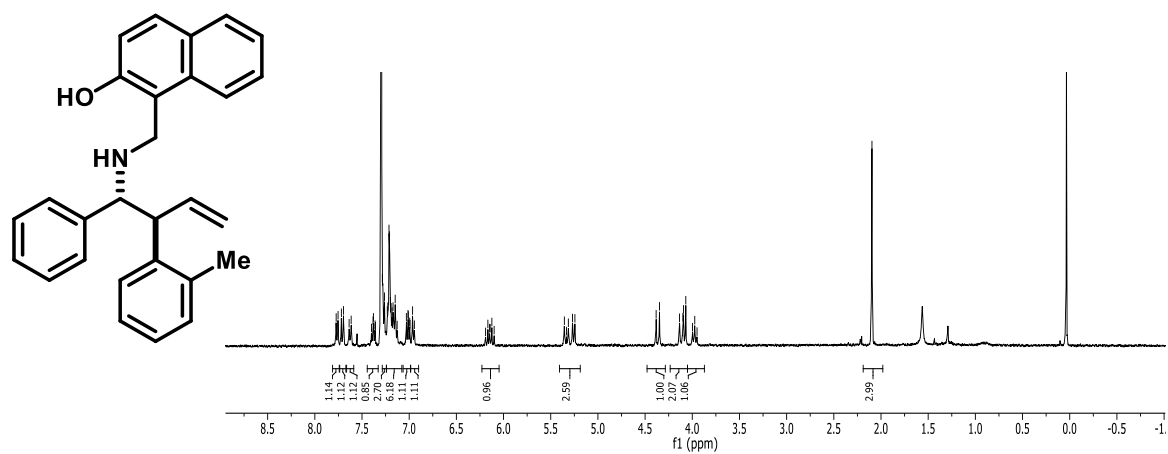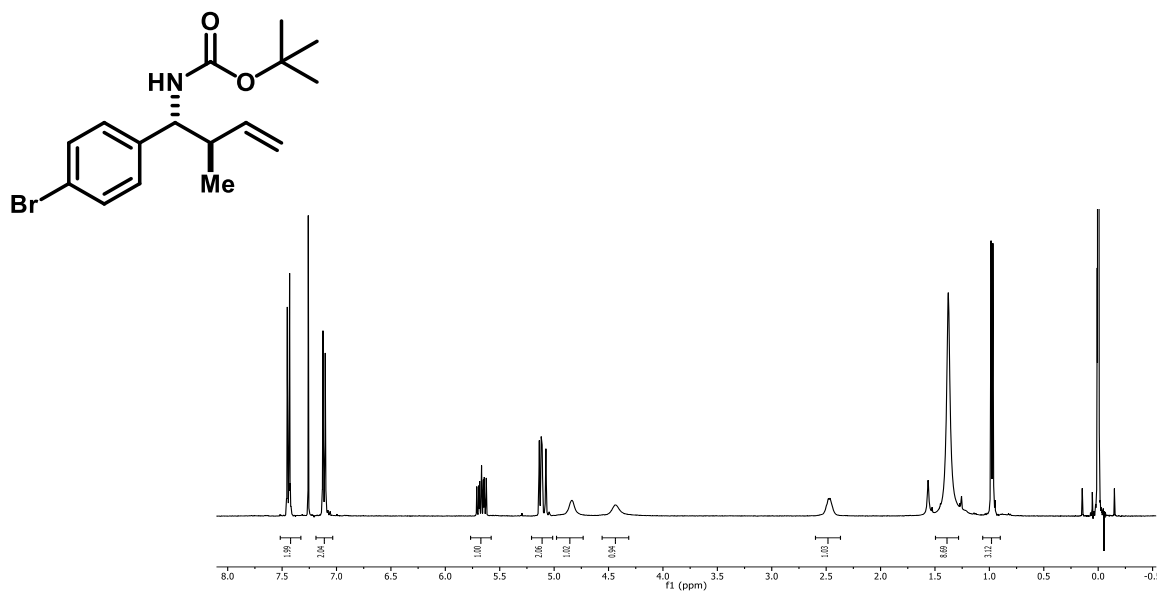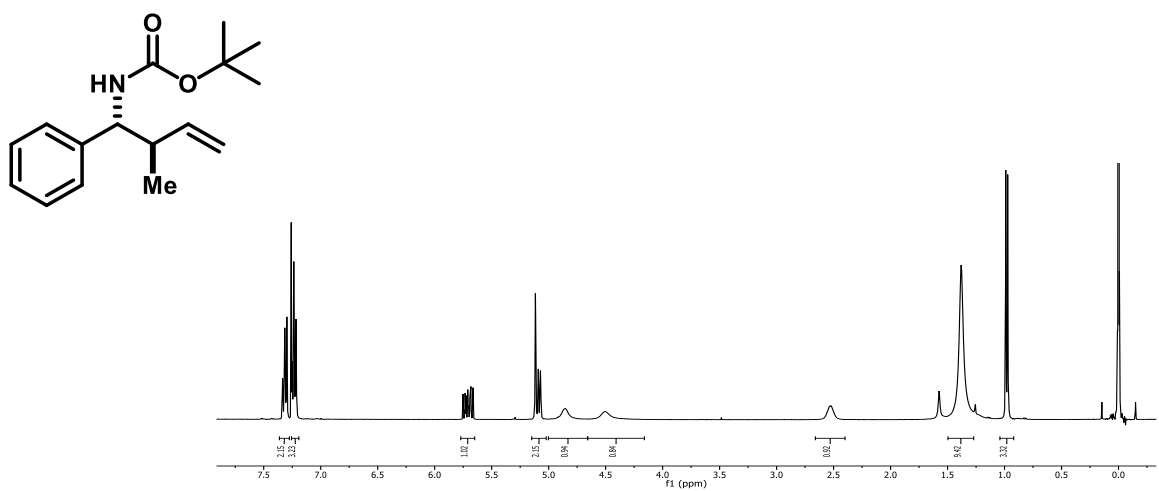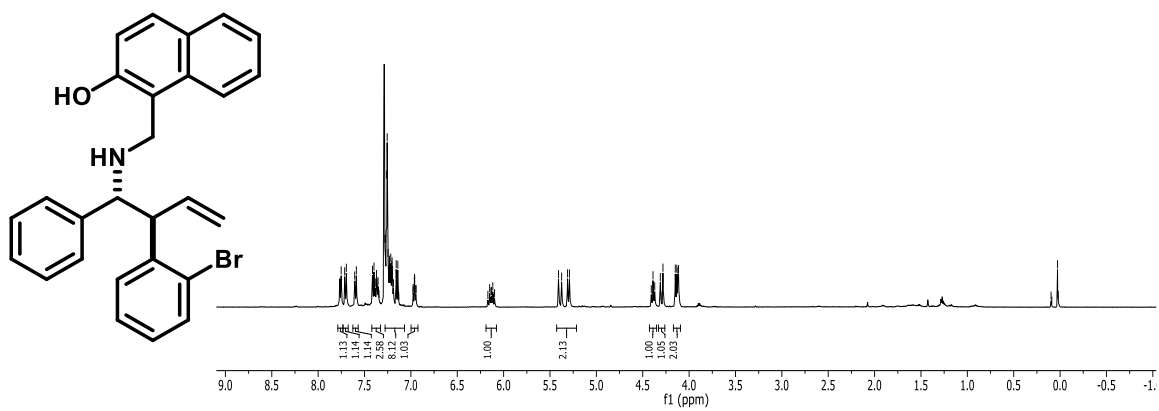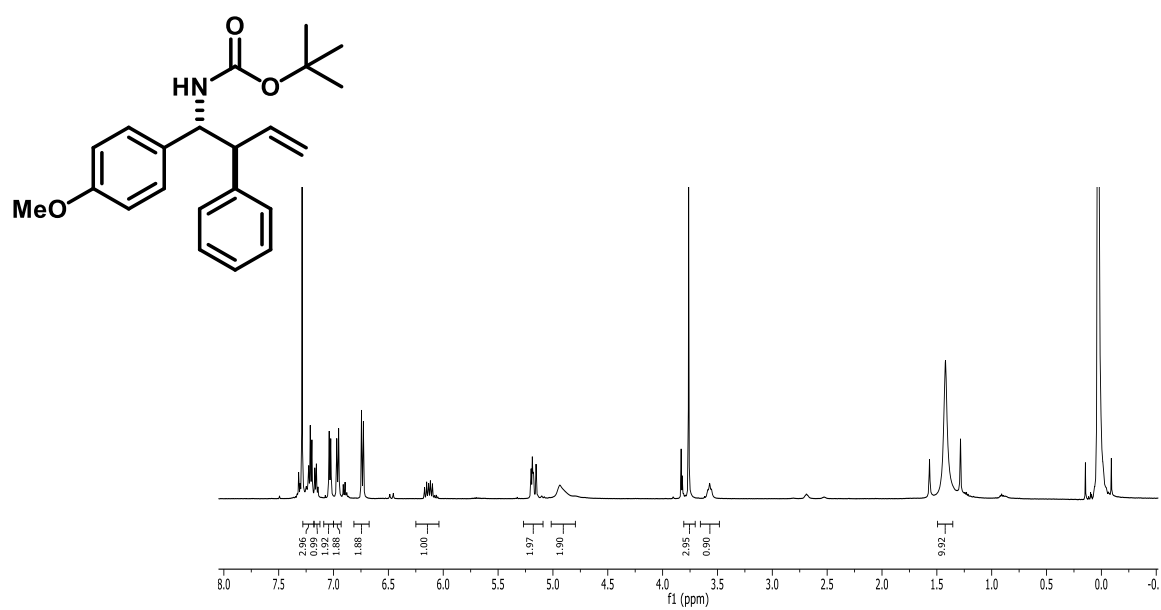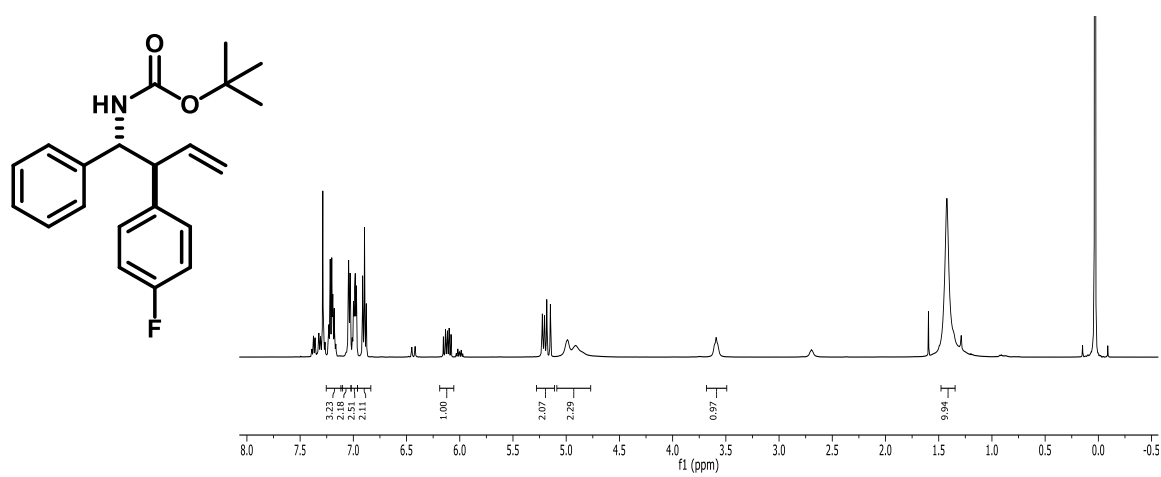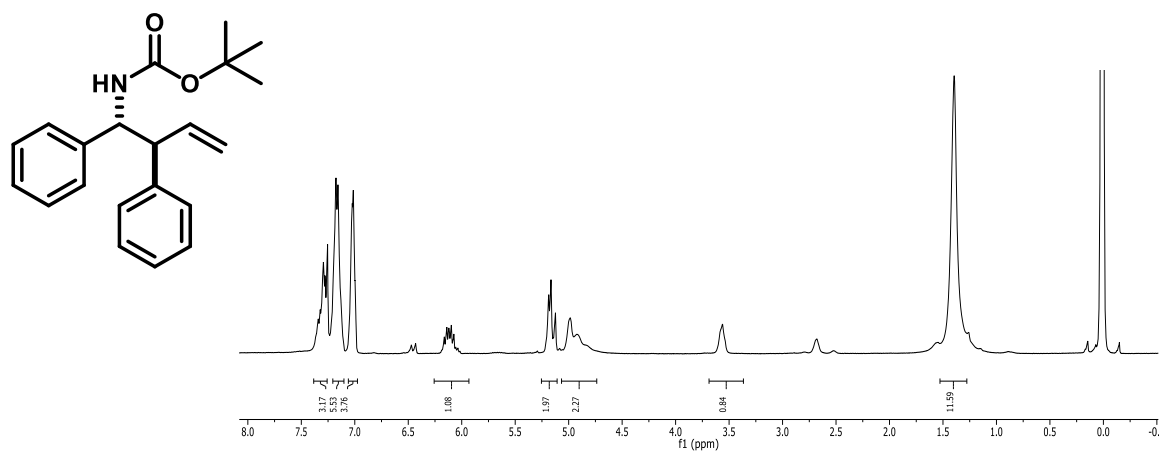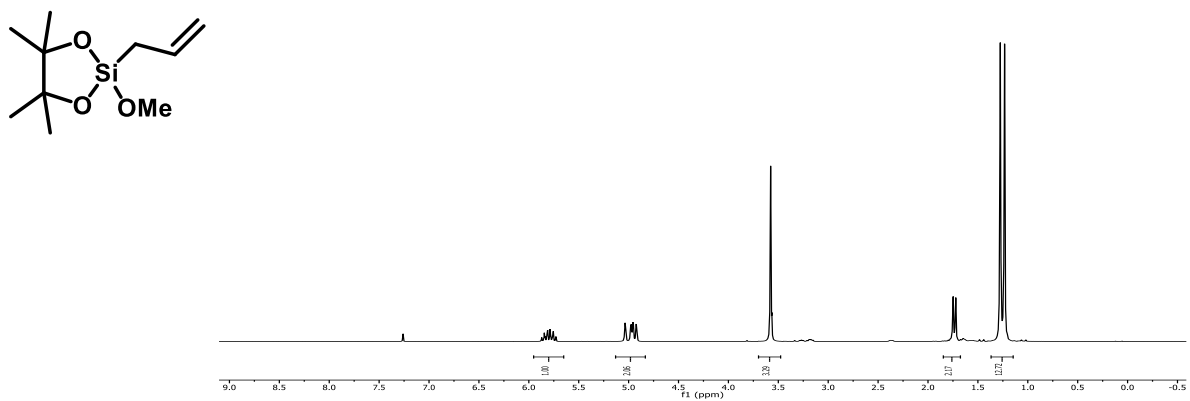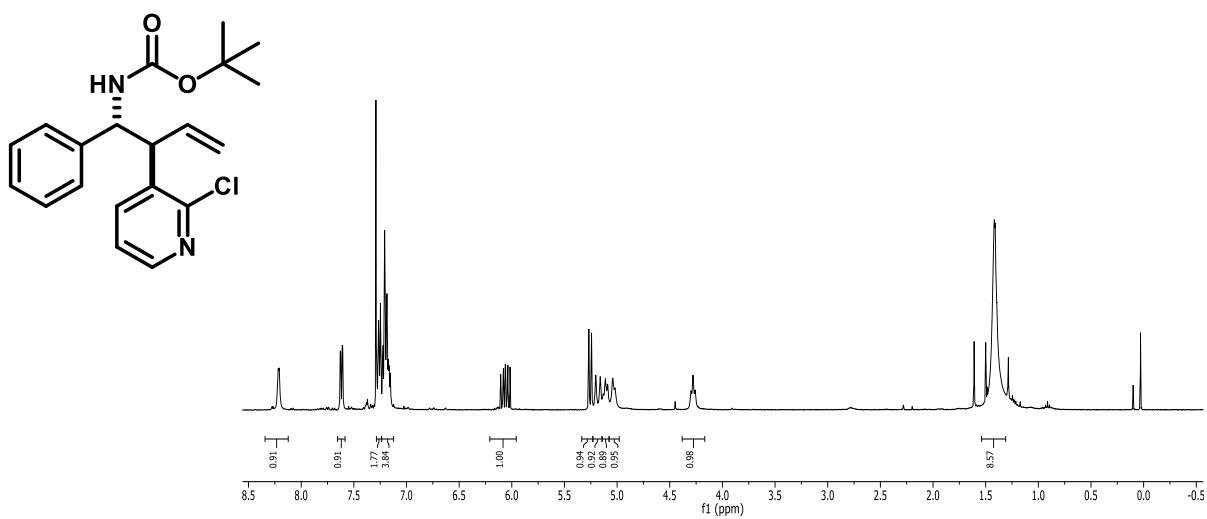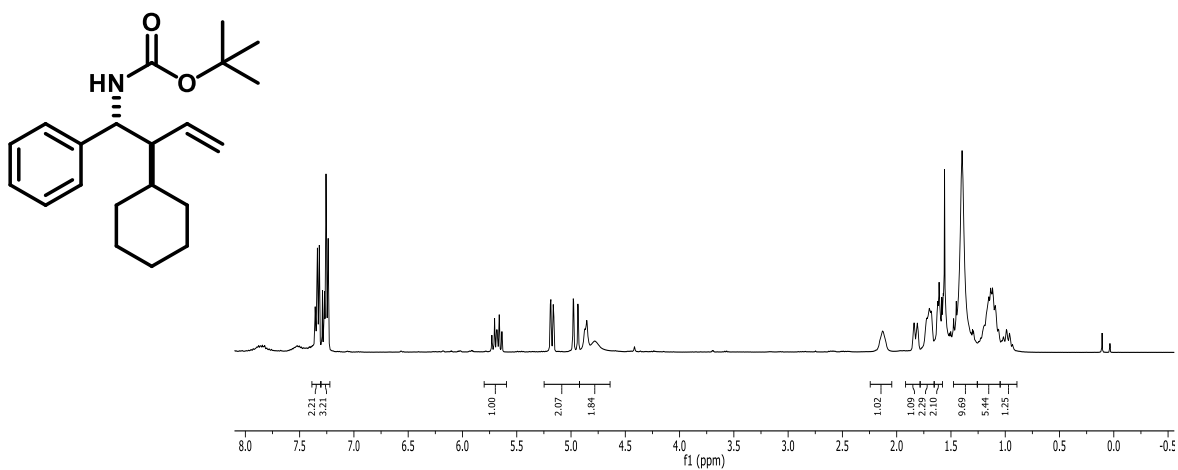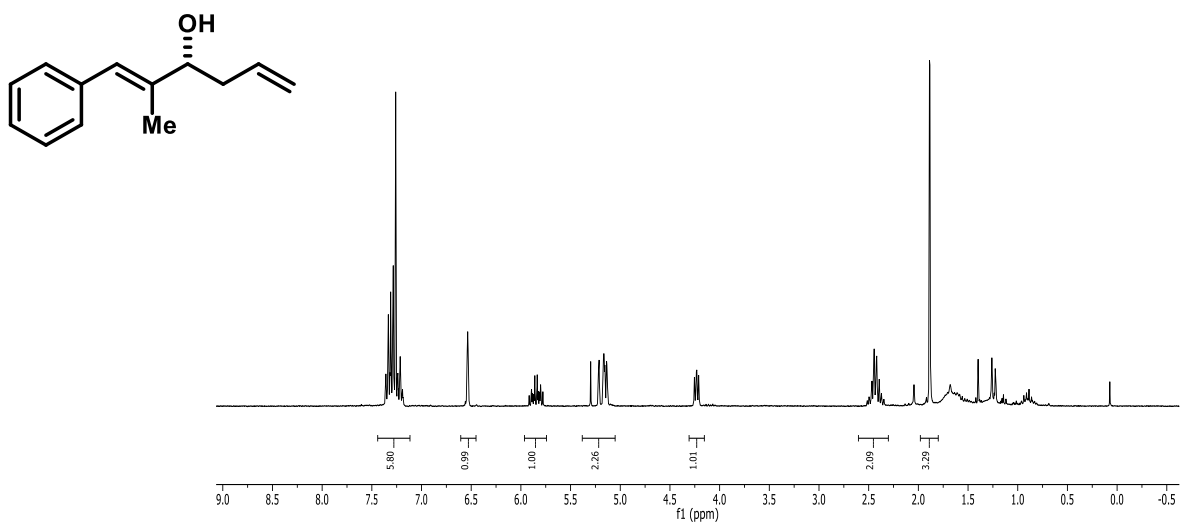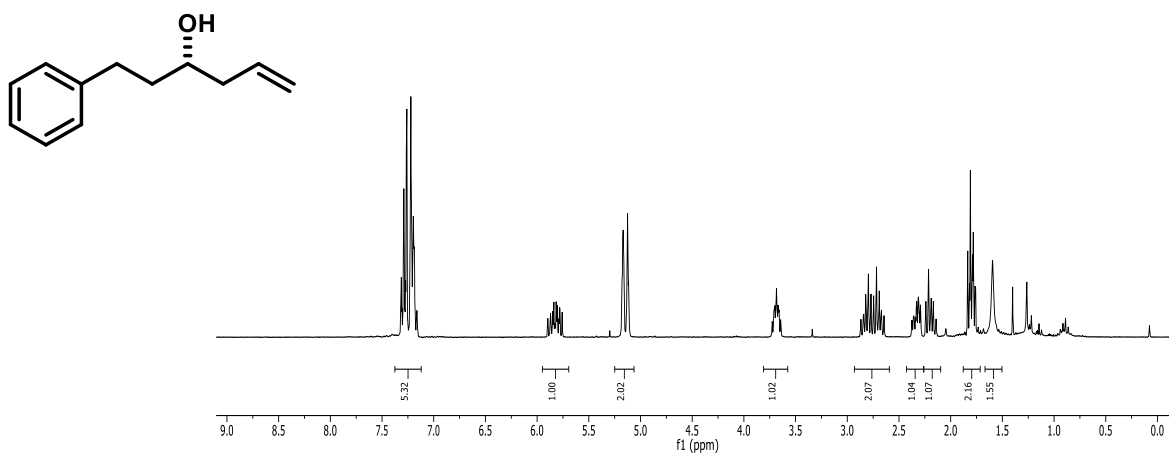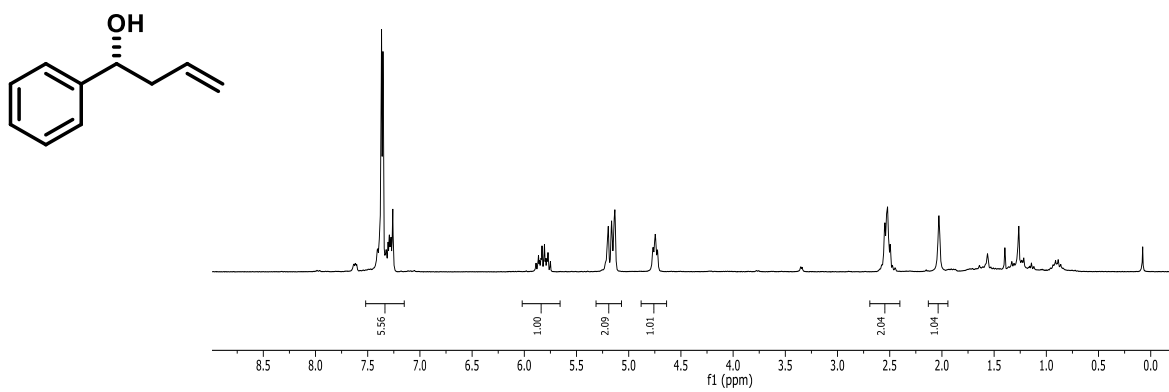
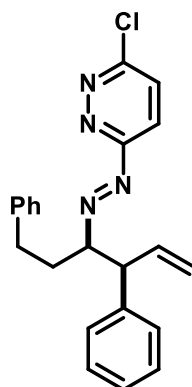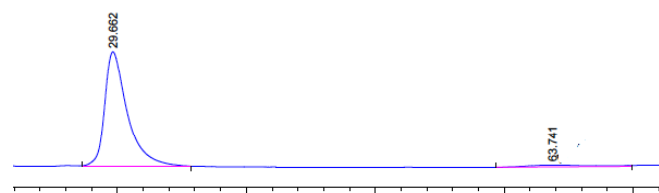## II.   HPLC Traces

Chiracel OJ-H, 85:15 hexane/isopropanol, 1.0 ml/min, 254 nm:
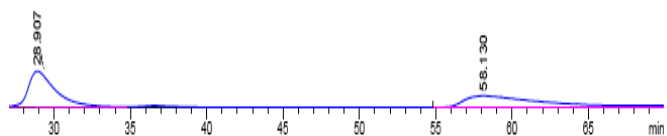
Peak #	RetTime [min]	Type	Width [min]	Area mAU *s	Height [mAU]	Area %
1	28.907	MM	2.0218	4.61628e4	380.54010	49.6589
2	58.130	VBA	5.1283	4.67970e4	123.74739	50.3411

Peak #	RetTime [min]	Type	Width [min]	Area mAU *s	Height [mAU]	Area %
1	29.662	BB	1.8195	1.80500e4	146.73602	95.4775
2	63.741	MM	4.4859	854.96753	2.27538	4.5225

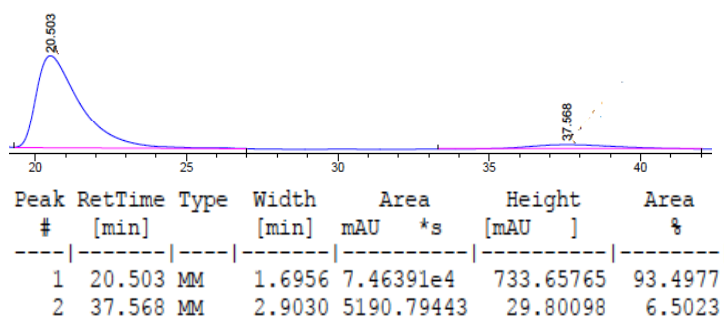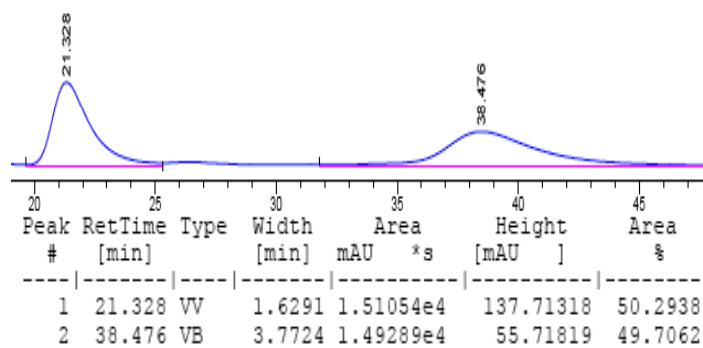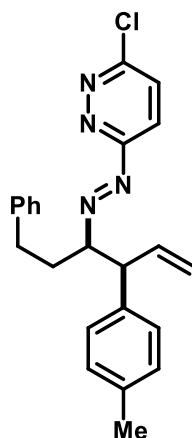Chiracel AD-H, 90:10 hexane/ethanol, 1.0 ml/min, 254 nm:
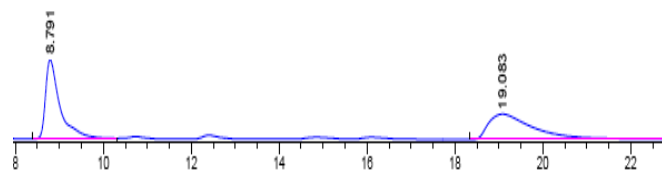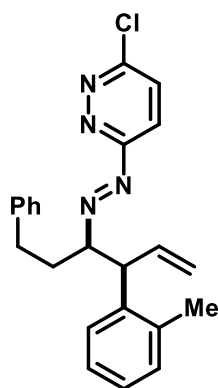
Peak #	RetTime [min]	Type	Width [min]	Area mAU *s	Height [mAU]	Area %
1	8.791	BV	0.3422	5.24742e4	2248.48169	50.5906
2	19.083	VV	1.0557	5.12490e4	716.56195	49.4094
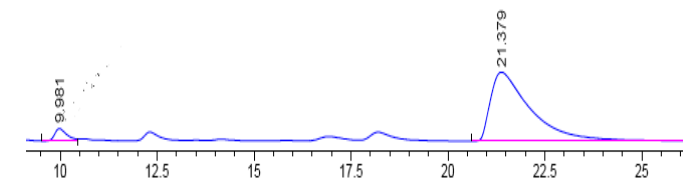
Peak #	RetTime [min]	Type	Width [min]	Area mAU *s	Height [mAU]	Area %
1	9.981	MM	0.3551	2863.60669	134.41820	4.9513
2	21.379	VV	1.0531	5.49713e4	760.36591	95.0487

Chiracel OJ-H, 85:15 hexane/isopropanol, 1.0 ml/min, 254 nm:

Peak #	RetTime [min]	Type	Width [min]	Area mAU *s	Height [mAU]	Area %
1	21.328	VV	1.6291	1.51054e4	137.71318	50.2938
2	38.476	VB	3.7724	1.49289e4	55.71819	49.7062

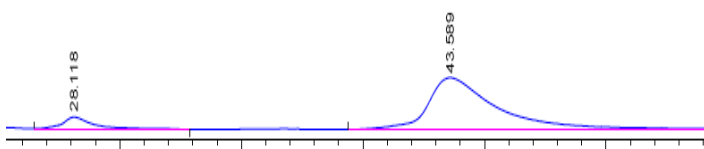| Peak #	RetTime [min]	Type	Width [min]	Area mAU *s	Height [mAU]	Area %
1	20.503	MM	1.6956	7.46391e4	733.65765	93.4977
2	37.568	MM	2.9030	5190.79443	29.80098	6.5023

Chiracel AD-H, 90:10 hexane/ethanol, 1.0 ml/min, 254 nm:

Peak #	RetTime [min]	Type	Width [min]	Area mAU *s	Height [mAU]	Area %
1	8.604	BV	0.3410	4.08094e4	1756.11438	49.6808
2	13.494	MM	0.6527	4.13339e4	1055.44531	50.3192

Peak #	RetTime [min]	Type	Width [min]	Area mAU *s	Height [mAU]	Area %
1	9.196	VV	0.3859	1401.98999	59.41528	6.8122
2	14.384	VV	0.6445	1.91784e4	443.34677	93.1878

Chiracel OJ-H, 90:10 hexane/isopropanol, 1.0 ml/min, 254 nm:
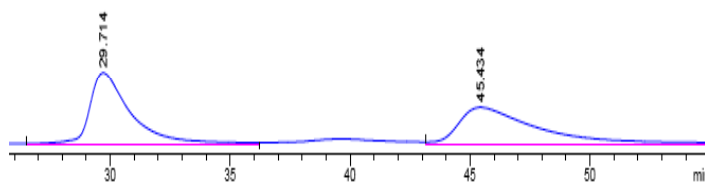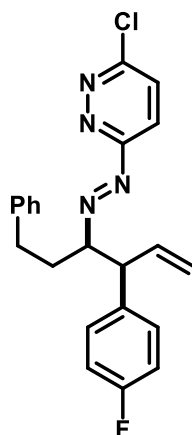
Peak #	RetTime [min]	Type	Width [min]	Area mAU *s	Height [mAU]	Area %
1	29.714	VV	1.6941	2.12097e4	180.11510	50.1046
2	45.434	VB	3.1998	2.11211e4	92.09474	49.8954

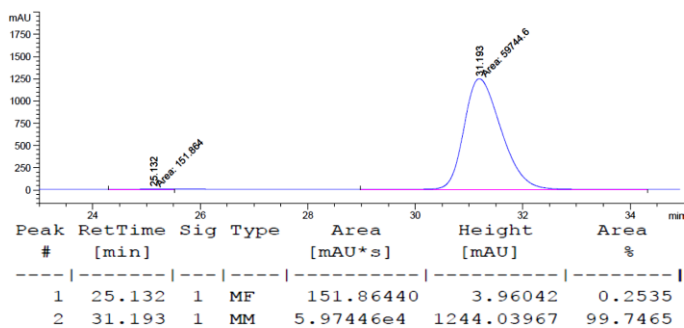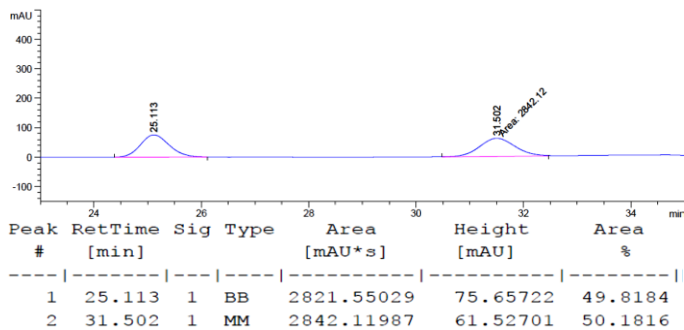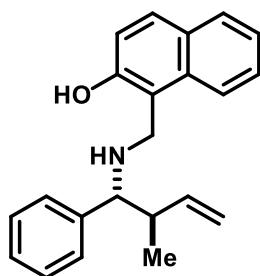| Peak #	RetTime [min]	Type	Width [min]	Area mAU *s	Height [mAU]	Area %
1	28.118	VB	1.1921	2272.99902	26.83359	9.2164
2	43.589	PB	2.6899	2.23895e4	118.06966	90.7836

Chiracel AD-H, 98:2 hexane/ethanol, 1.0 ml/min, 254 nm:
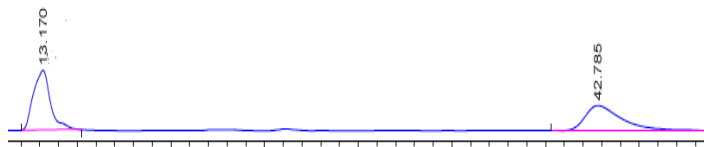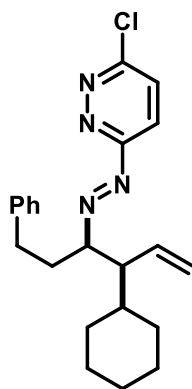
Peak #	RetTime [min]	Type	Width [min]	Area mAU *s	Height [mAU]	Area %
1	13.170	MM	1.0413	9178.11719	146.90779	50.4433
2	42.785	BB	2.0694	9016.79883	63.08501	49.5567
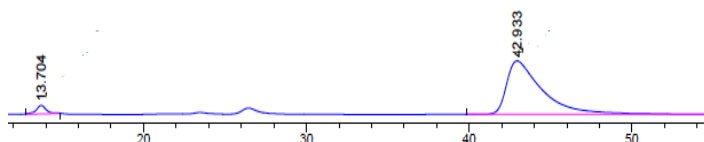
Peak #	RetTime [min]	Type	Width [min]	Area mAU *s	Height [mAU]	Area %
1	13.704	MM	0.7406	1212.38354	27.28281	4.5048
2	42.933	MM	2.5479	2.57010e4	168.11885	95.4952

Chiralpak AD-H 98:2 Hex/IPA, 1.0 mL/min, 230 nm

Peak #	RetTime [min]	Sig	Type	Area [mAU*s]	Height [mAU]	Area %
1	25.113	1	BB	2821.55029	75.65722	49.8184
2	31.502	1	MM	2842.11987	61.52701	50.1816

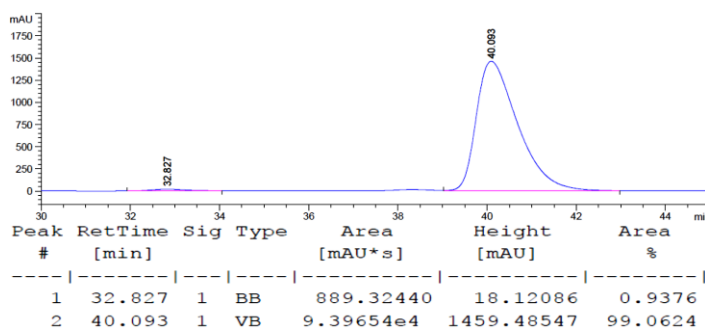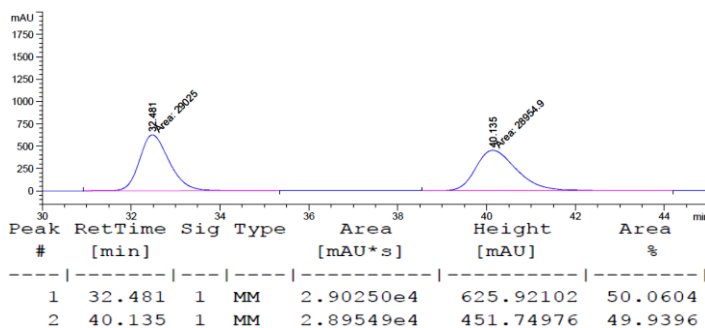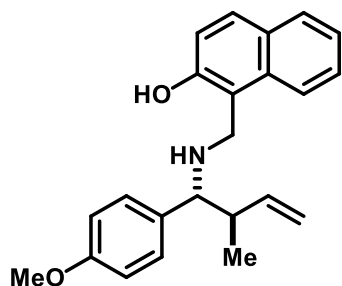| Peak #	RetTime [min]	Sig	Type	Area [mAU*s]	Height [mAU]	Area %
1	25.132	1	MF	151.86440	3.96042	0.2535
2	31.193	1	MM	5.97446e4	1244.03967	99.7465

Chiralpak AD-H 98:2 Hex/IPA, 1.0 mL/min, 230 nm

Peak #	RetTime [min]	Sig	Type	Area [mAU*s]	Height [mAU]	Area %
1	27.059	1	MM	3.92840e4	865.14886	49.6680
2	33.480	1	MM	3.98092e4	743.10284	50.3320

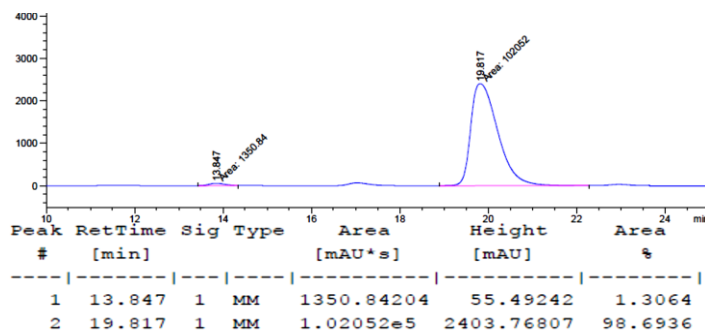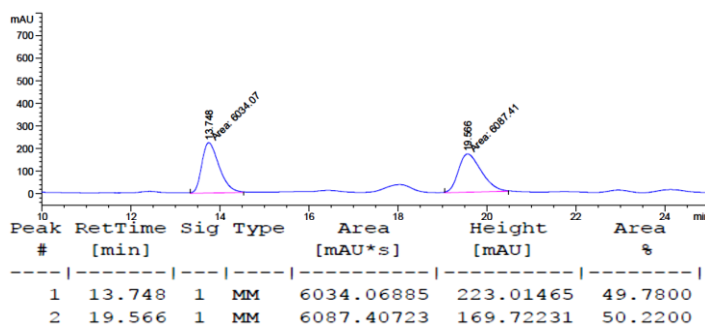| Peak #	RetTime [min]	Sig	Type	Area [mAU*s]	Height [mAU]	Area %
1	29.003	1	BB	1970.94495	44.44098	2.9750
2	34.993	1	BB	6.42783e4	1198.23181	97.0250

Chiralpak AD-H 98:2 Hex/IPA, 1.0 mL/min, 230 nm

Peak #	RetTime [min]	Sig	Type	Area [mAU*s]	Height [mAU]	Area %
1	32.481	1	MM	2.90250e4	625.92102	50.0604
2	40.135	1	MM	2.89549e4	451.74976	49.9396

Peak #	RetTime [min]	Sig	Type	Area [mAU*s]	Height [mAU]	Area %
1	32.827	1	BB	889.32440	18.12086	0.9376
2	40.093	1	VB	9.39654e4	1459.48547	99.0624

Chiralpak AD-H 95:5 Hex/IPA, 1.0 mL/min, 254 nm

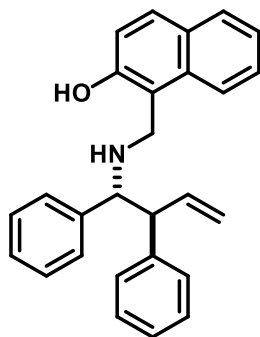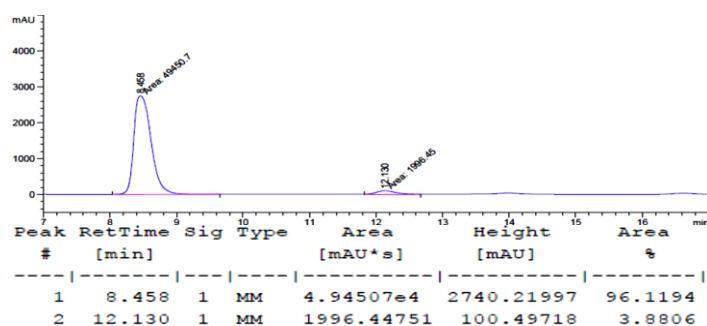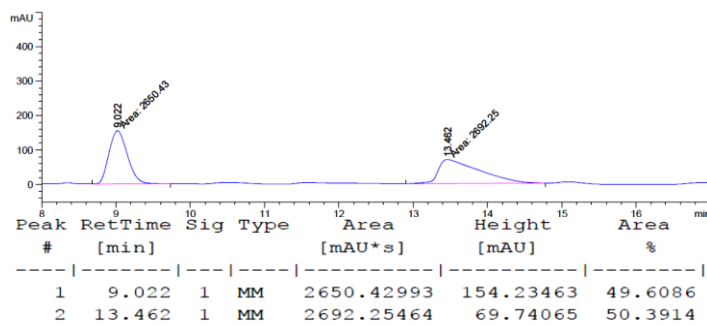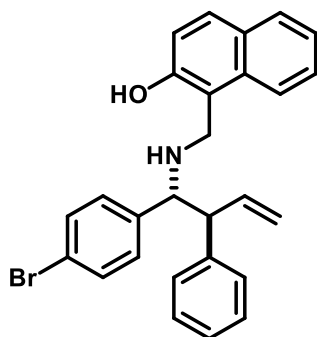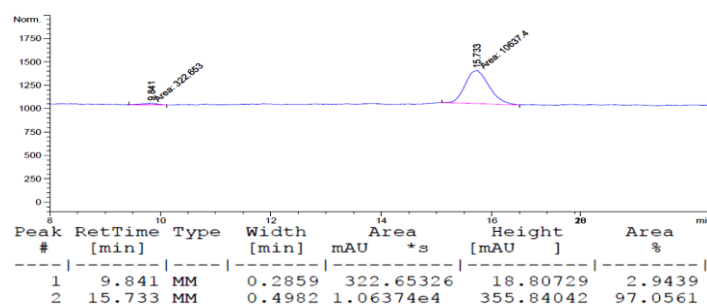| Peak #	RetTime [min]	Sig	Type	Area [mAU*s]	Height [mAU]	Area %
1	13.748	1	MM	6034.06885	223.01465	49.7800
2	19.566	1	MM	6087.40723	169.72231	50.2200

Peak #	RetTime [min]	Sig	Type	Area [mAU*s]	Height [mAU]	Area %
1	13.847	1	MM	1350.84204	55.49242	1.3064
2	19.817	1	MM	1.02052e5	2403.76807	98.6936

Chiralpak AD-H 92:8 Hex/EtOH, 1.0 mL/min, 254 nm

Peak #	RetTime [min]	Sig	Type	Area [mAU*s]	Height [mAU]	Area %
1	9.022	1	MM	2650.42993	154.23463	49.6086
2	13.462	1	MM	2692.25464	69.74065	50.3914

Peak #	RetTime [min]	Sig	Type	Area [mAU*s]	Height [mAU]	Area %
1	8.458	1	MM	4.94507e4	2740.21997	96.1194
2	12.130	1	MM	1996.44751	100.49718	3.8806

Chiralpak AD-H 83:17 Hex/IPA, 1.0 mL/min, 220 nm
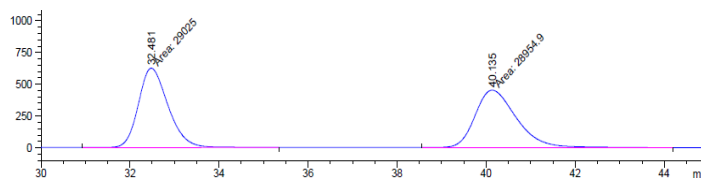
Peak #	RetTime [min]	Type	Width [min]	Area mAU*s	Height [mAU]	Area %
1	10.444	MM	0.3830	2.14882e4	934.97302	47.8801
2	16.760	MM	0.5654	2.33909e4	689.51880	52.1199

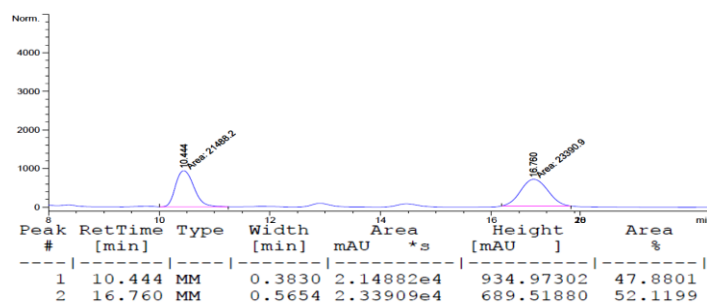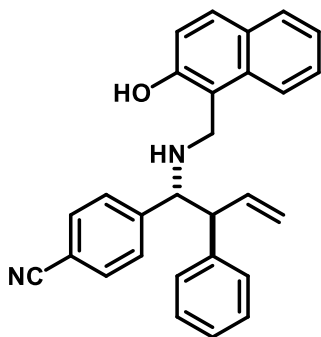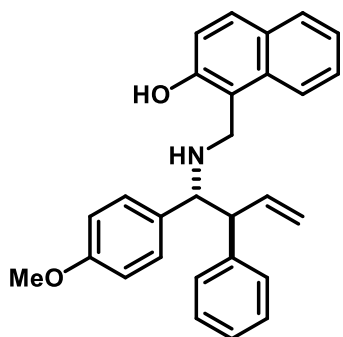| Peak #	RetTime [min]	Type	Width [min]	Area mAU*s	Height [mAU]	Area %
1	9.841	MM	0.2859	322.65326	18.80729	2.9439
2	15.733	MM	0.4982	1.06374e4	355.84042	97.0561

Chiralpak AD-H 98:2 Hex/IPA, 1.0 mL/min, 230 nm

Peak #	RetTime [min]	Sig	Type	Area [mAU*s]	Height [mAU]	Area %
1	32.481	1	MM	2.90250e4	625.92102	50.0604
2	40.135	1	MM	2.89549e4	451.74976	49.9396
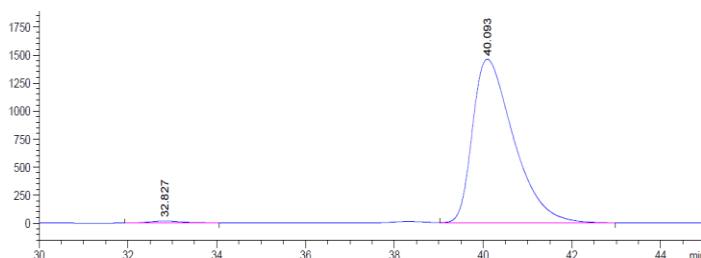
Peak #	RetTime [min]	Sig	Type	Area [mAU*s]	Height [mAU]	Area %
1	32.827	1	BB	889.32440	18.12086	0.9376
2	40.093	1	VB	9.39654e4	1459.48547	99.0624

Chiralpak AD-H 95:5 Hex/EtOH, 1.0 mL/min, 230 nm
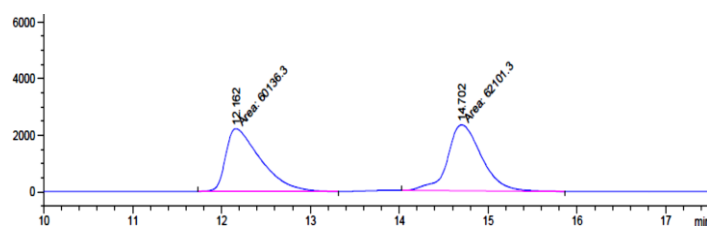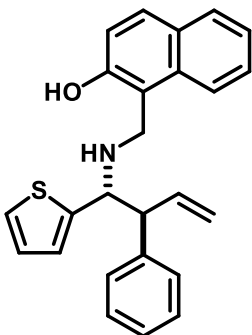
Peak #	RetTime [min]	Sig	Type	Area [mAU*s]	Height [mAU]	Area %
1	12.162	1	MM	6.01363e4	2220.97827	49.1962
2	14.702	1	MM	6.21013e4	2329.92456	50.8038
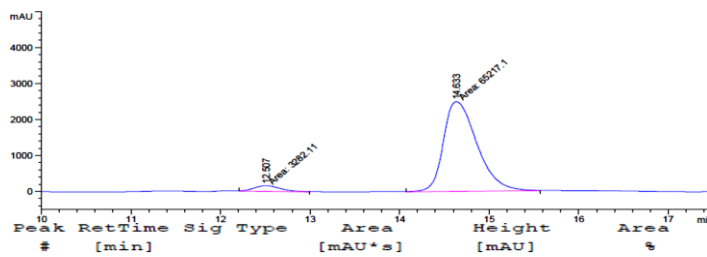
Peak #	RetTime [min]	Sig	Type	Area [mAU*s]	Height [mAU]	Area %
1	12.507	1	MM	3282.10669	158.85709	4.7914
2	14.633	1	MM	6.52171e4	2494.31104	95.2086

Chiralpak AD-H 95:5 Hex/IPA, 1.0 mL/min, 230 nm

Peak #	RetTime [min]	Sig	Type	Area [mAU*s]	Height [mAU]	Area %
1	23.824	1	MM	1.36743e4	353.87585	50.1336
2	34.190	1	BB	1.36015e4	271.63083	49.8664

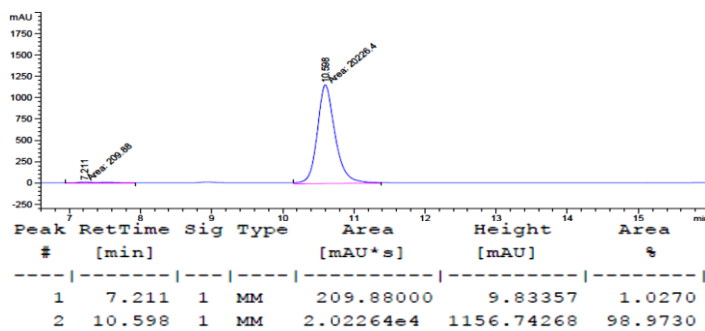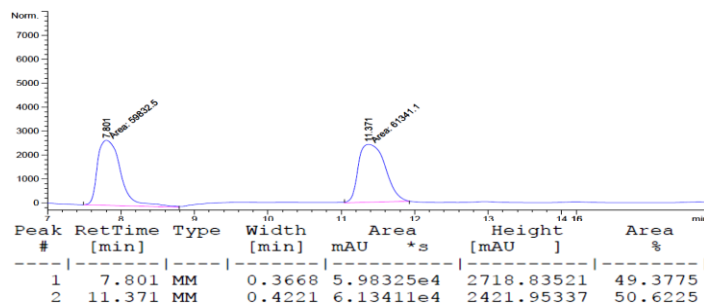| Peak #	RetTime [min]	Sig	Type	Area [mAU*s]	Height [mAU]	Area %
1	22.339	1	MM	9.97788e4	2141.64893	99.6509
2	33.003	1	MM	349.53891	4.60902	0.3491

Chiralpak AD-H 95:5 Hex/IPA, 1.0 mL/min, 230 nm

Peak #	RetTime [min]	Sig	Type	Area [mAU*s]	Height [mAU]	Area %
1	10.420	1	MM	5.41890e4	2417.12842	48.8646
2	16.315	1	MM	5.67073e4	1785.24365	51.1354

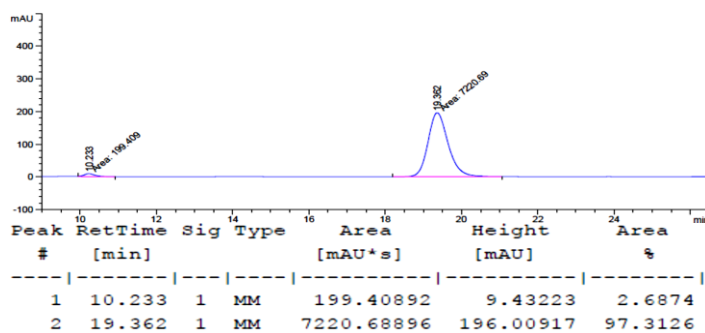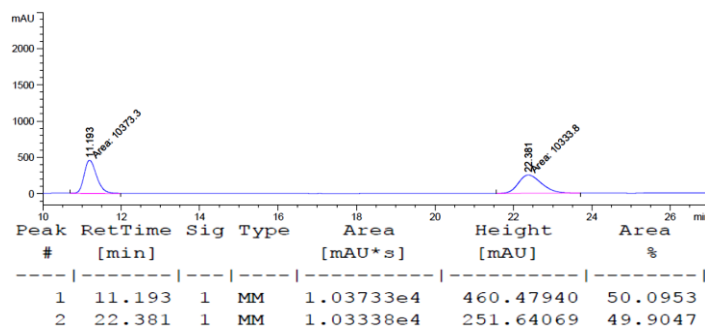| Peak #	RetTime [min]	Sig	Type	Area [mAU*s]	Height [mAU]	Area %
1	10.748	1	MM	36.48026	2.00763	0.4286
2	17.122	1	MM	8475.88965	277.94589	99.5714

Chiralpak AD-H 95:5 Hex/IPA, 1.0 mL/min, 220 nm

Peak #	RetTime [min]	Type	Width [min]	Area mAU *s	Height [mAU]	Area %
1	7.801	MM	0.3668	5.98325e4	2718.83521	49.3775
2	11.371	MM	0.4221	6.13411e4	2421.95337	50.6225

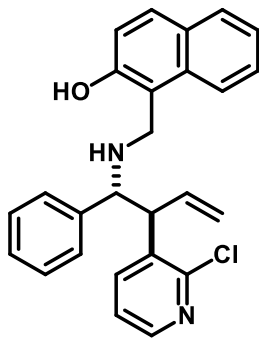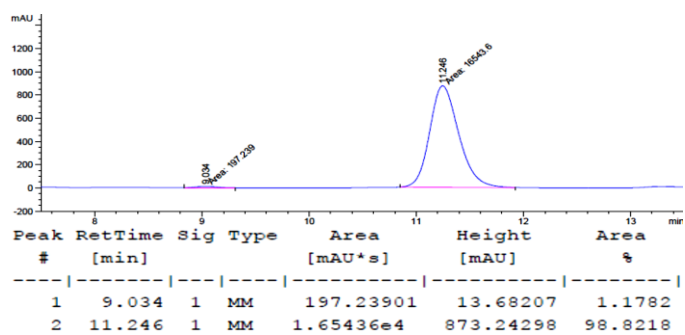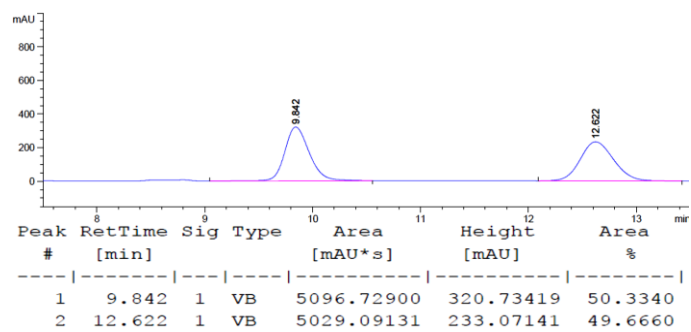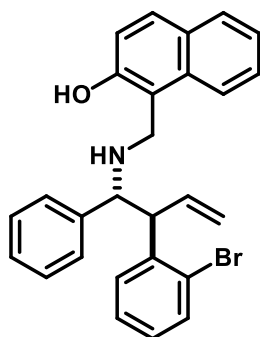| Peak #	RetTime [min]	Sig	Type	Area [mAU*s]	Height [mAU]	Area %
1	7.211	1	MM	209.88000	9.83357	1.0270
2	10.598	1	MM	2.02264e4	1156.74268	98.9730

Chiralpak AD-H 85:15 Hex/IPA, 1.0 mL/min, 230 nm

Peak #	RetTime [min]	Sig	Type	Area [mAU*s]	Height [mAU]	Area %
1	11.193	1	MM	1.03733e4	460.47940	50.0953
2	22.381	1	MM	1.03338e4	251.64069	49.9047

Peak #	RetTime [min]	Sig	Type	Area [mAU*s]	Height [mAU]	Area %
1	10.233	1	MM	199.40892	9.43223	2.6874
2	19.362	1	MM	7220.68896	196.00917	97.3126

Chiralpak AD-H 92:8 Hex/EtOH, 1.0 mL/min, 230 nm

Peak #	RetTime [min]	Sig	Type	Area [mAU*s]	Height [mAU]	Area %
1	9.842	1	VB	5096.72900	320.73419	50.3340
2	12.622	1	VB	5029.09131	233.07141	49.6660

Peak #	RetTime [min]	Sig	Type	Area [mAU*s]	Height [mAU]	Area %
1	9.034	1	MM	197.23901	13.68207	1.1782
2	11.246	1	MM	1.65436e4	873.24298	98.8218

Chiralcel OD 98:2 Hex/IPA, 1.0 mL/min, 220 nm
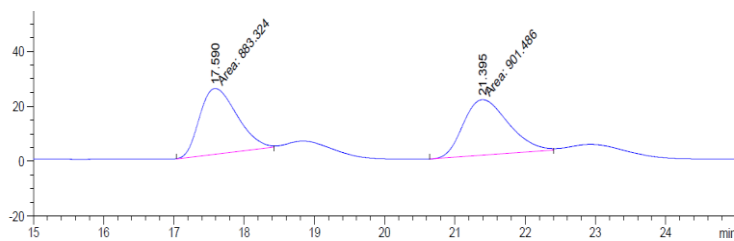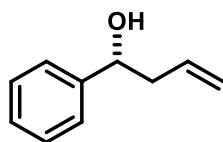
Peak #	RetTime [min]	Sig	Type	Area [mAU*s]	Height [mAU]	Area %
1	17.590	1	MM	883.32422	23.95174	49.4912
2	21.395	1	MM	901.48578	20.23991	50.5088
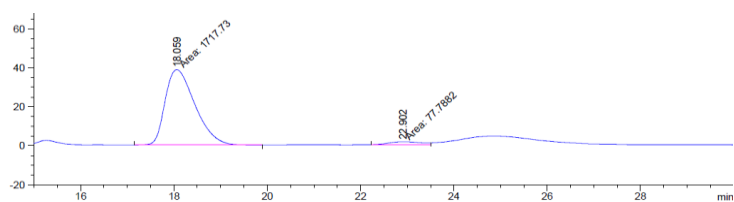
Peak #	RetTime [min]	Sig	Type	Area [mAU*s]	Height [mAU]	Area %
1	18.059	1	MM	1717.72681	38.63095	95.6676
2	22.902	1	MM	77.78824	1.62630	4.3324

Chiralcel OD 95:5 Hex/IPA, 1.0 mL/min, 220 nm
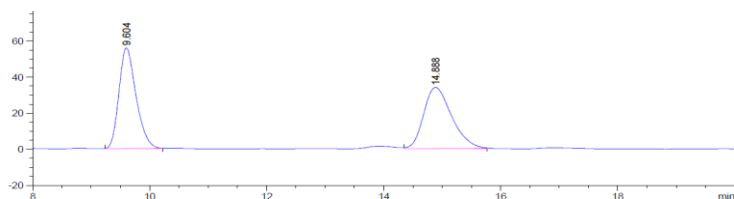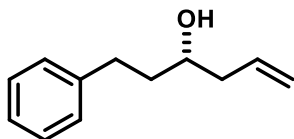
Peak #	RetTime [min]	Sig	Type	Area [mAU*s]	Height [mAU]	Area %
1	9.604	1	BB	1132.25732	55.72150	50.2155
2	14.888	1	BB	1122.54138	33.83898	49.7845
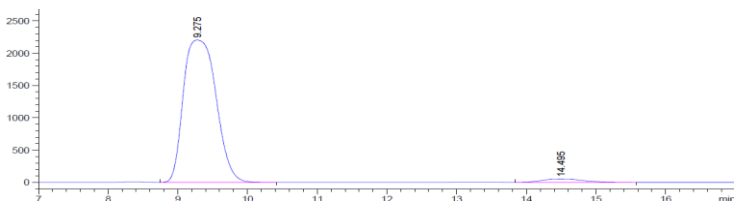
Peak #	RetTime [min]	Sig	Type	Area [mAU*s]	Height [mAU]	Area %
1	9.275	1	VB	7.18692e4	2200.56396	97.1667
2	14.495	1	VB	2095.68286	50.49832	2.8333

Chiralcel OD 95:5 Hex/IPA, 1.0 mL/min, 220 nm
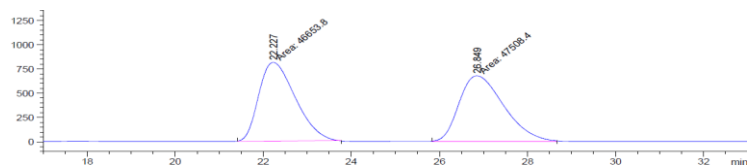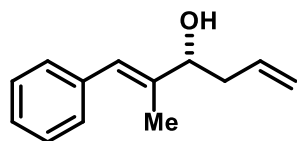
Peak #	RetTime [min]	Sig	Type	Area [mAU*s]	Height [mAU]	Area %
1	22.227	1	MM	4.66538e4	810.90723	49.5462
2	26.849	1	MM	4.75084e4	675.83887	50.4538
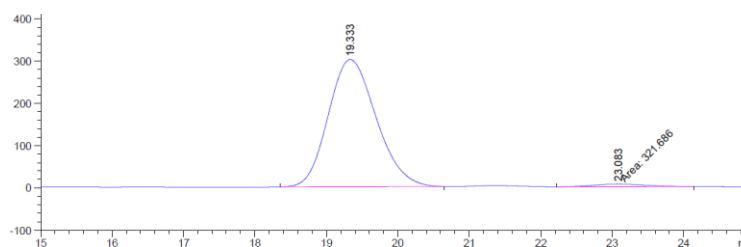
Peak #	RetTime [min]	Sig	Type	Area [mAU*s]	Height [mAU]	Area %
1	19.333	1	BB	1.40398e4	301.14352	97.7601
2	23.083	1	MM	321.68555	6.27789	2.2399